Diagnostics of Induction Machine Rotor Faults Using Analysis of Stator Signals

TOOMAS VAIMANN

TALLINN UNIVERSITY OF TECHNOLOGY
Faculty of Power Engineering
Department of Electrical Engineering

Dissertation was accepted for defence of the degree of Doctor of Philosophy on April 22, 2014.

Supervisors: Associate professor Aleksander Kilk, Department of Electrical Engineering, Tallinn University of Technology

Professor Anouar Belahcen, Department of Electrical Engineering, Tallinn University of Technology; Department of Electrical Engineering, Aalto University, Finland

Opponents: Professor Iraida Kolcunová, Department of Electrical Engineering, Košice University of Technology, Slovakia

Andrejs Podgornovs, Ph.D., Department of Electrical Engineering, Riga University of Technology, Latvia

Defence of the Thesis: August 21, 2014.

Authors declaration:

Hereby I declare that this Doctoral Thesis, my original investigation and achievement, submitted for the doctoral degree at Tallinn University of Technology, has not been submitted for any academic degree.

Toomas Vaimann

April 22nd, 2014

Asünkroonmasina rootori diagnostika staatorisignaalide uurimise meetodil

TOOMAS VAIMANN

CONTENTS

ABBREVIATIONS AND SYMBOLS

List of abbreviations

2D	two-dimensional
3D	three-dimensional
α-axis	current or voltage α component axis
A	ampere
β-axis	current or voltage β component axis
CO_2	carbon dioxide
CWT	continuous wavelet transform
d-axis	direct axis
d-q axis	direct-quadrature axis
DC	direct current
DWT	discrete wavelet transform
FE	finite element
FEM	finite element method
FFT	fast Fourier transform
Hz	hertz
IT	information technology
kW	kilowatt
MATLAB	science and engineering programming environment software
MCSA	motor current signature analysis
MUSIC	multiple signal classification
q-axis	quadrature axis
rms	root mean square
rpm	rotations per minute
STFT	short-time Fourier transform
V	volt

List of symbols

A	vector potential
a	scale parameter
A_k	amplitude of the kth sinusoid
AR	rotor first phase coil
AS	stator first phase coil
A_z	z-component of the vector potential
B	magnetic flux density
b	time parameter
BR	rotor second phase coil
BS	stator second phase coil
cosφ	power factor
CR	rotor third phase coil
CS	stator third phase coil
d	deviation of the ellipse from circular shape
d_s	gap between stator and rotor center points
DR	equivalent rotor coil on direct axis
DS	equivalent stator coil on direct axis
E	electric field strength
e(n)	additive complex white noise sample of variance σ^2
F	vector of total forces acting at some discrete location
f	local force vector
f	frequency
$\mathbf{f}^B$	body force vector
f_k	frequency of the kth sinusoid
$\mathbf{f}^S$	surface force vector
f_{sb}	sideband frequency
G	Jacobian matrix for the transformation from the reference finite element to the actual one
g	air-gap length

H	magnetic field strength
i_α	current alpha component
i_β	current beta component
i_a	first phase current
i_{as}	applied current to stator
i_b	second phase current
i_c	third phase current
i_d	d-axis current component
i_q	q-axis current component
I_n	rated current
J	current density
l	length of the conductor
N	vector length
n_n	rated speed
O_r	rotor symmetry axis
O_s	stator symmetry center
O_w	rotational center
O_sO_w	static transfer vector
O_wO_r	dynamic transfer vector
p	number of poles
P_n	rated power
QR	equivalent rotor coil on quadrature axis
Q_r	number of rotor bars
QS	equivalent stator coil on quadrature axis
Q_s	number of stator slots
R	resistance
R_M	eigenanalysis autocorrelation matrix
R_r	rotor radius
R_s	stator radius
s	slip

$\hat{S}_e$	reference element
U	vector of virtual displacements of each node
u_α	voltage alpha component
u_β	voltage beta component
u_a	first phase voltage
u_b	second phase voltage
u_c	third phase voltage
u_d	d-axis voltage component
u_q	q-axis voltage component
U_n	rated voltage
V_{as}	applied voltage to stator

List of Greek symbols

β	initial angle of eccentricity
β_d	initial angle of dynamic eccentricity
β_s	initial angle of static eccentricity
δ_d	dynamic eccentricity degree
δ_m	mixed eccentricity degree
δ_s	static eccentricity degree
ε	strain tensor
Θ	angle between stator and rotor center points
Θ	angular position
ν	magnetic reluctivity of the material
σ	electric conductivity
τ	stress tensor
Φ	scalar potential
φ_k	phase of the kth sinusoid
ψ	analyzing wavelet
ψ^*	complex conjugate of ψ
ω_N	Nth root of unity

LIST OF ORIGINAL PAPERS

Given doctoral thesis is based on following publications by the author. These publications are referred to in text using Roman numerals I-VI:

[I]   **Vaimann, T.**; Niitsoo, J.; Kivipõld, T.; Lehtla, T. (2012). Power quality issues in dispersed generation and smart grids. *Electronics and Electrical Engineering*, vol. 10, no. 8, pp. 23–26.

[II]   Kallaste, A.; Belahcen, A.; Kilk, A.; **Vaimann, T.** (2012). Analysis of the eccentricity in a low-speed slotless permanent-magnet wind generator. *Proceedings of the 8th International Conference PQ2012 Electric Power Quality and Supply Reliability*, Tartu, Estonia, June 11–13, 2012, pp. 47–52.

[III]   **Vaimann, T.**; Belahcen, A.; Kallaste, A. (2014). Changing of magnetic flux density distribution in a squirrel-cage induction motor with broken rotor bars. *Electronics and Electrical Engineering*, vol. XX, no. XX, [to be published].

[IV]   **Vaimann, T.**; Kallaste, A.; Kilk, A. (2011). Overview of sensorless diagnostic possibilities of induction motors with broken rotor bars. *Proceedings of the 12th International Scientific Conference Electric Power Engineering EPE 2011*, Kouty nad Desnou, Czech Republic, May 17–19, 2011, pp. 183–186.

[V]   **Vaimann, T.**; Belahcen, A.; Martinez, J.; Kilk, A. (2014). Detection of induction motor broken bars in grid and frequency converter supply. *Przeglad Elektrotechniczny (Electrical Review)*, vol. 90, no. 1, pp. 90–94.

[VI]   **Vaimann, T.**; Belahcen, A.; Martinez, J.; Kilk, A. (2012). Park's vector approach for detection broken rotor bars in frequency converter fed induction generator. *Proceedings of the 13th International Scientific Conference Electric Power Engineering EPE 2012*, May 23–25, 2012, Brno, Czech Republic, vol. 2, pp. 985–988.

Copies of listed publications are included in Appendix A.

Author's contribution per paper

Contribution of author to the listed papers included in the thesis is as follows:

[I]   Toomas Vaimann is the main author of the paper. He is responsible for gathering data, describing the effect of frequency converter influenced harmonic components on electrical machines and possible diagnostic methods. Also he is partly responsible for writing the paper. Other authors gave valuable inputs in other described parts and writing those parts in the paper. The main author made a presentation of the paper at the 16th International Conference ELECTRONICS'2012, Palanga, Lithuania.

[II]   Toomas Vaimann is one of the main authors of the paper. He is responsible for the data collection, explanation of the theoretic part of air-gap eccentricity, analysis and the writing of the paper. A. Kallaste was responsible for modelling the eccentricity for a slow speed permanent magnet generator. Other authors had the role of consultants in this paper. Paper was presented at the 8th International Conference Electric Power Quality and Supply Reliability PQ2012, Tartu, Estonia.

[III]   Toomas Vaimann is the main author of the paper. He is responsible for the data collection as well as the writing of the paper. Other authors had the role of consulting and assisting with the magnetic field modelling in this paper. The main author made a presentation of the paper at the 18th International Conference ELECTRONICS'2014, Palanga, Lithuania.

[IV]   Toomas Vaimann is the main author of the paper. He is responsible for the data collection as well as the writing of the paper. Other authors had the role of consultants in this paper. The main author made a presentation of the paper at the 12th International Scientific Conference Electric Power Engineering EPE 2011, Kouty nad Desnou, Czech Republic.

[V]   Toomas Vaimann is the main author of the paper. He is responsible for the data collection, measurements described in the paper as well as the writing of the paper. Other authors had the role of consulting and assisting during the measurements in this paper.

[VI]   Toomas Vaimann is the main author of the paper. He is responsible for the data collection, measurements described in the paper as well as the writing of the paper. Other authors had the role of consultants and assisting during the measurements in this paper. The main author made a presentation of the paper at the 13th International Scientific Conference Electric Power Engineering EPE 2012, Brno, Czech Republic.

ACKNOWLEDGEMENTS

1 INTRODUCTION

Diagnostic of electrical machines has gained popularity during the last two or three decades. During the years a lot of literature regarding this topic has been published. Induction motors are critical for many industrial processes because they are cost effective and robust in the sense of performance. They are also critical components in many commercially available equipment and industrial processes [1]. In developed countries today there are more than 3 kW of electric motors per person and most of it is from induction motors [2]. A good overview of induction machine diagnostic papers has been given in [3].

In the past years, interest towards diagnostic of electrical machines has been rising more rapidly. As the world is moving towards smarter grids, dispersed electricity generation and replacing traditional fossil fuels with alternative sources due to energy politics and CO_2 emission quotas, condition monitoring of electrical machines is becoming more important. Monitoring becomes necessary to keep a certain electric power quality and supply reliability level in the new dispersed and dynamic systems where many small generation units such as small hydro and wind power plants are integrated. Some of the possible hazards and necessities of implementing certain diagnostic procedures in dispersed generation and smart grid situation have been described in [I].

Online diagnostic makes detection of the faults easier and in some cases even may lead to prevention of failures. Minor faults can seem unimportant at the beginning, but when problems are not dealt with, failures can lead to catastrophic measures. In that way condition monitoring makes it possible to detect the faults in such stage, when repairing of the machines is still possible or reasonable. Also it would help to differentiate the deviations and harmonic distortions in the grid from the faulty cases of the machines [I].

1.1 Causes of electrical machine faults

There are many possible failures that can affect the performance of electrical machines. Usually the faults are caused by a combination of various stresses. Those stresses are as follows [4]:

- Thermal stress due to over-load, non-uniform heat distribution, hot spot and arc;

- Magnetic stresses due to electromagnetic forces, magnetic asymmetry forces, noises and electromagnetic vibrations;

- Residual stress from the fabrication process;

- Dynamic stress due to rotor axial torque and centrifugal forces;

- Circumferential stress due to wearing and pollution of rotor material by chemical materials and humidity;

- Mechanical stress due to mechanical fatigue of different parts, bearing damage, loosened laminations etc.

The main reasons however are usually related to poor manufacturing quality like defective casting or jointing. Another common reason is improper use of the machines. For example overcurrent due to jam conditions of the rotor may pose a threat to the health of the machines [5].

Another classification of the causes that lead to failures in electrical machines is presented in [6] and it is as follows:

- Harsh environment;
- Improper machine selection and application;
- Inadequate installation;
- Mechanical failure;
- Electrical problems;
- Voltage unbalance;
- Inadequate maintenance;
- Combination of one or more of the abovementioned causes.

One of the most common reasons for fault propagation is harsh environment. One of the elements of harsh environment is excessive temperature due to environmental reasons or problems in the motor. To ensure a long lasting exploitation time of the machines, they must operate on the nominal temperature rating. Every 10 degrees of overheating means halving of the insulation life time and can lead to different insulation problems. A very in-depth report of different insulation related problems in electrical machines can be found in [7].

Another common environmental factor that can cause machine failures is moisture. If for any reasons moisture forms on the surface of the machine insulation, the insulation may become conductive and result in insulation and whole machine failure. There is also a possibility that the insulation would absorb the moisture from its surface in time, which will cause the insulation resistance to lower to the level that a fault will occur [6]. Apart from the mentioned ones there are of course numerous harmful environments such as the ones containing harmful gases and fumes, salt rich air, excessive dirt, dust etc. [8].

It is essential that the right size and type of machine is selected to be working with the right load. Additionally there are many aspects beside load that have to be kept in mind when a machine is selected. For example severe duty cycles can cause the machine to prematurely fail. If those severe duty cycles are combined with the before mentioned harsh environments, one must be careful to make correct choices, so that the machines would last for their planned life time. Of course there are cases where the misapplication of the machine is so minor, that the machine will

last for significant time, but it should be kept in mind that even small mistakes and faults in machines can lead to severe failures, if not treated in time.

When the machine is mounted in an inadequate manner, the results might yet again be machine faults. Machines are usually coupled with some sort of load. This means that all those couplings, belts and other connections between machine and load must be aligned correctly, otherwise excessive vibrations might occur, which can be potentially damaging for the machine. Excessive vibrations can also occur due to wrongly sized or not enough tightened mounting bolts. Those vibrations can be extremely harmful to bearings and shaft of the machine and can even cause winding burnout [6].

One of the common causes of machine failure is overloading of the machines. If for some reason excessive load is connected to the motor, the motor will draw additional current and as a result the machine temperature will increase. Due to exceeding of the rated full load current and most probably nominal temperature ratings, the machine exploitation time will be shortened. In some occasions jam conditions of the rotor can be the source for overloading of the machine. This in turn can often be caused by a bearing failure that is considered to be one of the most common machine faults.

If the supply voltage of the electrical machine has been chosen incorrectly, it can shorten the exploitation period of the machine. In some cases, when the voltage deviations become severe, it can result in rapid failure of the machine. Copper losses can be reduced with high line voltage, but on the other hand, increased magnetic flux will result in higher iron losses. Tests have shown that if the supply voltage rises in the order of 10% or more over the rated voltage, it will cause the iron to saturate and will lead to harmful overheating of the machine [6].

Unbalanced voltage between the phases can also be harmful for the machines as they will lead to current unbalance, which will again result in overheating of the machine. This problem is becoming more and more severe due to excessive harmonics in the grid and the addition of nonlinear loads in the end user side of the grid. Those harmonics and unexpected nonlinear loads may also lead to unbalanced current of the machine and become harmful not only to the machine itself but also to power electronic converters that are very often used in hand with electrical machines. Some investigations of harmonics and nonlinear loads can be found in [9], [10]. Problems that harmonics pose to electrical machines are somewhat mentioned in [I].

Finally, diagnostics and condition monitoring is one of the key factors that can prevent or at least delay the failure of the machine. Most faults start as minor deviations from the normal conditions and they seem unimportant. The problem is that if those small deviations are not dealt with in time, the faults can start propagating until the repair of the machine is not reasonable or even possible. When condition monitoring or online diagnostic measures are taken, it is possible

to detect the faults at early stages and save the machine from larger faults in time. Reasons to use condition monitoring include [11]:

- preventing catastrophic failures and significant damage of the machines;

- avoiding loss of life, environmental harm and economic losses;

- stopping unscheduled outages;

- optimization of machine performance;

- reducing repair time and spare parts inventory;

- lengthening of the maintenance cycle;

- reducing price and raw material consumption;

- increasing product quality.

In other words, the reasons can be safety, production assurance, predictive maintenance and quality control [11].

Given thesis investigates the possibilities of using stator electrical parameters to identify rotor faults in induction machines. However, possible features to be monitored in the diagnostic purposes can include vibration, noise, heat, power consumption, displacement, rotation speed, as well as already mentioned electric parameters (such as voltage, current, frequency, resistance, etc.). The list is long and growing.

This is also one of the reasons why condition monitoring could be used in very different industries. These industries include power generation, oil and gas industry, petrochemical industry, pipelines, refineries, waste water treatment, food and pharmaceutical industries, marine propulsion, metal and mining industry, transportation, etc.

1.2 Mechanical and electrical faults

Statistically bearing faults are considered to be the most common machine failures. It has been estimated that even up to 50% of all machine faults are caused by bad bearings [6]. Depending on the data source, the exact percentage of the occurring fault type is varying.

A large survey on reliability of the industrial electric machines conducted by IEEE [12]–[14] lists bearing related faults as the most common faults in electric machines, forming 41% of all possible faults in the machines. Stator faults are occurring in 37% of the time, rotor related faults take up to 10% of the whole amount of failures and the remaining 12% of faults are the ones that cannot be classified to the three mentioned groups according to the survey. Similar statistical values are described in numerous publications, e.g. [15]–[18].

However the exact statistics may vary, rotor faults make up to 10–20% of the possible failures in the machines and a great number of these faults are broken rotor bar or end ring faults. Moreover, broken rotor bar faults can be the trigger for faults in other parts of machines, such as stator faults. This phenomenon is described more precisely in the Simulations chapter of the given dissertation.

1.2.1   Air-gap eccentricity

This fault is related to a condition of unequal air gap that exists between the stator and rotor. Some of the comprehensive descriptions of the fault can be found in [15], [19]–[24]. Additionally air-gap eccentricity fault has been investigated by the author of the thesis and his colleagues. Some results of the investigation are presented in [II]. In severe cases of the fault, there is even a possibility of a stator-rotor rub caused by the unbalanced radial forces due to the eccentricity.

Air-gap eccentricity can be caused by different inaccuracies during the production of the machine, such as construction strength, manufacturing tolerances, bending of the shaft and bearings etc. [25]. Eccentricity can be found to some extent in all electrical machines and it has been thoroughly investigated. In fact up to 10% of eccentricity is usually permissible for any electrical machine [19] Researches have been made on how eccentricity affects losses [26], eccentricity due to asymmetrical magnetic forces [27], [28], diagnostics of eccentricity [29]–[31] etc.

Fig. 1.1 shows possible types of eccentricity. A healthy machine (Fig. 1.1a), static eccentricity (Fig. 1.1b), elliptic eccentricity (Fig. 1.1c) and dynamic eccentricity (Fig. 1.1d and 1.1e) are shown on the figure.
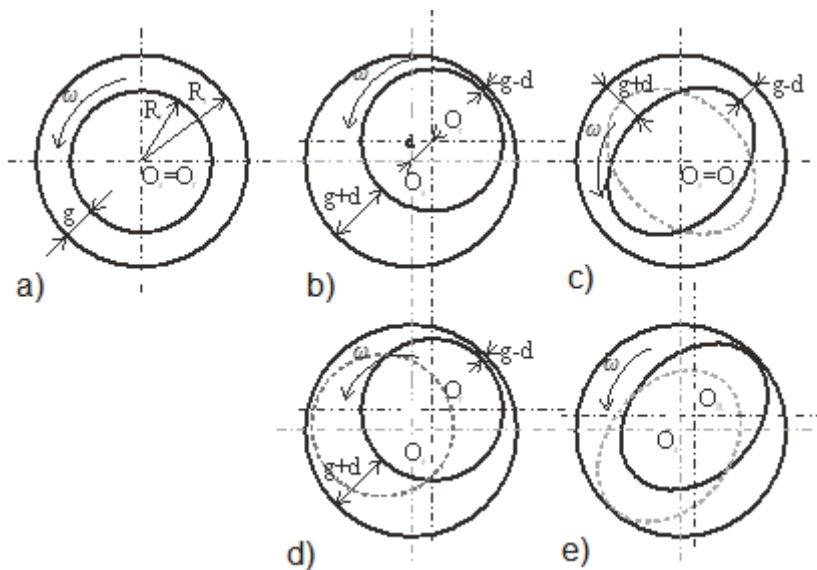

Fig. 1.1. Rotor eccentricity: a) healthy; b) static; c) elliptic; d) and e) dynamic [32].

Static eccentricity

In the case of static eccentricity fault, the rotational axis of the rotor coincides with the rotor symmetry axis, but at the same time, it is displaced from the stator symmetry axis. It means that the position of the minimal radial air-gap length is fixed in space. This can be caused by [19]:

- ovality of the stator core;

- incorrect positioning of the rotor or stator at the assembling stage.

Air-gap distribution around the rotor is not uniform and it is independent of time. The static eccentricity degree (δ_s) is defined using the following equation [32]:

$$\delta_s = \frac{|O_s O_w|}{g},$$
(1.1)

where O_s is the stator symmetry center, O_w is the rotational center, and g is the air-gap length.

In case of a static eccentricity fault, the width of the air-gap can be determined as follows:

$$g = R_s - R_r + \sqrt{R_r^2 - (d_s \cdot \sin \beta)^2},$$
(1.2)

where R_s is stator radius, R_r represents rotor radius and d_s is the gap between the stator and rotor center points.

Elliptic eccentricity

In case of elliptic eccentricity the rotor and stator symmetry points are matching, but as the rotor is shaped as an ellipse, there are still deviations in the uniformity of the air-gap. In such case the amount of eccentricity at a given angular position changes in time.

The width of the air-gap in such case can be found as follows [32]:

$$g(t) = R_s - \sqrt{\left[(R_r + d)\cos\left(\frac{\omega t}{p} - \beta\right)\right]^2 + \left[(R_r - d)\cos\left(\frac{\omega t}{p} - \beta\right)\right]^2},$$
(1.3)

where R_r represents the radius of cylindrical rotor, d is the deviation of the ellipse from circular shape and p expresses the number of rotor poles. Angle β is changing in time.

Dynamic eccentricity

In case of dynamic eccentricity the rotor symmetry point is shifted from the stator center, but the rotation of rotor is happening around the stator symmetry point. As the rotor center is not at the center of rotation, the position of minimum air-gap rotates with the rotor. This means it is a function of space and time and dynamic

eccentricity can be looked at as a time-varying phenomenon. This fault condition could be caused by [19]:

- bent rotor shaft;

- bearing wear or misalignment;

- mechanical resonance at critical speed;

- thermal bowing of the rotor etc.

The dynamic eccentricity degree (δ_d) can be found according to the following equation [32]:

$$\delta_d = \frac{|O_w O_r|}{g}, \tag{1.4}$$

where O_r represents the rotor symmetry axis and $O_w O_r$ is the dynamic transfer vector. That vector is fixed in case of all angular positions of the rotor, but its angle varies in time as the rotor rotates.

Mixed eccentricity

Mixed eccentricity is the most severe combination of eccentricity phenomena. In such case symmetry points of rotor, stator and the point of rotational symmetry are all shifted from each other. So both static and dynamic eccentricities are present in the generator. Mixed eccentricity is the result of static and dynamic transfer vectors and in that case mixed eccentricity degree (δ_m) can be written as follows:

$$\delta_m = \frac{|O_w O_r|}{g} = \left|\frac{O_s O_w}{g} + \frac{O_w O_r}{g}\right| = \sqrt{d_t^2 + d_d^2 + 2 d_t d_d \cos q}. \tag{1.5}$$

As mixed eccentricity is a time-varying phenomenon, the width of the air-gap depends on the mechanical position of the rotor and it can be found using the following equation:

$$g(t) = R_s - \delta_m g \cos\left(\frac{\omega t}{P} - \beta\right) - \sqrt{R_r^2 - \delta_m^2 g^2 \sin\left(\frac{\omega t}{P} - \beta\right)}. \tag{1.6}$$

Fig. 1.2 presents positions of stator and rotor cross-sections under different eccentricity phenomena in the stator reference frame. Fig. 1.2a shows the case of static eccentricity. In the figure β_s is the initial angle of static eccentricity and $O_s O_w$ is the static transfer vector. This vector remains the same in all angular positions of the rotor. Fig. 1.2b shows dynamic eccentricity, where β_d is the initial angle of the dynamic eccentricity. In Fig. 1.2c elliptic eccentricity can be seen, where β is the initial angle of the eccentricity and Θ is the angle between the center points of stator and rotor of the machine.
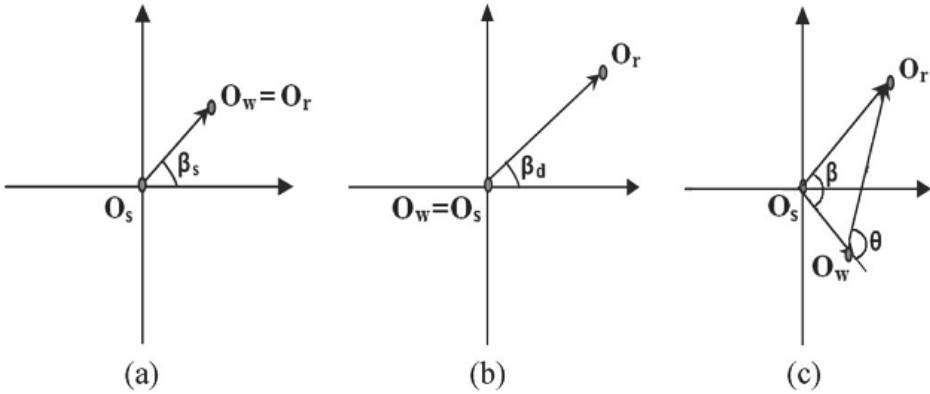
Fig. 1.2. Position of stator and rotor cross sections under (a) static eccentricity,
(b) dynamic eccentricity, and (c) elliptic eccentricity in the stator reference frame [32].

1.2.2   Bearings damage

Bearing damage is considered statistically one of the most common faults in electrical machines. Good explanations and overviews of the bearing damage fault can be found in [5], [15], [21], [33], [34].

The main causes for bearing damage are as follows [19]:
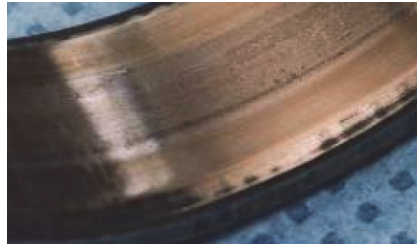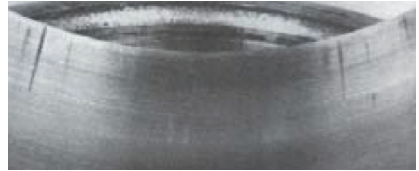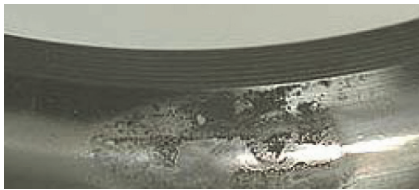
- contamination and corrosion;

- improper lubrication;

- improper installation of bearing (forcing the bearing onto the shaft or in the housing).

Bearing defects normally develop from fatigue but reasons for the damage can also start from poor lubrication, mechanical shock, overheating, impurities or mechanical overload [5]. A list of common bearing damage reasons and consequent damages is presented in Table 1.1.

In case of bearing damage, friction of the machine is affected, which in turn affects rotor currents and mechanical velocity [19], [23]. From this, the main symptoms of bearing damage include uneven running, reduced working accuracy and unusual running noise [5], [35]. Uneven running itself causes vibrations in the machine that can be potentially damaging and will speed up the propagation of the fault.

There are two main bearing types that are used in electrical machines. Sleeve bearings are used in large machines, as they can carry heavy loads. Faults of the sleeve bearings produce very low vibration levels because of the pressured oil between bearing surfaces [5]. Due to this, the faults are easily missed in case of vibration measurements and similar methods. Direct measurements of axle misalignment must be implemented to detect the fault.

Table 1.1. Common bearing damage reasons and consequent damages [5], [35]

Primary reason	Damage	Visual
Normal deterioration (normal fatigue)	Flaking	
Abrasive particles • Contamination during installation • Defect in seals • Contaminated lubricant	Worn contact surfaces, indentations	
Fail of the lubrication film • Inadequate lubricant • Improper lubricant	Surface distress, microscopic cracks, smearing, flaking	
Water or other corrosive material inside the bearing	Corrosion, flaking, cracks	
Bearing currents Rough installation	Fluting Indentations, fractures	
Heavy load Rough installation	Smearing (scored races), indentations if a heavy load is on non-running bearings Indentations, fractures	

Most of machines are equipped with roller or ball bearings. Each of the bearings consist of two rings: inner and outer ones; and a set of balls or rolling elements placed in raceways that rotate inside these rings [15], [19], [20], [33], [34]. Rolls are supported by a holder, which is usually referred to as a train cage. The main difference between roller bearings and ball bearings is the use of rolls and balls in respective cases [5]. From those two types ball bearings are the most used due to their low price, although roller bearings usually can carry heavier loads due to the larger contact surface between roll and race. Main four types of ball bearing rolling element faults are presented in Fig. 1.3.

Ball bearing faults can also be divided into cyclic and non-cyclic vibration faults [5], [36]. Cyclic vibrations derive from defects like flaking, cracks or scratches, which are usually one point faults and rolling element of the bearing rolls over the defected point in a cyclic manner over time periods. Surface roughness, corrosion, fluting and similar faults can be considered as non-cyclic faults, as the defect is usually not localized to a certain point, but is spread over the surface, causing non-cyclic vibrations [5], [37]. In both cases, the faults diminish life time of the bearings and also increase the failure probability of the whole machine, which in hand decreases the reliability of the machine and is therefore a not desirable phenomenon.
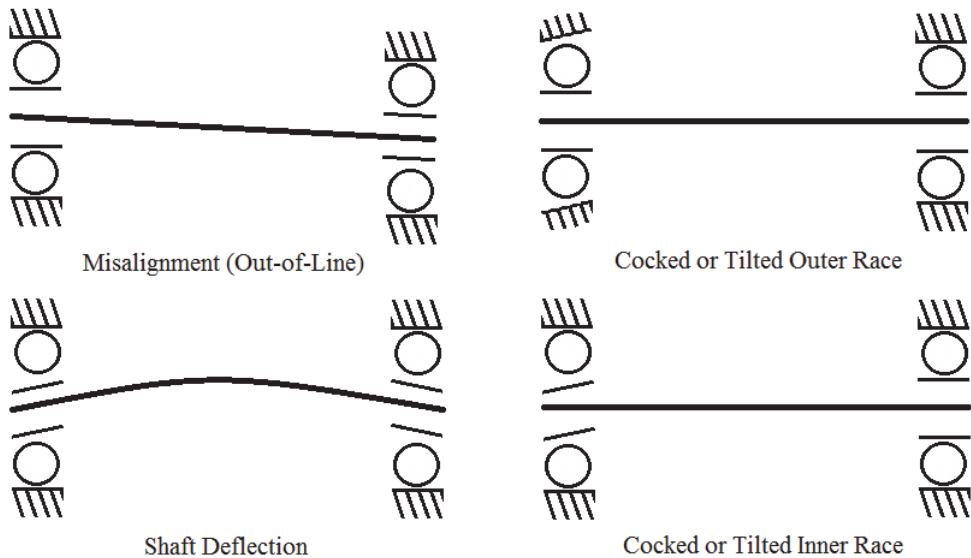
Fig. 1.3. Types of ball bearing rolling element misalignment [15], [33].

1.2.3   Stator and armature faults

Stator and armature faults are related to insulation failures in electrical machines [19]. These faults can be classified as winding failures and stator lamination stack short-circuits. Regardless of the main cause of the winding fault, the actual mode of the failure can be divided down into five groups, which are

illustrated in Fig. 1.4 [38]. In case of whichever stator winding malfunctions, it is very difficult to determine, what the initial failure was and which faults are the results of the initial fault propagation.
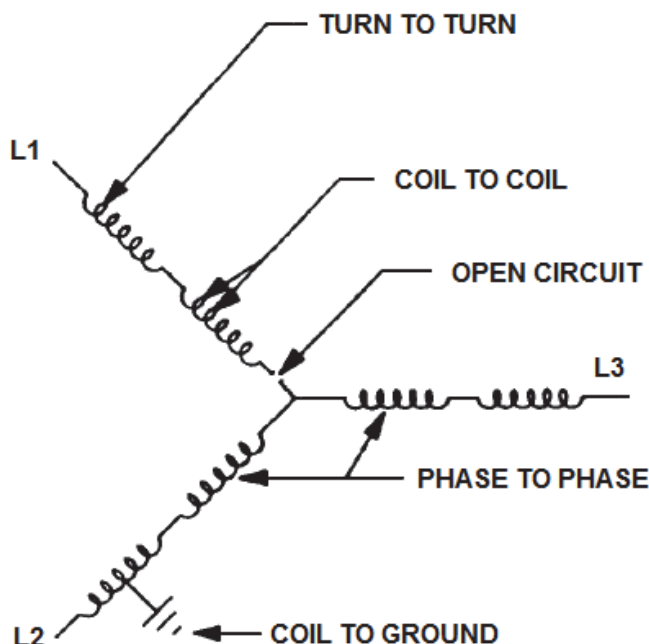
Fig. 1.4. Possible failure modes in a star-connected stator. Fault consisting of
a combination of those faults is also possible [38].

A very illustrating example is given in [38]. A failure in the machine stator can start with a minor turn-to-turn short circuit within one coil. When this fault is not detected and treated, it will propagate and excessive heat is generated within the shorted coil. This will result in insulation deterioration and at some point in a partial ground short-circuit through the slot liner. If again the fault is neglected and the machine would continue operation due to protection peculiarities or malfunction, increasing heat is generated in the damaged area until the phase or ground insulation is destroyed. This will lead to the occurrence of a direct phase-to-phase fault or ground fault, which will damage the machine to the extent that further operation is impossible.

In such cases it is very hard to say what the initial problem with the machine was. A minor turn-to-turn failure is usually very difficult to recognize due to the destructive nature of the resulting fault conditions [38]. Furthermore, turn-to-turn short circuits or minor lamination short circuits can be the result of local saturation and stray currents as is shown under the simulation chapter of the given thesis.

The main symptoms of the stator faults can be found in several publications [7], [15], [19], [38]. These can be:

- high stator core or winding temperatures;

- slack core lamination, slot wedges and joints;

- loose bracing for end winding;

- electrical discharges;

- leakage in cooling system.

1.2.4 Broken rotor bars and end-ring faults

Electric current that is induced by the stator field, flows through the rotor bars. It is producing magnetic force that will create necessary torque in the machine. Rotor bars that might crack, break or separate from the end rings prevent current to flow, which in hand limits motor performance. As a result, there is a thermal difference in the rotor, a lack of induced magnetic field, an unbalanced radial force and vibration components [19].

The worst case of such fault is when the broken rotor bars are situated closely one after another. This case is also most probable in practice as broken rotor bars are usually not detected at early stage. As the resistance of the broken bar is very high in comparison with the healthy ones, currents start to distribute disproportionally in the rotor cage. Parts of the rotor currents, which are unable to flow in broken bars, are flowing in adjacent bars. This increases the rms value of currents in the bars next to the broken ones [39]. As the healthy bars next to the broken one have too high current density, they will start to overheat, so these bars are under severe thermal stress. Those bars start cracking and breaking when attention to the problem is not paid. The fault will continue to cascade, until the rotor cage is destroyed.

A further explanation of the propagation of induction machine broken rotor bars fault is brought in simulations chapter. Also it is explained in [III].

Main reasons for such types of faults are [15], [19]–[21], [40], [41]:

- thermal stresses because of thermal overload, unbalance, hot spots or excessive losses, sparks etc.;

- magnetic stresses by unbalance magnetic pull, vibration;

- dynamic stresses arising from shaft torques, centrifugal forces and cyclic stresses;

- mechanical stresses because of loose lamination, fatigued parts, or bearing failure.

Figs. 1.5 and 1.6 show induction machine rotor bars that have broken because of different reasons. On Fig. 1.5 broken rotor bars due to heavy duty operation are presented. A trapped air bubble and broken rotor bar due to defective casting is shown on Fig. 1.6.
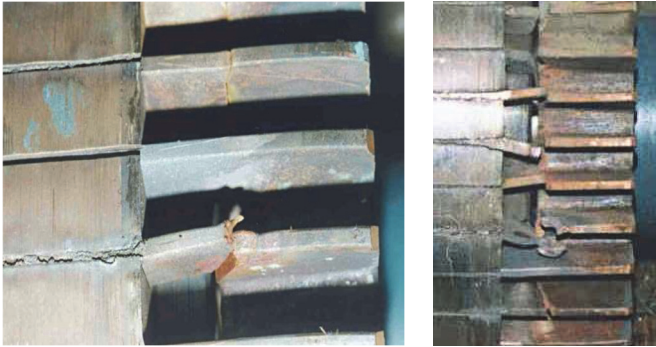
Fig. 1.5. Broken rotor bars due to heavy duty operation [43].

Fig. 1.6. Broken rotor bar due to defective casting [5].

Broken rotors bars can lead to vibration problems [42], but more likely, in severe cases, the bar pounds out of the slot and makes contact with the stator core or winding [38]. The biggest problem of those faults is that it is often not worth or possible to repair the rotor. However all of this can be avoided, when the motor is supervised by an appropriate condition monitoring or diagnostic system and the fault is identified early enough.

1.3   Diagnostic methods

Diagnostic of electrical machines has been an investigative interest for researchers for the past few decades. This also means that there are several diagnostic methods available that are used to identify the faults in machines. Some of the methods that can be used to detect faults in the machines are described in [IV].

A well-known indicator of broken bar fault is the appearance of sideband components [15], [21], [44]. These sideband frequencies can be found in the power spectrum of the stator current and they appear on the both sides of the fundamental frequency component. The lower sideband component is situated on the left side of the fundamental frequency peaks and it is caused by electrical

and magnetic asymmetries in the induction machine rotor cage [44]. The higher sideband lies on the right side of the fundamental component and it emerges due to consequent speed ripples caused by the resulting torque pulsations [21], [45]. The frequencies of these sidebands are described mathematically as follows:

$$f_{sb} = (1 \pm 2s)f ,$$ (1.7)

where s is slip per unit and f is the fundamental frequency of the stator current, which is set by the supply. The sideband components are extensively used for induction motor fault classification purposes [15], [44], [46]–[48].

When choosing an appropriate method for condition monitoring or diagnostics of the machines, it should be noted, that changes of the working cycle are not desired while diagnostic process is performed. In other words, in case of motors which are used in critical duty drives or perform on high risk conditions, no additional changes should to be made in order to perform the tests.

A growing number of machines are driven through frequency converters. This means that also diagnostic for appropriate setups with frequency converters should be investigated. Frequency converters add additional noise and harmonics to the traditional current spectrum of the machines and thus such drives need a slightly different approach in diagnostics than traditional grid supplied machines.

Most of the diagnostic methods and approaches that are used for induction machine diagnostics using stator signals nowadays can be associated with so-called motor current signature analysis (MCSA) methods. An inconclusive list and explanations of some of the methods used is given below.

1.3.1   Fast Fourier transform

Fourier analysis is very useful for many applications where the signals are stationary, as in diagnostic faults of electrical machines [49]. Purpose of the fast Fourier transform (FFT) is to monitor a single-phase stator current. A simple explanation of the signal processing using FFT is presented as follows.

For this, the fundamental excitation component is removed through low-pass filtering and the resulting signal is sampled. A current transformer senses and recognizes the single-phase current and the signal is sent to a 50 Hz notch filter where the fundamental component is reduced. After that, the analog signal must be amplified and filtered with a low-pass filter. The filtering removes the high-frequency components that produce aliasing of the sampled signal and are therefore undesired. At the same time amplification maximizes the use of the analog-to-digital converter input range. The analog-to-digital converter samples the filtered current signal at a predetermined sampling rate that is an integer multiple of 50 Hz [15]. This is continued over a sampling period that is sufficient to achieve the required FFT.

Calculation of the fast Fourier algorithm can be performed using science and engineering software, such as MATLAB, where computing of this transform can be done in a simple way. The MATLAB functions $Y = fft(x)$ and $y = ifft(X)$ implement the transform and inverse transform pair given for vectors of length N by:

$$X(k) = \sum_{j=1}^{N} x(j) \omega_N^{(j-1)(k-1)} \, , \tag{1.8}$$

$$x(j) = \frac{1}{N} \sum_{k=1}^{N} X(k) \omega_N^{-(j-1)(k-1)} \, , \tag{1.9}$$

where

$$\omega_N = e^{\frac{2\pi i}{N}} \tag{1.10}$$

is an Nth root of unity [50]. Equations 1.8 and 1.9 are known as FFT algorithms, which have been developed from the discrete Fourier transform to reduce the amount of computations involved [51].

It is well known that motor current is a non-stationary signal. Therefore the properties of the current vary in time with the normal time-varying operating conditions of the motor. As a result, it is difficult to differentiate fault conditions from the normal operating conditions of the motor using FFT [49]. Another drawback is the computational resources needed to run the FFT. Although the IT solutions and hardware of devices have improved a lot during the last decades, there might still be situations where high computational power is not available or not sensible to use. The differentiation of faulty conditions of the motor will be easier, if the figures of healthy motor state are used as comparison material for the faulty rotor figures and peculiarities of local electrical network are noted.

1.3.2 Wavelet transform

As has already mentioned before, FFT is suitable for analyzing stationary signals. Usage of FFT on transitory signals, such as drifts, abrupt changes, and frequency trends, is somewhat problematic. To overcome this problem, a method known as short-time Fourier transform (STFT), or windowing technique was adapted, to analyze small sections of signal at a time [15].

Using this method means mapping or dividing the signal into a 2D function of time and frequency. As both time and frequency are present in case of the windowing technique, there is information of both those parameters. However this information is available only with a limited precision, which is determined by the size of the window used for analysis [15]. Fixed size of the window can be considered the main drawback of STFT [52].

To overcome yet another precision problem, wavelet transform was introduced. It can be described as a windowing technique that is using a variable size window to analyses the signal such as current or voltage. This novel concept was first introduced by Morlet in 1984, receiving much criticism from his colleagues at the time [53]. Nevertheless, Morlet was able to formalize the continuous wavelet transform (CWT):

$$W_k\left(a;b;\psi\right) = a^{-\frac{1}{2}} \int x(t) \psi^* \left(\frac{t-b}{a}\right) dt \qquad (1.11)$$

where a is the scale parameter, b is the time parameter, ψ is an analyzing wavelet, and the ψ^* is the complex conjugate of ψ.

In the following years concept of discrete wavelet transform (DWT) was introduced, in the formalization of which the scale parameter a and the time parameter b are discretized as follows [53]:

$$\begin{cases} a = a_0^m \\ b = n a_0^m b_0 \end{cases}, \qquad (1.12)$$

where m and n are integers. Now the continuous wavelet function $\psi_{a,b}(t)$ in Equation 1.11 becomes a discrete wavelet function:

$$\psi_{m,n}(t) = a_0^{-\frac{m}{2}} \psi\left(a_0^{-m} t - n b_0\right). \qquad (1.13)$$

The discretization of the scale parameter and time parameter leads to the discrete wavelet transform [53]:

$$W_x\left(m;n;\psi\right) = a_0^{-\frac{1}{2}} \int x(t) \psi^* \left(a_0^{-m} t - n b_0\right) dt. \qquad (1.14)$$

CWT and DWT can be considered as the basis for all wavelet related techniques that have been developed in later years.

Different from the STFT, the wavelet transform can be used for multi-scale analysis of a signal through dilation and translation, so it can extract time–frequency features of a signal effectively [53]. Therefore, the wavelet transform is more suitable for the analysis of non-stationary signals [54].

The wavelet transform is a linear transform, whose physical pattern is to use a series of oscillating functions with different frequencies as window functions $\psi_{a,b}(t)$ to scan and translate the signal of $x(t)$, where a is the dilation parameter for changing the oscillating frequency [53]. Wavelet transform can be considered a flexible tool, providing the opportunity of using the analysis of smaller windows when high-frequency information is needed and also wider windows, when low

frequency information is desired. This has been called one of the most valuable and interesting features of wavelet analysis [15], [55].

The applications of the wavelet analysis have covered almost every aspect of the fault diagnostics and so it is considered to be a powerful tool for condition monitoring and fault diagnostics and it is actively used and improved. The improvement of the method also means that the advantages of using the method for diagnostic purposes is increasing and it can be used in case of different applications and operational states such as steady state operation or transients.

1.3.3   Eigenvalue analysis

Eigenvalue and eigenvector analysis can be classified as the high resolution spectral analysis methods [15]. Basically it means that first the machine input line currents are acquired proceeding with the computation of the principal directions (eigenvectors) and significant values (eigenvalues) that weight the spread of the data sample through the main directions [56]. This acquired information is then used to detect the fault of the machine.

Such diagnostic methods have been promoted in the digital signal processing research literature as they may improve or maintain high resolution without sacrificing as much stability, allowing the keeping of only the principal spectral components of the signal and to decrease noise influence [15]. According to [15] and [57] the data to be analyzed using the method are assumed to consist of pure sinusoids in white noise, a suitable model for the stator current

$$d(n) = \sum_{k=1}^{L} A_k \exp\left(j2\Pi f_k n + \phi_k\right) + e(n),$$ (1.15)

where $d(n)$ stands for the data, $e(n)$ is the additive complex white noise sample of variance σ^2, A_k is the amplitude of the kth sinusoid, f_k the frequency of the kth sinusoid and φ_k the phase of the kth sinusoid. Eigenanalysis divides the information in the autocorrelation matrix R_M into two vector subspaces, a signal subspace and a noise subspace. The index M of the autocorrelation matrix R_M stands for the matrix order. The eigenvalues of M are

$$\left\{ \lambda_1 + \sigma^2, \lambda_2 + \sigma^2, ..., \lambda_L + \sigma^2, \sigma^2, ..., \sigma^2 \right\}.$$ (1.16)

As illustration, two well-known eigenvalue analysis based frequency estimators have been used: multiple signal classification (MUSIC) and root-MUSIC for stator voltage unbalance underscoring [57]. In the case from [57], one of the principal spectral components modified by the electric fault is the third harmonic component (150 Hz) of the supply frequency. The amplitude of the third harmonic component amplitude increases in a significant way, under any load operation. The two principal spectral components of the stator current spectrum are the first and the fifth harmonics (50 and 250 Hz) for a healthy motor, and the first and third

harmonics (50 and 150 Hz) for a stator voltage unbalance. The MUSIC algorithm has been applied for each case and results are given in Fig. 1.7.
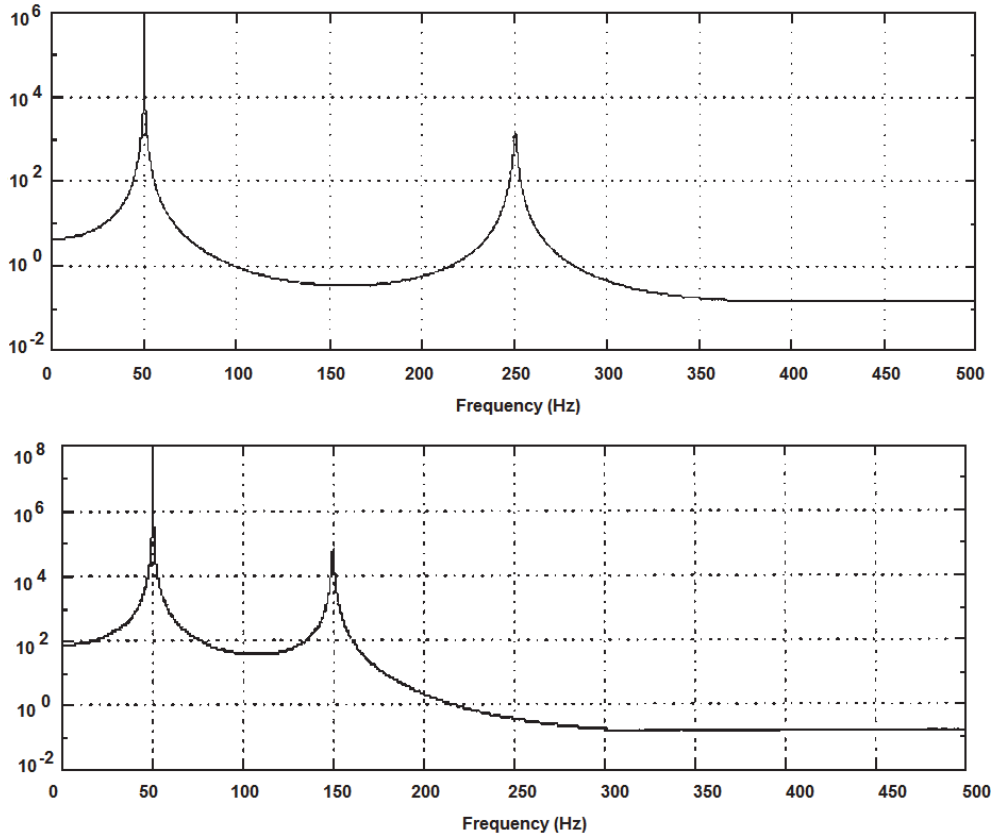
Fig. 1.7. MUSIC algorithm frequency estimate: upper – healthy machine, bottom – stator voltage unbalance [57].

The usage of MUSIC and root-MUSIC algorithms allows the keeping of only the needed main frequencies without other spectral information that would act as unnecessary noise in the analyzed spectrum of the machine. Moreover, stator current high-resolution spectral analysis, used as a medium for induction motors faults detection, can be useful in all faults modifying main spectral compo-nents [15].

1.3.4   Park's vector approach

Park's vector approach is based on space vector projection in d-q reference frame. It is a relatively simple reference figure, which gives the opportunity of deciding upon the state of machine under investigation. The approach itself is not a novel method for the diagnostics of electrical machines. It has been proposed more than twenty years ago by Cardoso [58]–[60].

The d-q reference frame makes it possible to transform a three-phase system into a simplified two-phase one. This transformation is explained through a schematic diagram shown on Fig. 1.8, where a three-phase induction motor with the d-q axes is superimposed. In this figure the q-axis lags the d-axis by 90°. Voltage V_{as} is applied to stator phase A, while the current flowing through it is i_{as}. Phases B and C are not shown on the diagram in an attempt to maintain clarity. In the d-q model, coils DS and QS replace the stator phase coils AS, BS and CS, while coils DR and QR replace the rotor phase coils AR, BR and CR [61].
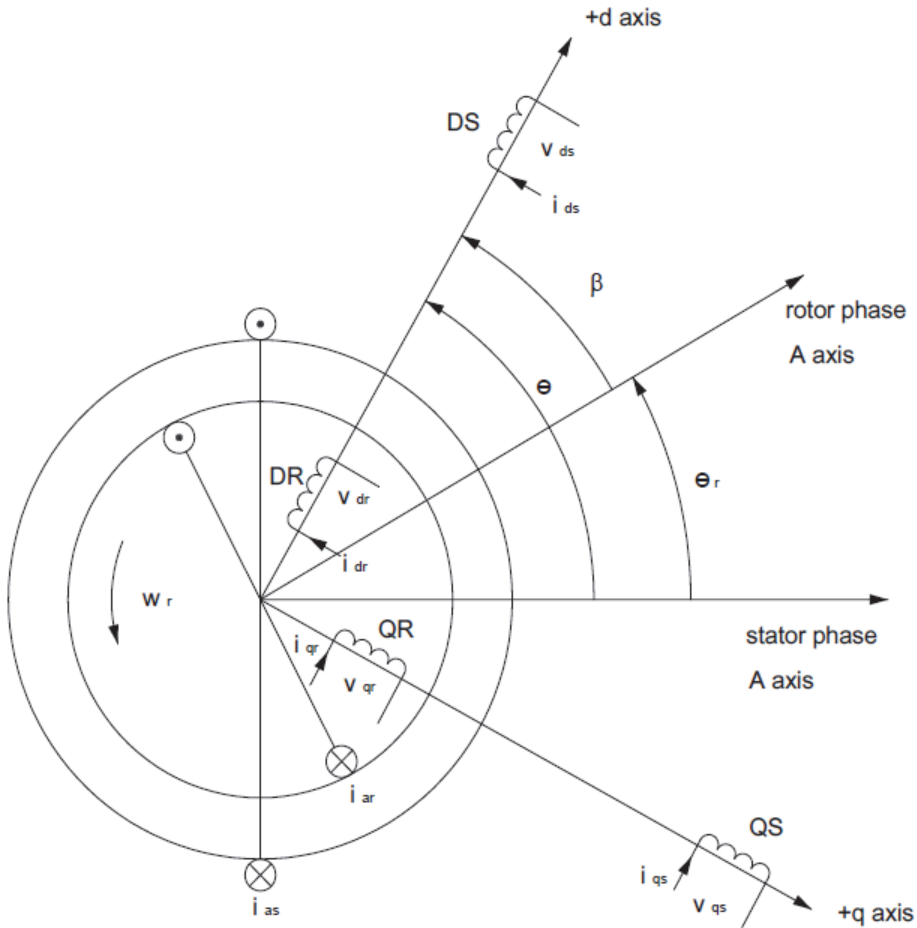
Fig. 1.8. d-q axes superimposed onto a three-phase induction motor [61].

In order to use Park's vector approach on a three-phase induction machine, the stator currents must be transformed into two equivalent phases. It means that the phase currents (i_a, i_b, i_c) are to be transformed into current d-axis and q-axis components (i_d, i_q) and placed on d-axis and q-axis respectively. This can be done using simple mathematic equations:

$$\begin{cases} i_d = i_a \\ i_q = \dfrac{1}{\sqrt{3}}\left(2i_b + i_c\right) \end{cases}.$$ (1.17)

Its representation is a circular pattern centered at the origin of the coordinates. This is a very simple reference figure, which allows the detection of an abnormal condition due to any fault of the machine by observing the deviations of the acquired picture from the reference pattern. The healthy pattern differs slightly from the expected circular one, because supply voltage is generally not exactly sinusoidal [62]. Pattern of the rotor with broken bars is however more like an ellipse shaped one. This pattern can be seen in Fig. 1.9.
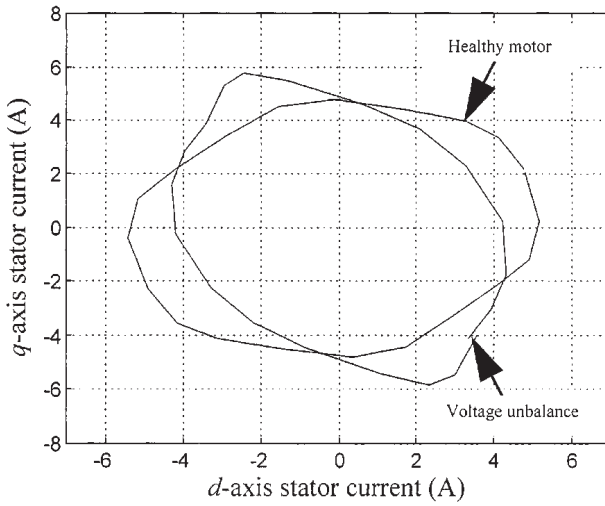
Fig. 1.9. Stator current Park's vector pattern [15].

Although traditionally used with stator current, the usage of voltage as input signal for Park's vector approach can prove to be a better method, because voltage is not influenced by torque. Both open loop and closed loop motor diagnostics is possible with using stator voltage for the reference pattern of this method.

To use the stator voltage as an indicator for three-phase induction machine diagnostics a similar transformation must be performed as when the stator current is used:

$$\begin{cases} u_d = u_a \\ u_q = \dfrac{1}{\sqrt{3}}\left(2u_b + u_c\right) \end{cases},$$ (1.18)

where u_a represents first phase voltage, u_b is second phase voltage and u_c is third phase voltage; u_d and u_q are voltage d-axis and q-axis components respectively.

Also different types of faults can be diagnosed using Park's vector approach. The main objective of the given thesis is to analyze diagnostic possibilities of broken rotor bar problem, but several researchers have found the mentioned method and similar 2D or 3D methods useful for stator fault diagnostics as well [63], [64].

1.3.5   Clarke transformation

Clarke transformation is a method relatively similar to the Park's vector approach explained in the previous chapter. The most important difference of the two methods lies in the reference frame where the methods are used. In case of Park's vector approach, a static d-q reference frame is used, which means that the rotor is moving in relation to the static stator, whereas a dynamic α-β reference frame is used in case of Clarke transform. This means that the machine is looked at from the stator side, where the rotor is moving in the dynamic reference frame.

The explanation of the method is very similar to the one of Park's vector approach. Implementation of the method requires the transformation phase currents (i_a, i_b, i_c) into current α and β components (i_α, i_β) which are then placed on α-axis and β-axis respectively. Even the mathematic formalization is similar, although indexes differ due to the different reference frame:

$$\begin{cases} i_\alpha = i_a \\ i_\beta = \dfrac{1}{\sqrt{3}} \left(2i_b + i_c \right) \end{cases} \tag{1.19}$$

Voltages are transformed in a similar way:

$$\begin{cases} u_\alpha = u_a \\ u_\beta = \dfrac{1}{\sqrt{3}} \left(2u_b + u_c \right) \end{cases} \tag{1.20}$$

Both Park's vector approach as well as Clarke transformation is usable in the same way. The vector patterns indicating the faulty operation of the machine are theoretically the same. Clarke transformation has been used as the fault detection method in the scope of the given thesis as it seems that usage of Clarke transformation has yielded results that are visually better traceable.

1.4   Aim of the study

This study is carried out using measurements performed on induction machines with broken rotor bars. Mostly stator voltage and current have been monitored and used as fault indicators, as those parameters are also measured online when frequency converters are used to drive the machines.

One of the aims of the study is to find a simple method to identify rotor faults in induction machines. The method must be mathematically simple and not in need of

large computational resources, so it would be possible to use it as an added algorithm in frequency converters. Clarke transformation was selected to be a sufficient and suitable diagnostic method.

Second aim of the study is to verify, in which cases if at all, it is more sensible to use voltage instead of the traditional usage of current to identify possible faults in the machine. Thus, phase voltage was measured at all tests in addition to current both in the cases of healthy and faulty machines.

Yet another aim of the study is to show with simulations, how the fields in rotor are changing when rotor cage is being demolished bar by bar. This gives the opportunity to emphasize the necessity of condition monitoring and diagnostics of induction machines due to the possible catastrophic outcomes in case of the propagation of broken rotor bar fault in the machines.

Last, but not least, one of the aims of the study is the comparison of diagnostic possibilities in case of both grid and frequency converter supply of the machines. As frequency converters are very often used to drive the induction machines, diagnostic of such setups must also be investigated, to know, how the fault patterns change due to additional harmonics and raised level of electromagnetic noise.

1.5   Scientific contribution

The doctoral thesis is based on six published journal and conference papers composed by the author of the thesis. The study was carried out during the years 2010–2014 in Tallinn University of Technology in Tallinn, Estonia. Measurements described in the thesis were performed by the author of the thesis during experiments in Ljubljana University, Slovenia in 2008 and Aalto University in Espoo, Finland in 2011. The originality of the thesis lies in the scientific and practical novelties, which are as follows:

- Clarke transformation, although historically left aside due to former problems of possible automization of the diagnostic process, which was not yet achievable because of computational possibilities, proves to be a sufficient method to decide upon the state of the machine;

- stator voltage can be effectively used as a fault indicator of induction machine rotor failures. This proves to be most efficient when the machine is connected to a weak grid or driven through a frequency converter using scalar control, in which case current data cannot be used;

- it is shown that in case of the usage of frequency converters, the fault pattern changes regardless of the used signal filtering and in such setups a slightly different pattern than in grid should be considered a fault indicator of induction machine broken rotor bars;

- same diagnostic procedures can be implemented with same efficiency both in case of induction motors and induction generators, which is necessary to

achieve desired power quality and supply reliability in case of small wind turbines and hydro power plants;

- simulation of broken rotor bars in squirrel-cage induction machines clearly shows that the magnetic field of the rotor will change rapidly and pose a real threat for further bars breaking, if the fault is not recognized and dealt with in time;

- feeding algorithms of Clarke transformation used in the thesis into a frequency converter is proposed, in which case online data of the state of the machine would be available and declinations from the normal operating mode could be registered.

The results of the doctoral thesis have been presented by the author at ten international conferences. Author of the thesis has published 14 international scientific papers directly linked to the thesis. Two of them are available in IEEE Xplore databases, seven listed in ISI Web of Science database and five have been published in international peer-reviewed journals.

2   MEASUREMENTS

Clarke transform was selected to be a sufficient and suitable method to indicate the broken rotor bars fault in induction machines. Therefore, all experiments and measurements are analyzed using the aforementioned method.

Measurements and necessary tests for this thesis were performed in two separate locations. The measurements of the machine with seven broken rotor bars on grid operation were conducted in Ljubljana University, Slovenia. Laboratory setup for the measurements in Slovenia is shown on Fig. 2.1. Data of the induction machine used in the experiments is presented in Table 2.1.
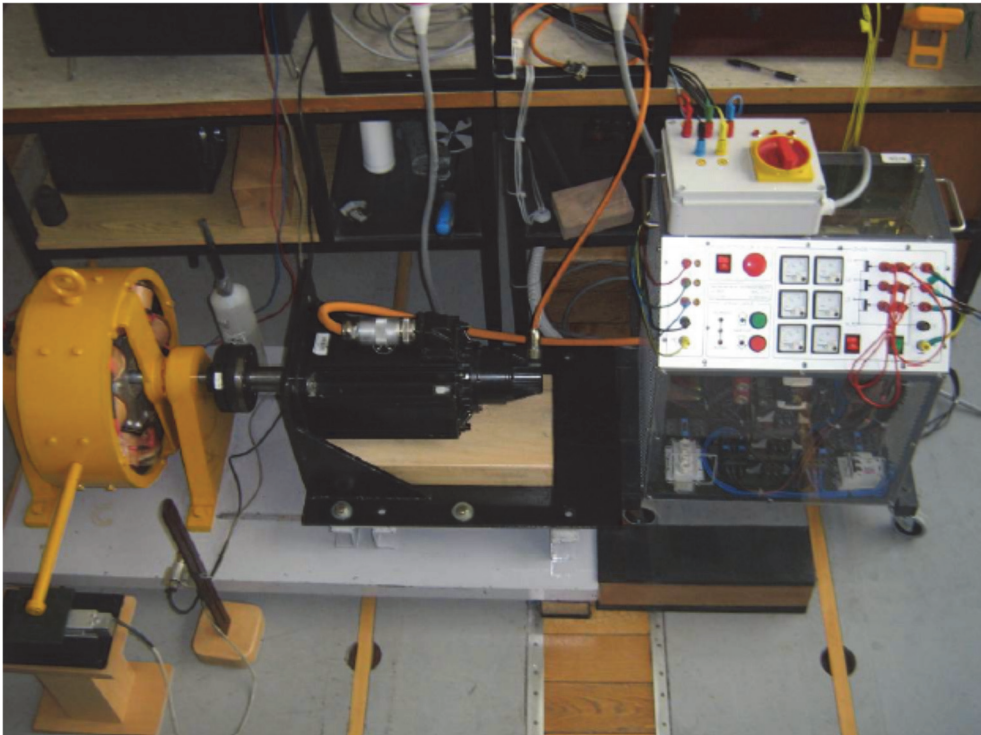
Fig. 2.1. Laboratory setup in Ljubljana University, Slovenia.

Machine was supplied directly from the grid through an autotransformer. Induction machine stator current and voltage were measured during the tests. All the measurements were made under different load conditions starting from no load and applying torque until rated load conditions were met. An electromagnetic brake was used to apply torque to the machine and the induction machine was connected to star throughout the test series. All the tests were performed using a rotor with seven broken bars situated next to each other and additionally a healthy rotor to have a reference with the healthy conditions of the tested machine. Schematic of the laboratory setup for the measurements is presented in Fig. 2.2.

Table 2.1. Data of the tested induction machine (Motor 1)

Parameter	Symbol	Value
Rated voltage	U_n	177 V
Rated current	I_n	14.8 A
Rated speed	n_n	1456 rpm
Rated power	P_n	3 kW
Frequency	f	50 Hz
Power factor	$\cos\varphi$	0.785
Number of poles	p	4
Number of rotor bars	Q_r	44
Number of stator slots	Q_s	36
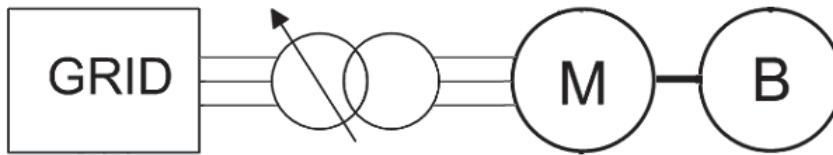
Fig. 2.2. Schematic of the laboratory setup.

The tests with the machine having three broken bars and using frequency converter supply were performed in Department of Electrical Engineering, Aalto University, Finland. Experimental setup of the studied machine used in these tests is shown on Fig. 2.3 and the data of the tested induction machine is presented in Table 2.2.
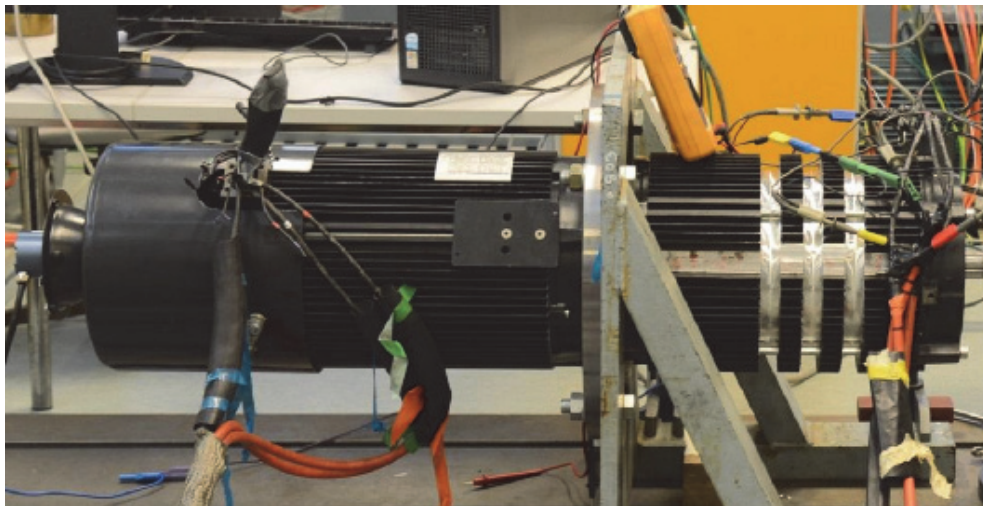
Fig. 2.3. Back-to-back mounting of the machine under investigation and the loading machine on a common mechanical support.

Table 2.2. Data of the tested induction machine (Motor 2)

Parameter	Symbol	Value
Rated voltage	U_n	400V@60 Hz; 333V@50 Hz
Rated current	I_n	41 A
Rated speed	n_n	1680 rpm@60 Hz; 1400 rpm@50 Hz
Rated power	P_n	22 kW@60 Hz; 18 kW@50 Hz
Frequency	f	50–60 Hz
Power factor	cosφ	0.860
Number of poles	p	4
Number of rotor bars	Q_r	40
Number of stator slots	Q_s	48

During these measurements the machine was supplied from the grid through an ABB ACSM1-04 frequency converter. Scalar control was used for driving the machine. The machine was loaded using an identical machine in generator mode and the machine was connected to star during the testing period. The two machines were coupled in a back-to-back configuration through their shafts and mounted on the same mechanical support. The DC-links of the frequency converters were connected in parallel and only the power losses from both machines and frequency converters were drawn from the grid.

As in the previous case, stator current and voltage was measured during different load conditions and in addition to the broken rotor with three broken bars, an identical healthy rotor was used for the experiments. Schematic describing the experimental setup is presented in Fig. 2.4.
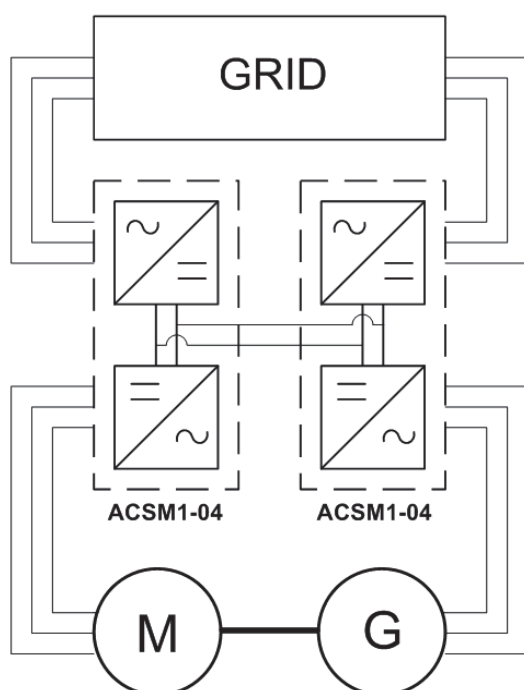
Fig. 2.4. Schematic of the experimental setup.

The machine under investigations was fed from a sinusoidal voltage supply at 50 Hz, whereas the loading machine was fed from a frequency converter to allow for different levels of loading. The electrical quantities of the machine, such as the current and phase voltages were measured separately using a Dewetron transient recorder.

3 RESULTS

The results on the conducted measurements and experiments are divided into two separate chapters, so that grid operation test results and frequency converter operation results would not be confused. However, these chapters have only the overviews of the obtained results. More comprehensive explanation of the measurement results and their analysis can be found in [V]. Generator mode tests and results of the same setup are presented in [VI].

3.1 Grid operation

Detection of broken rotor bars fault in grid supplied induction machines has been described numerously in related literature and is a quite deeply investigated and explained procedure compared for example to the closed-loop drives. As no switching frequencies or additional noise from driving converters influence the induction machine faulty conditions are usually clearly visible.

In the grid operation tests, an induction motor with a healthy rotor and a rotor with seven consecutive broken bars was used. The consecutive location of the broken bars is most probable case in practice and the asymmetry in such case is more severe. It should be also noted that the tested machine had a die-cast aluminum cage, which is prone to bad casting and thus could present several broken bars not only at operation but right away after the manufacturing process.
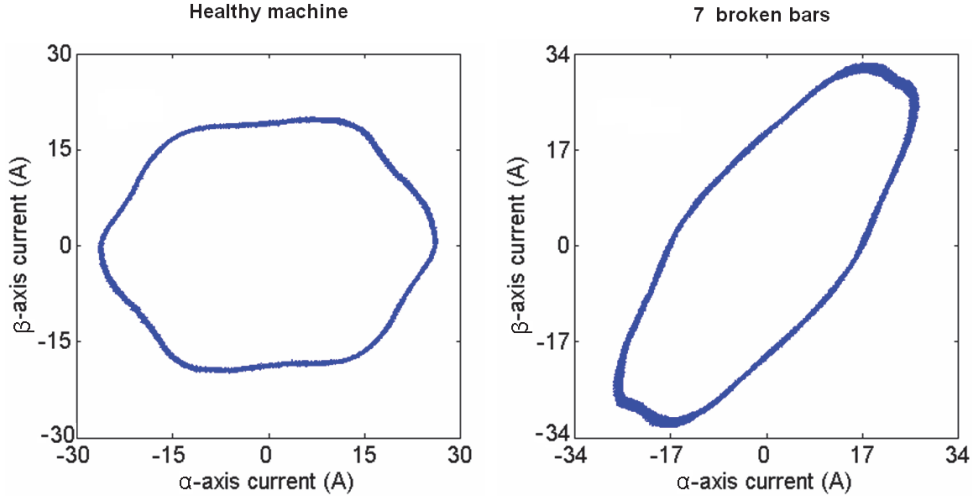
Fig. 3.1. Stator current Clarke vector patterns in case of healthy and faulty machines fed from the grid.

From the presented Figs. 3.1 and 3.2 [V], it can be seen that, there are some unexpected curves and declinations from the expected vector pattern. This is explained by the supply voltage used during the tests. As the supply was not exactly sinusoidal, the deviations from ideal sinusoid can also be traced in the resulting

figures. However, this phenomenon can be left aside, as the healthy and faulty conditions of the motor are clearly visible from the figures regardless of the imperfection in the grid supply.

As Fig. 3.1 shows [V], the healthy motor Clarke vector current pattern has indeed a more or less circular shape and the faulty one looks more close to an ellipse as referred to in the literature [58]. In addition, it was found that the absolute value of current is higher in the case of faulty motor, which was also expected prior to the testing. Faulty case can be traced easily in the full load figures as well, due to the major differences in the pattern shape of healthy and faulty conditions. If one compares the figures of no load and full load operations, it can also be clearly seen that the current amplitude rises as more torque is applied to the machine.
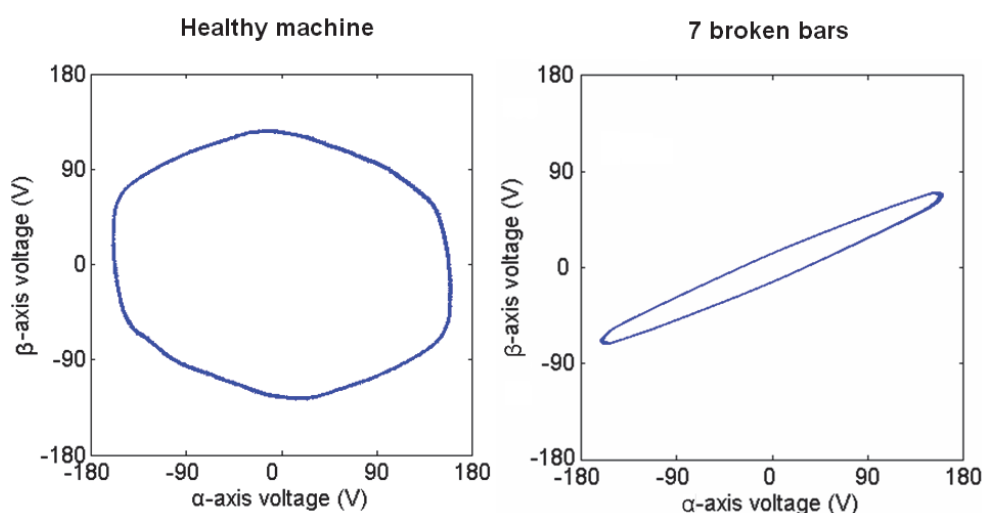
Fig. 3.2. Stator voltage Clarke vector patterns in case of healthy and faulty machines fed from the grid.

The voltage pattern of the healthy motor presented in Fig. 3.2 [V] looks again more as a circle and that of the faulty motor more like an ellipse. Such a dramatic change would not be expected if the supply network was enough rigid to withstand to effect of fault in the motor. Furthermore, changes in scale are more drastic and better traceable in case of the voltage graphs. Additionally, from the healthy case graph it can be seen that deviations due to the non-ideal sine voltage supply are not so vivid in the voltage case. The experiments conducted by the author of the given thesis using a different supply grid have shown that in case of a rigid and strong grid, almost no changes in the voltage pattern can be traced. In such circumstances, detection of faults using the traditional current pattern must be preferred.

3.2 Frequency converter operation

Most of the inverter-fed drives monitor and control the speed of the drive [65]. As frequency converters and other power electronic converters influence the machine current and voltage data, it soon became obvious that diagnostic methods, once developed for line-fed motor drives, are no longer effective in inverter-fed applications [65], [66]. When a certain type of fault occurs in such a drive, the control method of the inverter tries to preserve the normal operation of the machine. This leads to hindering and masking of the traditional fault indicators as sub-harmonic components in the current spectrum of the machine, mechanical oscillations etc.

In case of inverter fed drives, the electrical source can be looked at as a current or voltage source. Specification of the source nature depends upon the used control method of the drive. In the first case, the fault information would be contained in a voltage pattern applied to the stator terminals, whereas in the second, it appears in a current signature [65].

Regarding this phenomenon, several methods for induction machine fault detection have been combined with employed speed control scheme [66]–[68], which are usually relaying on the spectral analysis. In [66] the frequency spectrum of the stator magnetizing current is used to detect the fault, while in [67] and [68] the rotor flux is the indicator of induction machine fault. Such approaches tend to have the same limitations, namely, they are method specific and depend upon the accurate model of the machine [69]. To overcome these drawbacks and to be less dependent on the specific machine models, methods based on the observation of voltage signals have been proposed [65], [69].

Test results of the motor driven through a frequency converter in the frame of this dissertation are presented in [V]. The tested motor was supplied from the grid through ABB ACSM1-04 frequency converters and scalar control was used for driving the machine. Loading of the motor was performed using an identical machine in generator mode and the tested motor was connected to star during the testing period. The DC-links of the frequency converters were connected in parallel and only the power losses from both machines and frequency converters were drawn from the grid.

It can be seen from the test results presented in Fig. 3.3 [V] that there is a significant amount of noise in the stator signal pattern of the machine when it is driven though a frequency converter. This noise can be explained by the behaviour and peculiarities of the frequency converter operation. Frequency converters, due to slightly time-varying supply frequency and switching frequencies, induce additional harmonics to the current spectrum of the machines, which raises the amount of noise in the stator current and voltage spectra of the machine. Additionally, those induced harmonics will reduce or even hinder the sideband frequencies that are used as fault indicators for the detection of rotor faults. The severity of the noise amount is emphasized with the fact that the same filtering level was used for analyzing the results of grid supply tests and frequency converter tests presented in [V].
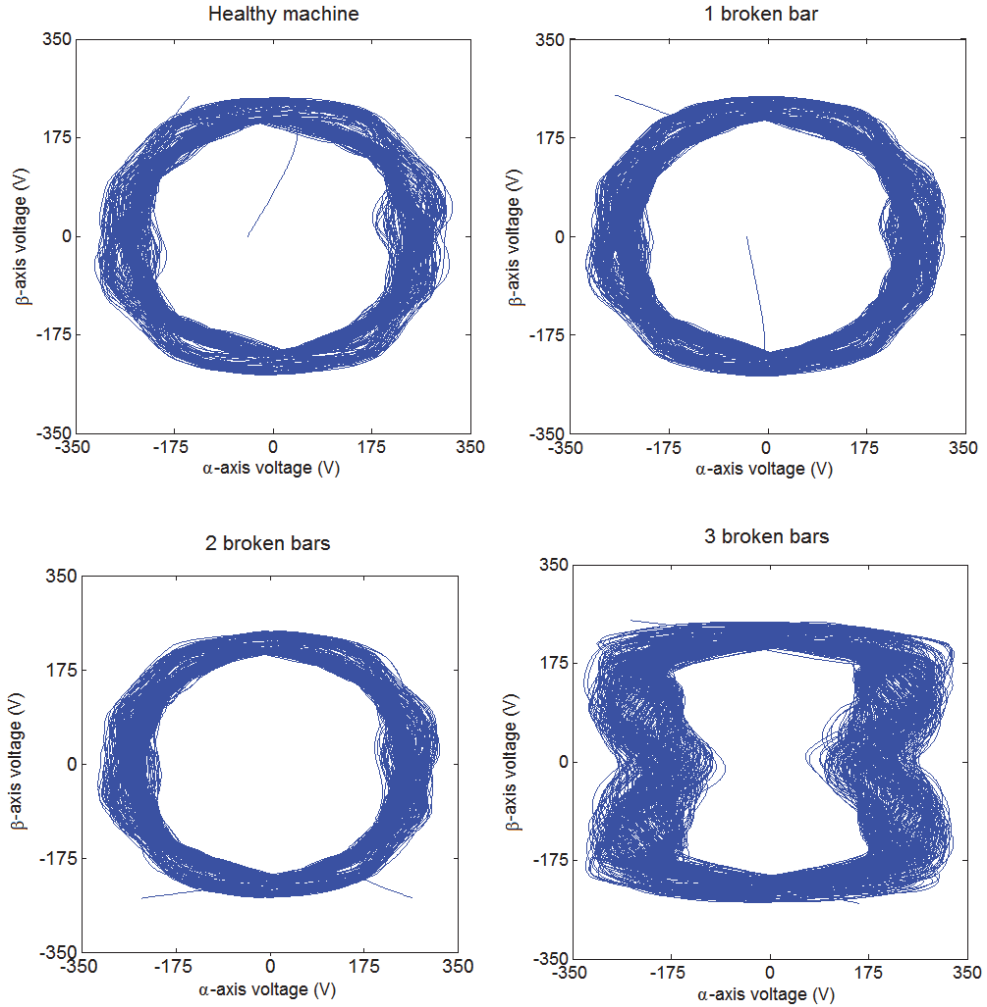
Fig. 3.3. Stator voltage Clarke vector patterns in case of different number of broken rotor bars when the machine was fed from a frequency converter.

However, changes in the faulty rotor machine stator voltage pattern are evident even irrespective to the vast amount of noise and additional harmonics. The faulty case can clearly be segregated from the healthy rotor case when the three broken bars fault is observed. In a number less than three broken bars (or less than 7.5% of the whole rotor case) the fault indicators become less evident and cannot be undoubtedly recognized by the human eye, as it becomes impossible to segregate an evident fault from fluctuations of the grid and other similar noise inducing phenomena. For the detection of faults in such cases, more precise pattern recognition method should be used. The stator voltage patterns in case of different severity levels of the broken rotor bar fault are presented in Fig. 3.3.

Similar results as measurements have shown for the diagnostics of induction motor driven with a frequency converter have been obtained also using the machine in generator mode. These results are very important, as many small scale wind applications as well as hydro power plants are equipped with induction generators. As the world is moving towards broader use of distributed energy generation and smart grid technologies, extensive emerging of such small scale power plants can be expected. To ensure needed power quality and desired supply reliability, condition monitoring of such setups will be of utmost importance in the near future.

Results of the generator mode tests are described in [VI]. However, the author must apologize for the improper use of the method definition (Park's vector instead of Clarke transformation) in that paper. As the methods are quite similar, having just few, but theoretically and mathematically relevant variations, they were at the time mixed up by the author due to inadequate knowledge in the field.

4   SIMULATION OF THE ROTOR FAULT

Breaking of induction machine rotor bars lead to local saturation around rotor teeth near the broken bars, as well as undesired asymmetrical distribution of the magnetic field in the whole machine. Therefore the study of asymmetrical distributed magnetic field of induction motors is a very significant part of the diagnostic procedure as the basis of any reliable diagnostic method is of the electric, magnetic and mechanical behavior of the machine in healthy state and under fault conditions [70].

Propagation of broken rotor bar fault in induction machines will force the magnetic field in the machine to become asymmetrical due to the lack of induced currents in the broken rotor bars. This leads to the local saturation in stator and rotor teeth near broken bars and disproportional distribution of magnetic field in the air-gap [70]. It can trigger several electromagnetic phenomena like increase of higher harmonic components, development of inverse magnetic field, torque pulsation, unbalanced magnetic pull etc. [39].

The aim of magnetic field simulations of the machine in the diagnostic point of view is to foresee and predict the changes in machine performance due to faulty conditions of the machine. Simulation results represent the contribution to the correct evaluation of the measured data in diagnostic procedures which are the important part of supervision systems based on expert systems and artificial intelligence methods [70]–[73]. The main reason for using magnetic field simulations in the scope of the given dissertation is the explanation of broken rotor bar fault propagation and its effect on the magnetic field distribution of the machine.

The necessity to detect the fault in an early stage, to prevent further damage of the equipment due to fault propagation, is one of the most important features of any condition monitoring or diagnostic techniques. At the same time, minor faults and early stages of the propagating fault are less obvious to detect and are significantly harder to grasp [65].

4.1   Simulation procedure

Simulation of the induction machine rotor fault is based on the modelling of the machine itself. Finite element method (FEM) is used for modelling of the machine and faulty conditions of the rotor bars. For the modelling of magnetic field flux density distribution in case of broken rotor bar fault of an induction machine, the same motor as in previously presented experiments was used (Motor 2).

The electromagnetic analysis is carried out in the cross section of the electrical machine using the 2D finite element (FE) approach with the time stepping scheme. The FEM is based on the A-Φ formulation of the magnetic field equations coupled with the winding circuit equations. The time integration is based on the Crank-Nicholson method.

The induction machine is considered as a quasi-static magnetic system where the Maxwell field equations altogether with the material laws reduce to

$$\nabla \times \mathbf{E} = -\frac{\partial \mathbf{B}}{\partial t}, \tag{4.1}$$

$$\nabla \times \mathbf{H} = \mathbf{J}, \tag{4.2}$$

$$\mathbf{H} = \nu \mathbf{B}, \tag{4.3}$$

$$\mathbf{J} = \sigma \mathbf{E}, \tag{4.4}$$

where $\mathbf{B}$ is the magnetic flux density, $\mathbf{E}$ the electric field strength, $\mathbf{H}$ the magnetic field strength, and $\mathbf{J}$ the current density. ν is the magnetic reluctivity of the material and σ its electric conductivity.

Using the vector potential $\mathbf{A}$ and the reduced scalar potential Φ defined by

$$\mathbf{B} = \nabla \times \mathbf{A}, \tag{4.5}$$

$$\mathbf{E} = -\frac{\partial \mathbf{A}}{\partial t} - \nabla \Phi. \tag{4.6}$$

The equation for the vector and scalar potentials reduces to

$$\nabla \times \left(\nu \nabla \times \mathbf{A} \right) = -\sigma \frac{\partial \mathbf{A}}{\partial t} - \sigma \nabla \Phi. \tag{4.7}$$

The stator and rotor cores of the machine are laminated and their conductivities are set to zero, resulting in the right hand term of Equation 4.7 vanishing for these regions. The reluctivity ν of the core material is represented in the software as a nonlinear function of the magnetic flux density in the form of a cubic spline. In conducting regions (except lamination) such as the rotor bars and stator windings, the reluctivity is set to that of vacuum and the gradient of the electric scalar potential can be defined as

$$\nabla \phi = -\frac{u}{l} e_z, \tag{4.8}$$

with u being the voltage over the conductor and l its length. Integrating the current density over the cross-section of the conductors leads to a relationship between the voltage u, the current i and the DC-resistance R as

$$u = Ri + R \int_s \sigma \frac{\partial A_z}{\partial t} \cdot dS, \tag{4.9}$$

where for 2D case only the z-component A_z of the vector potential is used as the other components are null.

The stator windings and rotor cage circuit equations are formed by applying Kirchhoff's laws and Equation 4.9. The end windings of the stator and rotor being ignored by the 2D field analysis are accounted for in the simulations through constant impedances in series with the 2D representation of the windings. For the stator windings, the current density is assumed uniform on each coil side in the slot area. This simplifying assumption is justified by the use of parallel and series connected thin wires to manufacture such a winding. It should be mentioned that in case of form-wound coils, the skin and proximity effects should not be ignored and thus an approach similar to the one used in [74] is to be adopted. The circuit equations from the stator and rotor windings are solved altogether with the magnetic and displacement field equations simultaneously at each time step.

In the given analysis, the magnetic forces form the load term for the mechanical problem. The magnetic forces are computed from the solution of the magnetic field at each iteration, applying a local version of the principle of virtual work, which results in local forces known as generalized nodal forces [75]. The equation to compute these forces is:

$$F^T = -\int_{\hat{S}_e} \left[\nu \nabla A_z \cdot \frac{\partial}{\partial \mathbf{U}} (\nabla A_z) |G| + \int_0^B \mathbf{H} \cdot d\mathbf{B} \frac{\partial}{\partial \mathbf{U}} (|G|) \right] d\hat{S}_e, \qquad (4.10)$$

where G is the Jacobian matrix for the transformation from the reference finite element to the actual one. $\hat{S}_e$ stands for the reference element and $\mathbf{U}$ the vector of virtual displacements of each node. The integration with respect to magnetic flux density in Equation 4.10 as well as the differentiation with respect to displacements is made analytically and implemented in the FE software. For this purpose and for FE iteration purpose, a cubic spline representation of the HB-curve of the iron sheets is used.

The computation of the electromagnetic torque is also based on the principle of virtual work as presented in [76]

$$T = \sum_{airgap-elements} \int_{\hat{S}_e} \left[\nu \nabla A_z \cdot \frac{\partial}{\partial \Theta} (\nabla A_z) |G| + \int_0^B \mathbf{H} \cdot d\mathbf{B} \frac{\partial}{\partial \Theta} (|G|) \right] d\hat{S}_e, \qquad (4.11)$$

with all the quantities as in Equation 4.10 and Θ the angular position.

The displacement field in the stator region of the induction machine is formulated according to the procedure presented in [77], where the total internal virtual work is equated to the total external work according to

$$\int_V \bar{\varepsilon}^T \tau dV = \int_V \overline{\mathbf{U}}^T \mathbf{f}^B dV + \int_S \overline{\mathbf{U}}^T \mathbf{f}^S dS + \sum_i \overline{\mathbf{U}}^{iT} \mathbf{F}^i, \qquad (4.12)$$

where ε is the strain tensor, τ the stress tensor, $\mathbf{f}$ the local force vector (the super-scripts B and S stand respectively for surface and body forces), and $\mathbf{F}$ the vector of

total forces acting at some discrete locations. The dash over the quantities stands for virtual quantities as required by the principle of virtual work. The inertia and damping forces are included in Equation 4.12 as body forces, which are functions of respectively the acceleration and the velocity. From Equation 4.12 we obtained a second-order time-differential equation for the elastic field problem. The solution of such an equation is achieved using the three point recurrence schemes as presented by Zienkiewicz [78].

The mechanical problem is solved in the stator of the machine only and the boundary conditions are set so that the circumferential displacements on the outer surface of the stator are zero. This condition ensures the non-singularity of the system matrix without introducing nonphysical excessive local stresses. Such a boundary condition is implemented in the FE-package in a procedure similar to the one presented in [77] by transforming the related unknowns and the stiffness and damping matrix terms from Cartesian to polar coordinate system. The elastic and magnetic field equations are discretized and solved following a standard FE procedure.

Based on this, the fault propagation in the given thesis is modelled from healthy rotor cage up to three consecutive broken bars (which is 7.5% of all the rotor bars of the machine). The broken bars were modelled as areas with significantly higher resistance and low conductivity, so they would not contribute to the cage circuit [79], [80]. Simulation results are described in [III]. Parameters used in the simulation of the machine are presented in Table 4.1.

Table 4.1. Parameters used in the simulation of the machine

Parameter	Value
Total simulated time	2.0 s (60000 time-step)
Time step length	0.0333 ms
Number of elements (mesh)	5328
Number of nodes (mesh)	3431
Stator temperature	120 °C
Rotor temperature	140 °C

4.2   Simulation results

From the performed simulations it was found as expected that presence of broken rotor bars results in uneven distribution of magnetic field in the rotor cage and the whole machine. Magnetic field density starts increasing around the broken bar in the rotor and also in stator facing the broken bar. In addition to that, the magnetic field density also starts increasing on the opposite side of the broken rotor bar and even in the shaft of the machine.

As it can be seen from Fig. 4.1 [III], the difference in the magnetic flux density distribution between the healthy machine and the ones with one to three consecutive broken bars corresponds to an asymmetric two poles field inducing eddy-currents in the shaft of the machine. Such current if free to circulate, will cause bearing currents that usually result in damaging the bearings. It should however, be noted that since the simulations are 2D ones, they do not account for the unipolar flux circulating through the shaft and thus slightly over estimate the induced currents.

SHADING: FLUX DENSITY DISTRIBUTION

0.00 T   0.40 T
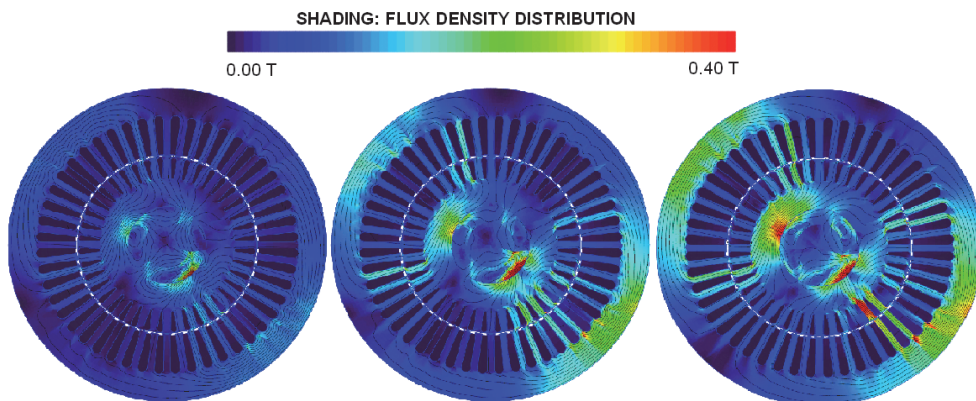
Fig. 4.1. The computed difference in the magnetic flux density distribution between the healthy machine and the ones with one to three consecutive broken bars at full load. The plot corresponds to the last time step. Left – difference between healthy and one broken bar case; middle – difference between healthy and two broken bars case; right – difference between healthy and three broken bars case.

When the fault propagates and the number of broken bars in the rotor cage increases, the magnetic field asymmetry is rising, resulting in higher local saturation in both rotor and stator teeth. Uneven magnetic field distribution starts affecting the machine phase voltage, resulting in the presence of higher harmonic components in the voltage spectrum. With increase of the number of consecutive broken bars, higher harmonic amplitude in phase voltage is also increasing, which means that various disturbances and undesired phenomena (i.e. increase of acoustic noise, increase of mechanical vibrations etc.) can be expected.

The computed vibration displacements of a node on the outer surface of the stator shown in Fig. 4.2 are compared with the measured ones shown in Fig. 4.3. The results are very close to each other except for some additional frequencies due to the 3D effects, which are not accounted for in the simulations such as the additional stiffness of the endplates and axial modes.
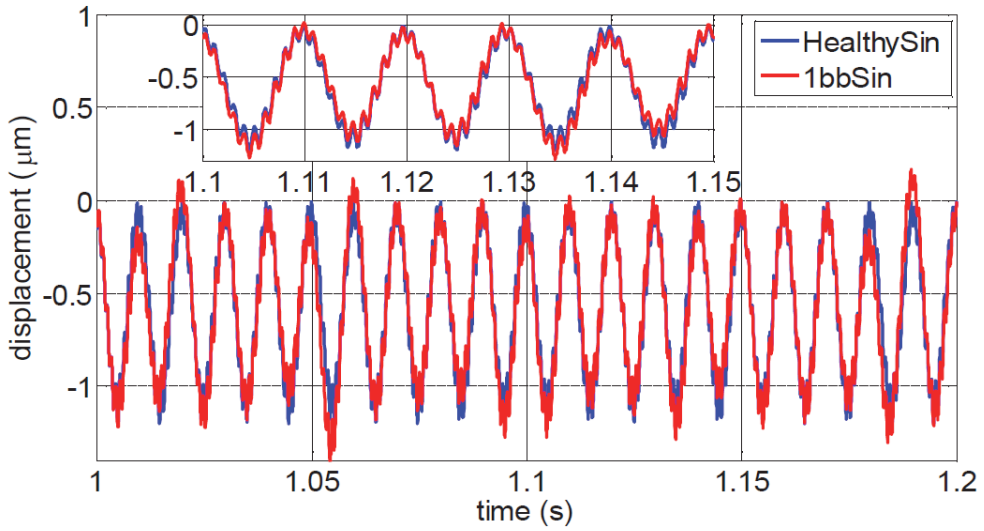
Fig. 4.2. Simulated radial displacements of a node on the outer surface of the stator core under healthy and one broken bar operation. The slotting effect and the modulation to the broken bar can be easily seen in the vibrations.
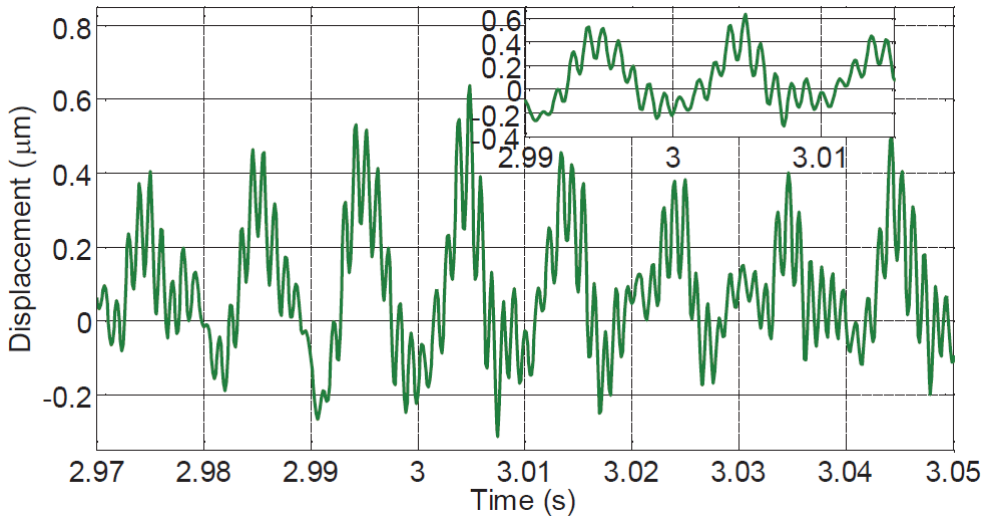
Fig. 4.3. Measured displacements under one broken bar operation at full load. Some additional frequency components are observed due to the 3D effects.

The computed spectrum of the current is shown in Fig. 4.4 and the spectrum of the torque is shown in Fig. 4.5. Both quantities as well as the phase voltages, not shown here, show strong increase in many frequencies and a substantial increase of the floor of the spectrum. Special attention is paid to the side-band frequencies around the fundamental harmonic and these around the principal slot harmonic. The broken rotor bar fault is also strongly seen in the vibration as shown in Fig. 4.6.
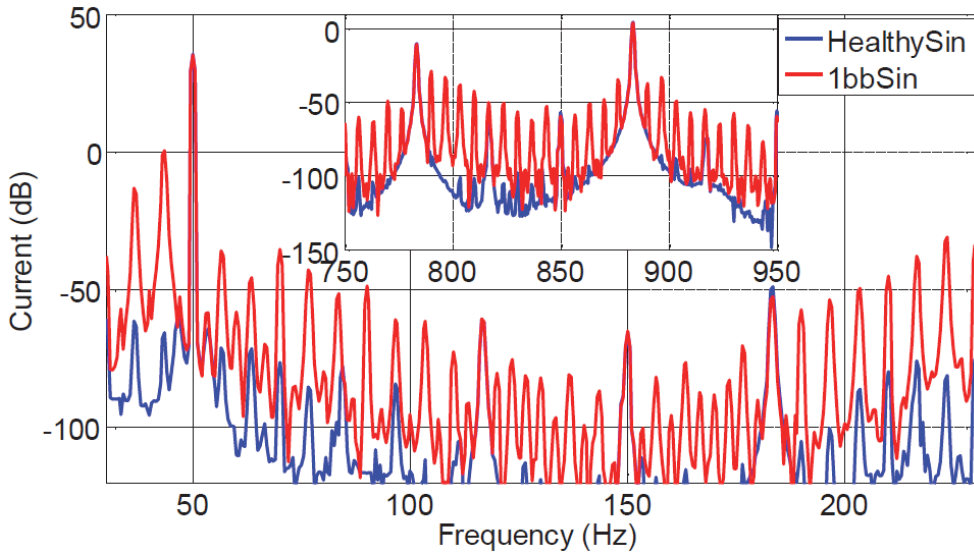
Fig. 4.4. Simulated spectrum of the stator current under healthy and one broken bar operation at full load.
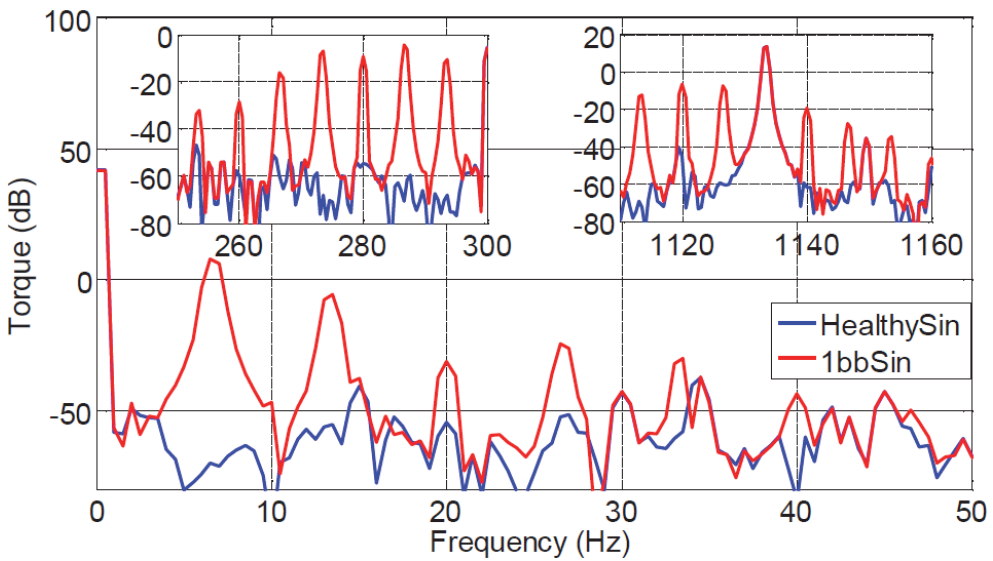
Fig. 4.5. Simulated spectrum of the torque under healthy and one broken bar operation at full load.
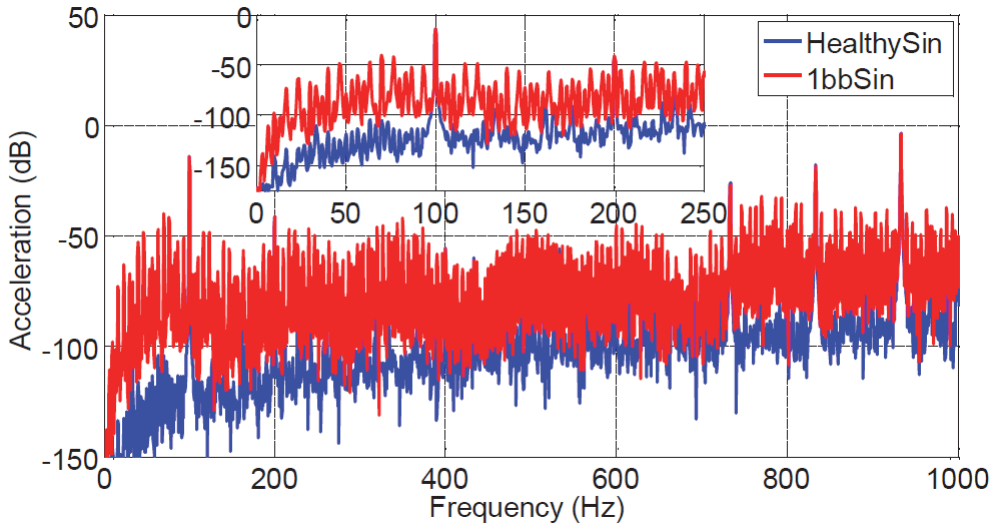
Fig. 4.6. Simulated spectrum of vibration acceleration under healthy and one broken bar operation at full load. A substantial increase in the floor level of the spectrum is noticed at faulty operation. Such increase is also seen in the current spectrum (Fig. 4.4).

Based on the magnetic field distribution Fig. 4.1, which are also presented in [III], it can be estimated that broken rotor bars fault can lead to severe consequences if the fault is not dealt with in an early stage. The propagation of the fault will not only result in the destruction of the rotor cage but can also lead to various stator failures (i.e. stator winding turn to turn short circuits, lamination short circuits etc.) due to the broken rotor bar influenced local saturation in and around stator teeth.

5 DISCUSSION

If one would choose the proposed method to be suitable for diagnostics of electrical machine, one must first set the desired results of the fault detection procedure. It is undoubtedly clear that non-invasive diagnostic methods are to be used as such procedures do not raise the necessity of disturbing the working cycle of the electrical machines under diagnosis.

Most of the non-invasive diagnostic techniques described in scientific papers and researches are MCSA related methods. The main problem with most of such methods is the complexity of the calculations, which means that many of the methods need excessive computational resources to solve the needed algorithms, before any analysis can be performed. This sets boundaries to the usability of the methods, as the algorithms cannot be implemented in various small measurement equipment or control devices themselves. The carrying idea behind the choosing of the method described in this thesis was to find a method mathematically as simple as possible, so that minimal amount of computational resources would be needed to implement the method. Simplicity and low resource demand of the proposed method broadens the usability area of the method as it can be used in a wider range of devices.

Another drawback of many MCSA related methods is the fact that their usage is often connected to the knowledge of certain machine models. This again sets boundaries as such methods are not universal enough to be used in any emerging case without knowing the peculiarities of the tested setup. In case of the proposed method, this will not be a problem. As the method can be used for analyzing both current and voltage, and both of the parameters are often measured together, it can be used in a number of possible setups. When the electrical machine under investigation is connected to a weak grid or is driven through a frequency converter using scalar control, voltage pattern would be the fault indicator. If the machine is connected to a strong grid or inverters with different control methods are used, so that the failures are not visible in the voltage pattern, those faults can be found observing the current spectrum of the electrical machine.

Segregation of the fault can also be a problem with a number of MCSA techniques. In case of proposed method, it might also be so. Relying on the literature, it can be said that in certain situation, the nature of the fault should be possible to segregate, but as this was not in the scope of this dissertation, no practical investigation regarding fault segregation has been performed by the author. Yet it has been found based on literature and practice, that using the method, segregation of a faulty machine from the healthy one is possible.

On the other hand, fault segregation is often overemphasized by the academic community. In industrial practice, it is often not that important. The segregation of rotor faults from stator faults are no doubt needed also in case of industrial machines, but being as precise as to localize the faulty stator phase or the exact position or number of broken bars, often has low practical value. When a machine

is diagnosed with a rotor or a stator fault, the whole winding will be changed during the reparation of the machine. The further specification and localization of the fault might be useful in rare occasions or special machines (either very large or using special materials for windings), when the change of the whole stator or rotor winding is economically not reasonable.

Using the method described in the dissertation enables the detection of the fault in a relatively early stage (7.5–10% of broken rotor bars). This is important, as the propagation of the fault may lead to irreversible damage to the machines. Cascading rotor bar fault will not pose threat only to the rotor cage of the machine, but as magnetic field simulations have shown, also saturate stator teeth opposing the broken rotor bars. This may easily lead to various stator faults and even further damage to the machine.

It can be concluded, that although drawbacks and uncertainties exist, usage of the method for condition monitoring of electrical machines will lead to early detection of the faults. This also means the rising of overall reliability of the setups where the method is used, possibly lower economical risks in case of failures and safer working environment for the people manipulating the electrical machines.

6   CONCLUSION AND FUTURE WORK

Conducted experiments and analyses show that although traditionally used for transformation of current data, Clarke's transform can be very effectively used for transformation of three-phase voltage. For diagnostic purposes this might be a better use of the method, as in the case of voltage, load conditions, as well as deviations of supply voltage do not have as high effect on the outcomes as in the case of current. In some cases such as machines that are equipped with frequency converters using scalar control, monitoring of voltage would in fact be the only option for such diagnostics as stator current signals in such setup do not show any fault patterns.

If the figures of stator current and voltage patterns in both load conditions of the machine with direct grid supply are observed, it can be seen that voltage graphs do not have alterations in amplitude when load is changed. This peculiarity of voltage patterns gives the opportunity for better and more precise decisions as healthy and faulty case data can be compared without any changes or recalculations of amplitudes.

When diagnostics via the comparison of induction motor performance models is desired, the described method could be used in a sufficiently effective way to decide upon the state of the motor. The needed information is the model or figure of the healthy case of the motor, which would also be the master model, to which other graphs would be compared to. It could prove to be a very good way for performing diagnostics also in the sense that no disturbance in the working cycle of the motor is needed in order to perform the needed measurements and analysis.

Frequency converters, due to slightly time-varying supply frequency, induce additional harmonics to the current spectrum of the machines, which reduces or even hinders the sideband frequencies that are used as fault indicators. Also they create more noise in the signals, which makes detection of the fault more complicated.

Simulation of the fault showed significant local saturation in and around rotor and stator teeth in the vicinity of the broken rotor bars. This phenomenon may lead to further occurrence of failures, such as stator winding turn to turn short circuits, lamination short circuits, which in such case would not be the primary failures but already resulting faults due to the propagation of the initial broken bar fault. Another easily traceable problem is the occurrence of eddy-currents in the shaft of the machine induced by the asymmetric two poles field. Such current if free to circulate, will cause bearing currents that usually result in damaging the bearings, which again lead to failures starting initially from the cracking and breaking of the rotor bars. Such results of simulation lead to the possibility that the statistically more probable faults in bearings and stator may not always be the initial faults themselves, but the results of broken rotor and the initial rotor bar problem might sometimes be overlooked during the maintenance and repair of the machines.

Further study in the field is needed to find more accurate and effective solutions to detect faults in machines driven through frequency converters. Furthermore, investigation is needed for better understanding the impact of frequency converters to the Clarke vector pattern of stator voltage. Clarke transformation seems to be a sufficient method of detecting a fault in induction machines regardless of the supply, but segregation of the nature of the fault requires more investigations.

It is essentially necessary to analyze the possibilities of using similar diagnostic methods in case of machine with lesser faults, such as one or two broken or even cracked bars. This would bring better understanding to at which level of the fault proposed methods would be usable.

To segregate the broken rotor bar fault from other possible failures of the machine, possibilities of classification and analysis of features or symptoms should be investigated. Features such as different fault signals, machine parameters, conditions under which the machine is used etc., could prove essentially important to decide in a quick way, where are the probabilistically vulnerable areas and grant a pre-diagnostic segregation possibility of the fault.

Attention should also be paid to implementation of pattern recognition techniques on the healthy and faulty rotor patterns to achieve a degree of automation to the diagnostic process. Automation of the process would grant the possibility of feeding diagnostic algorithms to a frequency converter and thus make online condition monitoring easier, as most of machines in use today are equipped with such devices, which measure and control supply voltage and current at all time. Mathematically simple and computationally easy diagnostic procedure would not need excessive amounts of memory and energy of frequency converters and would be possible to implement.

7   ABSTRACT

The main purpose of this thesis is to analyze and improve existing induction machine diagnostic methods. The aim was set to find a simple mathematical method that could be implemented to an induction machine to evaluate the state of the machine, bearing in mind that the working cycle of the machine would not be interrupted and some automization of the diagnostic procedure could be possible in future.

There are many possible failures that can affect the performance of electrical machines. Online diagnostic makes detection of the faults easier and in some cases even may lead to prevention of failures. Minor faults can seem unimportant at the beginning, but when problems are not dealt with, failures can lead to catastrophic measures. In that way condition monitoring makes it possible to detect the faults in such an early stage, when repairing of the machines is still possible or reasonable. Also it would help to differentiate the deviations and harmonic distortions in the grid from the faulty cases of the machines.

Furthermore, as the world is moving towards smarter grids and dispersed generation, condition monitoring of electrical machines is becoming more important. Monitoring becomes necessary to keep a certain electric power quality and supply reliability level in the new dispersed and dynamic systems where many small generation units such as small hydro and wind power plants are integrated.

In this thesis induction machine broken rotor fault diagnostics has been investigated. The tests have been performed on different machines, both in motor and generator regime, using different supply setups (straight from the grid and through frequency converters) and different severity of the fault. Clarke transformation has been selected to be the sufficient diagnostic method in this thesis. Both stator voltage and current have been used as indicators of the fault while performing the diagnostic procedures, comparison of which has also been presented in the thesis.

The conclusions of the thesis show that diagnostic of induction machines performing responsible tasks is undoubtedly important and necessary procedure that must not be forgotten. It raises the reliability of the machines and, depending where the machines are used, it can raise even the supply reliability of customers. Also, diagnostic helps to raise the life span of the machines and helps to avoid unnecessary safety and economical risks for the machine users. It has also been shown, that frequency converters add additional harmonic components to the classical current (or voltage) spectrum of the machines, which makes the decision upon the state of the machine more difficult.

The necessity of further work on the topic has been pointed out. Some of the tasks in future would involve segregation of the nature of the fault, better understanding of frequency converter influence and behaviour in case of faulty machines as well as modeling of different faults to validate testing results.

REFERENCES

[1] K. Kim, A. Parlos, and R. Bharadwaj, "Sensorless fault diagnosis of induction motors," *IEEE Transactions on Industrial Electronics*, vol. 50, no. 5, pp. 1038–1051, 2003.

[2] I. Boldea and S. Nasar, *The Induction Machine Handbook*. Boca Raton, FL: CRC Press, 2002, 950 p.

[3] M. Benbouzid, "Bibliography on induction motors faults detection and diagnosis," *IEEE Transactions on Energy Conversion*, vol. 14, no. 4, pp. 1065–1074, 1999.

[4] J. Faiz, B. Ebrahimi, and M. Sharifian, "Time stepping finite element analysis of broken bars fault in a three-phase squirrel-cage induction motor," *Progress in Electromagnetic Research*, PIER 68, pp. 53–70, 2007.

[5] T. Lindh, *On the Condition Monitoring of Induction Machines*. Doctoral dissertation, Lappeenranta: Lappeenranta University of Technology, 2003, 148 p.

[6] R. Lawrie, *Electric Motor Manual*. New York: McGraw & Hill, 1987, 129 p.

[7] G. Stone, E. Boulter, I. Culbert, and H. Dhirani, *Electrical Insulation for Rotating Machines: Design, Evaluation, Aging, Testing, and Repair*. Piscataway: IEEE Press, 2004, 370 p.

[8] J. Lepa, *Elektrimootorite hooldamine ja kaitse*. Tallinn: Valgus, 1976, 203 p. (In Estonian).

[9] J. Niitsoo, J. Kilter, I. Palu, P. Taklaja, and L. Kütt, "Harmonic levels of domestic and electrical vehicle loads in residential distribution networks," *IEEE AFRICON 2013 Conference*, pp. 184–188, 2013.

[10] J. Niitsoo, I. Palu, J. Kilter, P. Taklaja, and T. Vaimann, "Residential load harmonics in distribution grid," *3rd International Conference on Electric Power and Energy Conversion Systems*, pp. 1–6, 2013.

[11] L. Menozzi, "Technologies for machine condition monitoring," *SDEMPED 2011 Tutorials, 8th IEEE Symposium on Diagnostics for Electrical Machines, Power Electronics and Drives*, pp. 51–88, 2011.

[12] Motor Reliability Working Group, "Report of large motor reliability survey of industrial and commercial installations, Part I," *IEEE Transactions on Industry Applications*, vol. IA-21, no. 4, pp. 853–864, 1985.

[13] Motor Reliability Working Group, "Report of large motor reliability survey of industrial and commercial installations, Part II," *IEEE Transactions on Industry Applications*, vol. IA-21, no. 4, pp. 865–872, 1985.

[14] Motor Reliability Working Group, "Report of large motor reliability survey of industrial and commercial installations, Part 3," *IEEE Transactions on Industry Applications*, vol. IA-23, no. 1, pp. 153–158, 1987.

[15] M. Benbouzid, "A review of induction motor signature analysis as a medium for faults detection," *International Conference of the IEEE Industrial Electronics Society*, vol. 4, pp. 1908–1913, 1998.

[16] O. Thorsen and M Dalva, "A survey of faults on induction motors in offshore oil industry, petrochemical industry, gas terminals, and oil refineries," *IEEE Transactions on Industry Applications*, vol. 31, no. 5, pp. 1186–1196, 1995.

[17] P. Albrecht, J. Appiarius, R. McCoy, E. Owen, and D. Sharwa "Assessment of the reliability of motors in utility applications – updated," *IEEE Transactions on Energy Conversion*, vol. EC-1, no. 1, pp. 39–46, 1986.

[18] G. Kliman, W. Premerlani, B. Jazici, R. Koegl, and J. Mazereeuw, "Sensorless, online motor diagnostics," *IEEE Computer Applications in Power*, vol. 10, no. 2, pp. 39–43, 1997.

[19] D. Campos-Delgado, D. Espinoza-Trejo, and E. Palacios, "Fault-tolerant control in variable speed drives: a survey," *IET Electric Power Applications*, vol. 2, no. 2, pp. 121–134, 2008.

[20] W. Thomson and J. Gilmorer, "Motor current signature analysis to detect faults in induction motors drives–fundamentals, data interpretation, and industrial case histories," *32nd Turbomachinery Symposium*, pp. 145–156, 2003.

[21] S. Nandi, H. Tolyat, and X. Li, "Condition monitoring and fault diagnosis of electrical motors – a review," *IEEE Transactions on Energy Conversion*, vol. 20, no. 4, pp. 719–729, 2005.

[22] M. Haji and H. Tolyat, "Rotor eccentricity fault detection of a DC motor," *27th Annual Conference of IEEE Industrial Electronics Society – IECON2001*, vol. 1, pp. 591–596, 2001.

[23] M. Hajiaghajani, H. Tolyat, and I. Panahi, "Advanced fault diagnosis of a DC motor," *IEEE Transactions on Energy Conversion*, vol. 19, no. 1, pp. 60–65, 2004.

[24] S. Nandi, R. Bharadwaj, and H. Tolyat, "Performance analysis of a three-phase induction motor under mixed eccentricity condition," *IEEE Transactions on Energy Conversion*, vol. 17, no. 3, pp. 392–399, 2002.

[25] T. Kim, S. Hwang, W. Jung, and C. Kim, "Comparison of dynamic responses for IPM and SPM motors by considering mechanical and magnetic coupling," *IEEE Transactions on Magnetics*, vol. 37, no. 4, pp. 2818–2820, 2001.

[26] A. Belahcen and A. Arkkio, "Computation of additional losses due to rotor eccentricity in electrical machines," *IET Electric Power Applications*, vol. 4, no. 4, pp. 259–266, 2010.

[27] G. Dorrell, M. Hsieh, and Y. Guo, "Unbalanced magnet pull in large brushless rare-earth permanent magnet motors with rotor eccentricity," *IEEE Transactions on Magnetics*, vol. 45, no. 10, pp. 4586–4589, 2009.

[28] Y. Chin, P. Kanninen, P. Maki-Ontto, R. Sakki, and H. Lendenmann, "Phenomenon of magnetic force in permanent magnet wind turbine generators," *International Conference on Electrical Machines and Systems*, pp. 1–6, 2009.

[29] B. Ebrahimi, J. Faiz, and M. Roshtkhari, "Static-, dynamic-, and mixed-eccentricity fault diagnoses in permanent-magnet synchronous motors," *IEEE Transactions on Industrial Electronics*, vol. 56, no. 11, pp. 4727–4739, 2009.

[30] M. Hajiaghajani, L. Hao, S. Madani, and H. Toliyat, "A method for detection of eccentricity in permanent magnet machines," *38th IAS Annual Meeting and Industry Applications Conference*, vol. 3, pp. 1833–1838, 2003.

[31] W. le Roux, R. Harley, and T. Habetler, "Detecting rotor faults in low power permanent magnet synchronous machines," *IEEE Transactions on Power Electronics*, vol. 22, no. 1, pp. 322–328, 2007.

[32] A. Kallaste, *Low Speed Permanent Magnet Slotless Generator Development and Implementation for Windmills*. Doctoral dissertation, Tallinn: Tallinn University of Technology, 2013, 141 p.

[33] R. Schoen, T. Habetler, F. Kamran, and R. Bartfield, "Motor bearing damage detection using stator current monitoring," *IEEE Transactions on Industry Applications*, vol. 31, no. 6, pp. 1274-1279, 1995.

[34] J. Stack, R. Harley, and T. Habetler, "An amplitude modulation detector for fault diagnosis in rolling element bearings," *IEEE Transactions on Industrial Electronics*, vol. 51, no. 5, pp. 1097–1102, 2004.

[35] FAG Bearings Corporation, "Rolling bearing damage," FAG South East Asia PTE Ltd., 1997, Publ. No. WL 82 102/2 Esi, 71.

[36] B. Rao, *Handbook of Condition Monitoring*. Oxford: Elsevier Advanced Technology, 1996, 604 p.

[37] D. Busse, J. Erdman, R. Kerkman, D. Schleger, and G. Skibinski, "Characteristics of shaft voltage and bearing currents," *IEEE Transactions on Industry Applications*, vol. 3, no. 6, pp. 21–32, 1997.

[38] A. Bonnett and G. Soukup, "Cause and analysis of stator and rotor failures in three-phase squirrel-cage induction motor," *IEEE Transactions on Industry Applications*, vol. 28, no. 4, pp. 921–937, 1992.

[39] R. Fišer and S. Ferkolj, "Calculation of magnetic field asymmetry of induction motor with rotor faults," *1998 IEEE Mediterranean Electrotechnical Conference*, vol. 2, pp. 1175–1179, 1998.

[40] A. Siddique, G. Yadava, and B. Singh, "A review of stator fault monitoring techniques of induction motors," *IEEE Transactions on Energy Conversion*, vol. 20, no. 1, pp. 106–114, 2005.

[41] R. Tallam, S. Lee, G. Stone, G. Kliman, J. Yoo, T. Habetler, and R. Harley, "A survey of methods for detection of stator related faults in induction machines," *IEEE Transaction on Industry Applications*, vol. 43, no. 4, pp. 920–933, 2007.

[42] P. J. Rodriguez, A. Belahcen, and A. Arkkio, "Signatures of electrical faults in the force distribution and vibration pattern of induction motors," *IEE Proceedings – Electric Power Applications*, vol. 153, no. 4, pp. 523–529, 2006.

[43] R. Fišer and H. Lavric, "On-line detection and diagnostics of induction motor rotor faults using spectral analyses of stator current," *5th International Symposium on Topical Problems in the Field of Electrical and Power Engineering, Doctoral School of Energy and Geotechnology*, pp. 7–11, 2008.

[44] A. Bellini, F. Filippetti, G. Franceschini, C. Tassoni, and G. B. Kliman, "Quantitative evaluation of induction motor broken bars by means of electrical signature analysis," *IEEE Transactions on Industry Applications*, vol. 37, pp. 1248–1255, 2001.

[45] F. Filippetti, G. Franceschini, C. Tassoni, and P. Vas, "AI techniques in induction machines diagnosis including the speed ripple effect," *IEEE Transactions on Industry Applications*, vol. 34, pp. 98–108, 1998.

[46] W. Thomson and M. Fenger, "Industrial application of current signature analysis to diagnose faults in 3-phase squirrel cage induction motors," *Annual Pulp and Paper Industry Technical Conference*, pp. 205–211, 2000.

[47] G. Kliman, R. Koegl, J. Stein, R. Endicott, and M. Madden, "Noninvasive detection of broken rotor bars in operating induction motors," *IEEE Transactions on Energy Conversion*, vol. 3, pp. 873–879, 1988.

[48] J. Ramirez-Cruz, V. Garcia-Colon, F. Carvajal-Martinez, and M. Angeles, "Induction motors broken bar and eccentric gap on-line detection using motor signature current analysis under laboratory and field conditions," *Large Engineering Systems Conference on Power Engineering – LESCOPE*, pp. 65–69, 2004.

[49] M. Benbouzid and G. Kliman, "What stator current processing-based technique to use for induction motor rotor faults diagnosis," *IEEE Transactions on Energy Conversion*, vol. 18, no. 2, pp. 238–244, 2003.

[50] MathWorks: http://www.mathworks.com/help/techdoc/ref/fft.html

[51] V. Ingle and J. Proakis, *Digital Signal Processing Using MATLAB, 2nd edition*. Toronto: Thompson, 2007, 605 p.

[52] A. Da Silva and B. Upadhyaya, "Rotating machinery monitoring and diagnosis using short-time Fourier transform and wavelet techniques," *International Conference on Maintenance and Reliability*, vol. 1, pp. 1401–1415, 1997.

[53] Z. Peng and F. Chu, "Application of the wavelet transform in machine condition monitoring and fault diagnostics: a review with bibliography," *Mechanical Systems and Signal Processing*, vol. 18, no. 2, pp. 199–221, 2004.

[54] F. Auger and P. Flandrin, "Improving the readability of time–frequency and time–scale representations by the reassignment method," *IEEE Transactions on Signal Processing*, vol. 43, no. 5, pp. 1068–1089, 1995.

[55] A. Galli, G. Heydt, and P. Ribeiro, "Exploring the power of wavelet analysis," *IEEE Computer Applications in Power*, vol. 9, pp. 37–41, 1996.

[56] V. Fernão Pires, J. Martins, and A. Pires, "Eigenvector/eigenvalue analysis of a 3D current referential fault detection and diagnosis of an induction motor," *Energy Conversion and Management*, vol. 51, no. 5, pp. 901–907, 2010.

[57] M. Benbouzid, M. Vieira, and C. Theys, "Induction motors faults detection and localization using stator current advanced signal processing techniques," *IEEE Transactions on Power Electronics*, vol. 14, no. 1, pp. 14–22, 1999.

[58] A. Cardoso and E. Saraiva, "On-line diagnostics of three-phase induction motors, by Parks vector," *International Conference on Electrical Machines*, vol. 1, pp. 231–234, 1988.

[59] A. Cardoso and E. Saraiva, "On-line diagnostics of current source inverter-fed induction machines, by Park's vector approach," *International Conference on Electrical Machines*, pp. 1000–1005, 1990.

[60] A. Cardoso, S. Cruz, J. Carvalho, and E. Saraiva, "Rotor cage fault diagnosis in three-phase induction motors, by Park's vector approach," *Industry Applications Conference*, vol. 1, pp. 642–646, 1995.

[61] R. Lee, P. Pillay, and R. Harley, "D,Q reference frames for the simulation of induction motors," *Electric Power Systems Research*, vol. 8, pp. 15–26, 1984/85.

[62] A. Cardoso and E. Saraiva, "Computed-aided detection of airgap eccentricity in operating three-phase induction motors by Park's vector approach," *IEEE Transactions on Industry Applications*, vol. 29, no. 3, pp. 897–901, 1993.

[63] J. Martins, V. Pires, and T. Amaral, "Induction motor fault detection and diagnosis using a current state space pattern recognition," *Pattern Recognition Letters*, vol. 32, pp. 321–328, 2011.

[64] J. Martins, V. Pires, and A. Pires, "On-line diagnosis of three-phase closed loop induction motor drives using an eigenvalue αβ–vector approach," *7th International Conference on Power Electronics and Drive Systems*, pp. 689–693, 2007.

[65] M. Nemec, K. Drobnic, D. Nedeljkovic, R. Fišer, and V. Ambrožic, "Detection of broken bars in induction motor through the analysis of supply voltage modulation," *IEEE Transactions on Industrial Electronics*, vol. 57, no. 8, pp. 2879–2888, 2010.

[66] A. Bellini, F. Filippetti, and G. Franceschini, "Closed-loop control impact on the diagnosis of induction motor faults," *IEEE Transactions on Industry Applications*, vol. 36, no. 5, pp. 1318–1329, 2000.

[67] S. Cruz and A. Cardoso, "Analysis and diagnosis of rotor faults in high performance induction motor drives," *International Conference on Electric Machines*, 2006, CDROM.

[68] D. Pires, V. Fernão Pires, J. Martins, and A. Pires, "Rotor cage fault diagnosis in three-phase induction motors based on a current and virtual flux approach," *Energy Conversion and Management*, vol. 50, no. 4, pp. 1026–1032, 2009.

[69] M. Nemec, V. Ambrožic, D. Nedeljkovic, R. Fišer, and K. Drobnic, "Detection of broken bars in induction motors using voltage pattern analysis," *IEEE International Symposium on Diagnostics for Electric Machines, Power Electronics and Drives, SDEMPED*, pp. 1–6, 2009.

[70] R. Fišer and S. Ferkolj, "Magnetic field analysis of induction motor with rotor faults," *COMPEL – The International Journal for Computation and Mathematics in Electrical and Electronic Engineering*, vol. 17, no. 1/2/3, pp. 206–211, 1998.

[71] S. Ferkolj, R. Fišer, and H. Šolinc, "Magnetic fields calculation of induction motor under load conditions," *Electric and Magnetic Fields – From Numerical Models to Industrial Applications*, pp. 365–368, 1995.

[72] R. Fišer, S. Ferkolj, and H. Šolinc, "Steady state analysis of induction motor with broken rotor bars," *7th International Conference on Electrical Machines and Drives*, pp. 42–46, 1995.

[73] R. Fišer, and S. Ferkolj, "Modelling of dynamic performance of induction machine with rotor faults," *International Conference on Electrical Machines ICEM 1996*, vol. 1, pp. 17–22, 1996.

[74] M. J. Islam, J. Pippuri, J. Perho, and A. Arkkio, "Time-harmonic finite element analysis of eddy currents in the form-wound stator winding of a cage induction motor," *IET Electric Power Applications*, vol. 1, no. 5, pp. 839–846, 2007.

[75] A. Bossavit, "Edge-element computation of the force field in deformable bodies," *IEEE Transactions on Magnetics*, vol. 28, no. 2, pp. 1263–1266, 1992.

[76] J. L. Coulomb, "A methodology for the determination of global electromechanical quantities from a finite element analysis and its application to the evaluation of magnetic forces, torques and stiffness," *IEEE Transactions on Magnetics*, vol. 19, no. 6, pp. 2514–2519, 1983.

[77] K. J. Bath, *Finite Element Procedure in Engineering Analysis*. New Jersey: Prentice-Hall International, 1982, 735 p.

[78] O. C. Zienkiewicz, *The Finite Element Method*. London: McGraw-Hill, 1977, 787 p.

[79] D. Spyropoulos, K. Gyftakis, J. Kappatou, and E. Mitronikas, "The influence of the broken bar fault on the magnetic field and electromagnetic torque in 3-phase induction motors," *International Conference on Electrical Machines ICEM 2012*, pp. 1868–1874, 2012.

[80] J. Gierras, C. Wang, and J. Lai, "Noise of polyphase electric motors," CRC Press, Taylor & Francis Group, pp. 37–44, 2006.

8 KOKKUVÕTE

Käesoleva doktoritöö ülesandeks on analüüsida ja parendada olemasolevaid asünkroonmasinate diagnostikameetodeid. Doktoritöö peaeesmärgiks seati lihtsa matemaatilise meetodi leidmine, mis sobiks asünkroonmasinate diagnostikaks ja võimaldaks tuvastada nende rikkeid. Silmas tuleb pidada, et diagnostiliste protseduuride läbiviimine ei tohi mingil moel segada masina normaalset tööprotsessi. Leitud diagnostikameetodi kasutamist peaks olema tulevikus võimalik ka mingil määral automatiseerida.

Elektrimasinate tööd võivad häirida mitmesugused rikked. Reaalaja diagnostika võimaldab rikete tuvastamist varajases staadiumis ja mõnel juhul isegi rikete ennetamist. Tihti peetakse väikeseid rikkeid algstaadiumis ohututeks ja ebaolulisteks, kuid kui neile õigeaegselt tähelepanu ei pöörata, võib olukord aja möödudes muutuda ja rikked areneda lausa katastroofiliste mõõtmeteni. Masinate seisukorra monitoorimine võimaldab rikke olemasolu avastada piisavalt vara – siis, kui selle kõrvaldamine on veel reaalne ja majanduslikult mõttekas. Diagnostikameetodite rakendamine võimaldab ühtlasi eristada masinate rikkeid elektrivõrgus toimuvate kõikumiste ja harmooniliste võnkumiste põhjustatud talitlushäiretest.

Arvestades, et maailm liigub üha enam tarkvõrgu ja hajatootmise suunas, muutub elektrimasinate diagnostika järjest olulisemaks. Diagnostika muutub tähtsaks, sest võimaldab uutes dünaamilistes ja hajutatud süsteemides, milles kasutatakse palju väikesi tootmisüksusi nagu väikesed hüdro- ja tuuleelektrijaamad, säilitada ettenähtud elektrikvaliteedi ja toitekindluse taset.

Käesolevas doktoritöös uuritakse asünkroonmasina purunenud rootorivarraste diagnostikat. Katsed on sooritatud erinevate masinatega nii mootori kui ka generaatori režiimis, rakendatud on erinevaid toiteviise (toide otse võrgust või sagedusmuundurite vahendusel) ja erineva raskusastmega rikkeid. Töös kasutatavaks diagnostikameetodiks on valitud Clarke'i teisendus. Rikkeindikaatorina on kasutatud nii staatorivoolu kui ka –pinget ning nende võrdlus on välja toodud.

Töö põhjal saab järeldada, et vastutusrikkaid ülesandeid täitvate asünkroonmasinate diagnostika on äärmiselt tähtis ja vajalik protseduur, mida ei tohiks eirata. Diagnostika abil on võimalik tõsta elektrimasinate töökindlust ja mõnel juhul ka tarbijate toitekindlust. Elektrimasinate diagnostika aitab pikendada masinate eluiga, ära hoida ootamatuid kasutajatele ohtlikke olukordi ja masinate riketest tingitud suurt majanduslikku kahju. Töös on näidatud, et elektrimasinatega koos kasutatavad sagedusmuundurid raskendavad masinate rikete tuvastamist, kuna lisavad klassikalise elektrimasina voolu(pinge)spektrisse rikkesignaali leidmist segavaid harmoonilisi komponente.

Töös on põhjendatud edasiste uuringute vajadust. Olulisemateks uurimissuundadeks tuleks lugeda eri tüüpi rikete eristamist, rikkis masinatega kasutatavate sagedusmuundurite käitumise ja mõju uurimist ning erinevate rikete simuleerimist, et tuletatud diagnostikameetodeid katsete abil kinnitada.

AUTHOR'S PUBLICATIONS

[A1]   Vaimann, T.; Belahcen, A.; Martinez, J.; Kilk, A. (2014). Detection of induction motor broken bars in grid and frequency converter supply. *Przeglad Elektrotechniczny (Electrical Review)*, vol. 90, no. 1, pp. 90–94.

[A2]   Niitsoo, J.; Palu, I.; Kilter, J.; Taklaja, P.; Vaimann, T. (2013). Residential load harmonics in distribution grid. *Proceedings of the 3rd International Conference on Electric Power and Energy Conversion Systems EPECS 2013*, October 2–4, 2013, Istanbul, Turkey, pp. 1–6.

[A3]   Vaimann, T.; Belahcen, A.; Kallaste, A.; Kilk, A. (2013). Lifecycle-based design and optimization of electrical motor-drives – challenges and possibilities. *Proceedings of the 3rd International Conference on Electric Power and Energy Conversion Systems EPECS 2013*, October 2–4, 2013, Istanbul, Turkey, pp. 1–4.

[A4]   Vaimann, T.; Belahcen, A.; Kallaste, A.; Kilk, A. (2013). Magnetic properties of reduced Dy NdFeB permanent magnets and their usage in electrical machines. *Proceedings of the IEEE AFRICON 2013 Conference*, September 9–12, 2013, Pointe-Aux-Piments, Mauritius, pp. 1124–1128.

[A5]   Tuttelberg, K.; Vaimann, T.; Kallaste, A. (2013). Analysis of a slow-speed slotless permanent magnet synchronous generator. *Proceedings of the 4th International Youth Conference on Energy IYCE 2013*, June 6–8, 2013, Siófok, Hungary, ID-71.

[A6]   Kallaste, A.; Vaimann, T.; Janson, K.; Bolgov, V. (2013). Components selection of local power supply system for sparsely populated areas. *Proceedings of the 14th International Scientific Conference Electric Power Engineering EPE 2013*, May 28–30, 2013, Kouty nad Desnou, Czech Republic, pp. 181–186.

[A7]   Vaimann, T.; Janson, K.; Bolgov, V.; Kallaste, A. (2013). Analysis of off-grid hybrid power supply for sparsely populated areas. *Proceedings of the 14th International Scientific Conference Electric Power Engineering EPE 2013*, May 28–30, 2013, Kouty nad Desnou, Czech Republic, pp.175–179.

[A8]   Lindh, P.; Vaimann, T.; Kallaste, A.; Pyrhönen, J.; Vinnikov, D.; Naumanen, V. (2013). Influence of slot wedge material on permanent magnet losses in a traction motor with tooth coil windings. *International Journal of Applied Electromagnetics and Mechanics*, vol. 42, no. 2, pp. 227–236.

[A9]   Vaimann, T.; Belahcen, A.; Martinez, J.; Kilk, A. (2013). Stator voltage analysis of frequency converter fed induction generator with broken rotor bars. *Proceedings of the 13th International Symposium "Topical Problems in the Field of Electrical and Power Engineering" and "Doctoral School of Energy and Geotechnology II"*, January 14–19, 2013, Pärnu, Estonia, pp. 249–251.

[A10] Vaimann, T.; Niitsoo, J.; Kivipõld, T.; Lehtla, T. (2012). Power quality issues in dispersed generation and smart grids. *Electronics and Electrical Engineering*, vol. 10, no. 8, pp. 23–26.

[A11] Vaimann, T.; Kallaste, A.; Kilk, A. (2012). Using Clarke vector approach for stator current and voltage analysis on induction motors with broken rotor bars. *Electronics and Electrical Engineering*, vol. 123, no. 7, pp. 17–20.

[A12] Kazakov, A.; Janson, K.; Vaimann, T.; Järvik, J. (2012). DC microgrid protection means. *Proceedings of the 8th International Conference Electric Power Quality and Supply Reliability PQ2012*, June 11–13, 2012, Tartu, Estonia, pp. 311–316.

[A13] Vaimann, T.; Belahcen, A.; Martinez, J.; Kilk, A. (2012). Detection of broken rotor bars in frequency converter fed induction motor using Park's vector approach. *Proceedings of the 8th International Conference Electric Power Quality and Supply Reliability PQ2012*, June 11–13, 2012, Tartu, Estonia, pp. 53–56.

[A14] Kallaste, A.; Belahcen, A.; Kilk, A.; Vaimann, T. (2012). Analysis of the eccentricity in a low-speed slotless permanent-magnet wind generator. *Proceedings of the 8th International Conference Electric Power Quality and Supply Reliability PQ2012*, June 11–13, 2012, Tartu, Estonia, pp. 47–52.

[A15] Mõlder, H.; Järvik, J.; Vaimann, T.; Gordon, R. (2012). Investigation of molten metal mixing in a DC electric arc furnace with added AC component on different frequencies. *Proceedings of the 8th International Conference Electric Power Quality and Supply Reliability PQ2012*, June 11–13, 2012, Tartu, Estonia, pp. 33–36.

[A16] Kallaste, A.; Kilk, A.; Belahcen, A.; Vaimann, T.; Janson, K. (2012). Demagnetization in permanent magnet slotless generator using halbach array. *Proceedings of the 13th International Scientific Conference Electric Power Engineering EPE 2012*, May 23–25, 2012, Brno, Czech Republic, vol. 2, pp. 1053–1057.

[A17] Kütt, L.; Järvik, J.; Vaimann, T.; Shafiq, M.; Lehtonen, M.; Kilter, J. (2012). High-frequency current sensor for power network on-line measurements. *Proceedings of the 13th International Scientific Conference Electric Power Engineering EPE 2012*, May 23-25, 2012, Brno, Czech Republic, vol. 1, pp. 367–371.

[A18] Vaimann, T.; Belahcen, A.; Martinez, J.; Kilk, A. (2012). Park's vector approach for detection broken rotor bars in frequency converter fed induction generator. *Proceedings of the 13th International Scientific Conference Electric Power Engineering EPE-2012*, May 23–25, 2012, Brno, Czech Republic, vol. 2, pp. 985–988.

[A19] Mõlder, H.; Järvik, J.; Vaimann, T.; Gordon, R. (2012). Multi-electrode arc furnace technology with improved metal processing capability using current driven mixing. *Proceedings of the 11th Conference on Environment and Electrical Engineering EEEIC 2012*, May 18–25, 2012; Venice, Italy, pp. 313–316.

[A20] Vaimann, T.; Kallaste, A. (2012). Condition monitoring of electrical machines. *Proceedings of the 11th International Symposium "Topical Problems in the Field of Electrical and Power Engineering" and "Doctoral School of Energy and Geotechnology II"*, January 16–21, 2012; Pärnu, Estonia, pp. 209–212.

[A21] Järvik, J.; Mõlder, H.; Vaimann, T. (2012). Impact of conducting and insulating material to electric field. *Proceedings of the 11th International Symposium "Topical Problems in the Field of Electrical and Power Engineering" and "Doctoral School of Energy and Geotechnology II"*, January 16–21, 2012; Pärnu, Estonia, pp. 107–112.

[A22] Kallaste, A.; Vaimann, T.; Pabut, O. (2012). Slow-speed ring-shaped permanent magnet generator for wind applications. *Proceedings of the 11th International Symposium "Topical Problems in the Field of Electrical and Power Engineering" and "Doctoral School of Energy and Geotechnology II"*, January 16–21, 2012; Pärnu, Estonia, pp. 66–69.

[A23] Kazakov, A.; Janson, K.; Vaimann, T. (2012). Microgrids performance challenges. *Proceedings of the 11th International Symposium "Topical Problems in the Field of Electrical and Power Engineering" and "Doctoral School of Energy and Geotechnology II"*, January 16–21, 2012; Pärnu, Estonia, pp. 42–46.

[A24] Vaimann, T.; Niitsoo, J.; Kivipõld, T. (2011). Dispersed generation accommodation into smart grid. *Proceedings of the 52nd International Scientific Conference of Riga Technical University. Section of Power and Electrical Engineering*, October 13–14, 2011, Riga, Latvia, ID-42.

[A25] Vaimann, T.; Kallaste, A.; Kilk, A. (2011). Sensorless detection of induction motor rotor faults using the Clarke vector approach. *Scientific Journal of Riga Technical University. Power and Electrical Engineering*, 29, pp. 43–48.

[A26] Niilo, H.; Vaimann, T. (2011). Problems in the operation of parallel-series converter when using two switch forward inverter. *Student Forum Proceedings of the 7th International Conference-Workshop Compatibility and Power Electronics CPE 2011*, June 1–3, 2011, Tallinn, Estonia, pp. 28–33.

[A27] Vaimann, T.; Kallaste, A.; Kilk, A. (2011). Overview of sensorless diagnostic possibilities of induction motors with broken rotor bars. *Proceedings of the 12th International Scientific Conference Electric Power Engineering EPE 2011*, Kouty nad Desnou, Czech Republic, May 17–19, 2011, pp. 183–186.

[A28] Vaimann, T.; Kallaste, A.; Kilk, A. (2011). Using analysis of stator current for squirrel-cage induction motor rotor faults diagnostics. *Proceedings of the 6th International Conference on Electrical and Control Technologies ECT 2011*, May 5–6, 2011, Kaunas, Lithuania, pp. 245–251.

[A29] Mõlder, H.; Järvik, J.; Janson, K.; Gordon, R.; Vaimann, T. (2011). Method for mixing molten metal and compatible electric arc furnace. *Estonian Journal of Engineering*, 17(3), pp. 220–240.

[A30] Niilo, H.; Vaimann, T. (2011). 2 switch forward inverter for parallel-series resonance alternating (PSA) converter for supplying electric welding arc. *Proceedings of the 10th International Symposium "Topical Problems in the Field of Electrical and Power Engineering" and "Doctoral School of Energy and Geotechnology II"*, January 10–15, 2011, Pärnu, Estonia, pp. 140–144.

[A31] Vaimann, T.; Kallaste, A. (2011). Detection of broken rotor bars in three-phase squirrel-cage induction motor using fast Fourier transform. *Proceedings of the 10th International Symposium "Topical Problems in the Field of Electrical and Power Engineering" and "Doctoral School of Energy and Geotechnology II"*, January 10–15, 2011, Pärnu, Estonia, pp. 52–56.

[A32] Vaimann, T. (2009). Diagnostics of induction motor rotor faults using analysis of stator current. *Proceedings of the 6th International Symposium "Topical Problems in the Field of Electrical and Power Engineering. Doctoral School of Energy and Geotechnology II"*, January 12–17, 2009, Kuressaare, Estonia, pp. 13–17.

APPENDIX / LISA A

AUTHORS PUBLICATIONS RELATED TO THE STUDY [I]–[VI]

Paper I

Vaimann, T.; Niitsoo, J.; Kivipõld, T.; Lehtla, T. (2012). Power Quality Issues in Dispersed Generation and Smart Grids. *Electronics and Electrical Engineering*, vol. 10, no. 8, pp. 23–26.

Power Quality Issues in Dispersed Generation and Smart Grids

T. Vaimann[1], J. Niitsoo[2], T. Kivipold[2], T. Lehtla[3]

[1]Department of Fundamentals of Electrical Engineering and Electrical Machines, Tallinn University of Technology,
Ehitajate tee 5, 19086 Tallinn, Estonia, phone: +372 620 3800
[2]Department of Electrical Power Engineering, Tallinn University of Technology,
Ehitajate tee 5, 19086 Tallinn, Estonia, phone: +372 620 3754
[3]Department of Electrical Drives and Power Electronics, Tallinn University of Technology,
Ehitajate tee 5, 19086 Tallinn, Estonia, phone: +372 620 3704
toomas.vaimann@ttu.ee

Abstract—The world today is moving toward smart distribution grids and dispersed generation. Those tendencies are caused by different reasons. These include the decrease of fossil fuel consumption, EU directives of CO_2 emissions and climate objectives etc. Innovation and change in technology is a highly welcomed trend but one must not forget that there are drawbacks as well as benefits. One of the most important issues in future grids are the power quality and supply reliability issues. This paper describes how the change to dispersed generation and smart grids should look like and what are the main problems, that need quick and active solutions, so that future grids would be fully functional and reliable.

Index Terms—Power distribution faults, smart grids, power system dynamics, harmonic distortion.

I. INTRODUCTION

If centralized generation is characterizing factor for nowadays energy systems, then smart grids of the future mean also the spreading of dispersed generation. The cause of these changes is the strict environmental norms and liberalization of electricity markets [1].

Dispersed generation has been recommended as one of the environmentally friendly solutions for improving the energy system, decreasing the losses and increasing effectiveness [2]. In addition increasing the ratio of small producers in electricity generation has been proposed.

Connecting new producers and generators to the distribution network can drastically change the working parameters of the grid. This situation is extremely important when the new connected power plant is equal to or even greater than the load in this particular area. In such case the new power plant affects the voltage adjustment and power flux. It is important to evaluate the existing grid, capacity and loads in this certain area of the distribution network [2].

Dispersed units affect the current quality and through the grid also the voltage quality as experienced by other customers [2]. Power quality concerns the electrical interaction between the network and its customers. It consists of two parts: the voltage quality concerns the way in which the supply voltage impacts equipment; the current quality on the other hand concerns the way in which the equipment current impacts the system [3].

For these reasons it is important changing of the loads have to be observed in smart grids as well as the growth of dispersed generation. In addition loads are getting more and more nonlinear which means that the cooperation of untraditional generation and loads affect the grid in unpredictable ways.

One of the key aspects of electricity production and distribution is the power quality and supply reliability for the customers. Traditionally the problems have been solved but as the world is moving towards smart grids and dispersed generation, those problems need more active and precise control.

As it can be expected, a great number of small generation units will be connected to distribution grids in quite near future. Most probably it would require certain online diagnostic systems to secure the full functionality and reliability of those units.

As due to the rise of harmonics in the grid, the machines would become more vulnerable, their faults become even more difficult to detect, so one could expect a growing number of unexpected downtimes due to different faults of the generators. This is the issue why real time condition monitoring is of utmost importance in the dispersed generation situation.

II. DISPERSED GENERATION

Dispersed generation is the production of electricity at or near the point of use. Most or part of consumed energy is produced at point of use and rest of the electricity goes into the distribution grid [3].

In most cases it is assumed that the electrical current and voltage have a sinusoidal wave shape. But if hundreds or thousands of small power production plants are connected to

a grid, it could mean that the sinusoidal current and voltage waveform are distorted and the waveform is no longer sinusoidal. Also, all small generators themselves produce harmonics. So the large-scale use of renewable energy sources for the production of electricity will bring major challenges for the electricity network.

Generators are typical electrical devices that are usually setup together with frequency converters to drive them and different inverters to synchronize their work with the grid. Not only generators themselves but also frequency converters and other electronic devices produce a vast number of harmonics that can be a problem to electrical machines they are set up with and also the grid they are working in. Due to financial benefits usually no additional filters are used to lessen the amount of induced harmonics. A typical harmonic distortion of a frequency converter is shown on Fig. 1.

As dispersed generation means also a growing number of small power plants such as small hydro and wind applications, this harmonic problem can become a serious issue for the power quality and supply reliability in smart grid or dispersed generation situation.
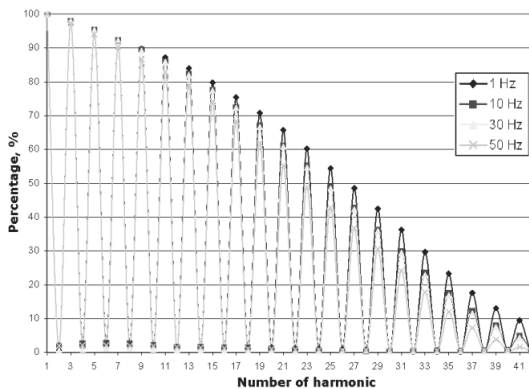

Fig. 1. Typical harmonic distortion of frequency converter.

For showing the probability of large extent of distributed generation in near future the potential is pointed out. The Estonian potential for dispersed generation, which currently is greater than the annual electricity consumption, is chosen as the example [3]. The potential of different energy sources in Estonia are shown in Table I.

TABLE I. ESTONIAN POTENTIAL OF DISPERSED GENERATION [3].

Name	Energy MWh/year	%
Wind energy	6 224 400,00	53
Litter oddments (biomass)	1 280 400,00	11
Wood (biomass)	1 279 800,00	11
Boiler plant reconstruction to CHP	1 179 000,00	10
Energy brush (biomass)	1 079 133,30	9
Solar Energy	224 000,00	2
Dung (biogas)	185 435,20	2
Hydropower	102 514,00	1
Reed (biomass)	50 000,00	0
Landfill gas (biogas)	25 974,40	0
Wastewater sludge (biogas)	21 201,60	0
Total:	11 651 858,50	100

III. POWER QUALITY

Connection of dispersed resources and changing dispersed generation to the distribution grid can affect the power quality in a great amount [2]. Smart distribution grid must secure the end users with power that has the demanded quality [4]–[6]. This is why the modern control systems, that are monitoring the important components of the distribution grid, must react precisely to the changes in power quality.

Power quality can be controlled and improved in whatever point of the electric system beginning from the means in the system or the grid and ending with single devices at the consumer level.

Connection of the dispersed generation of renewable energy to distribution grid can have both positive and negative effects to the power quality. It depends on possibilities of information and communication systems to control and maintain voltage in the feeders, turn the loads in or out and replace lost power with the reserves.

For example small amounts of wind power have negligible effects on electricity networks, but when electricity generation from wind power exceeds a certain threshold level, investments in the power system will be required. This threshold level is known as the hosting capacity [4].

The principle of hosting capacity is explained at Fig. 2. Hosting capacity does not say anything about how much generation from renewable energy sources that is connected to the grid, only how much can be connected without having to invest in measures to strengthen the grid.
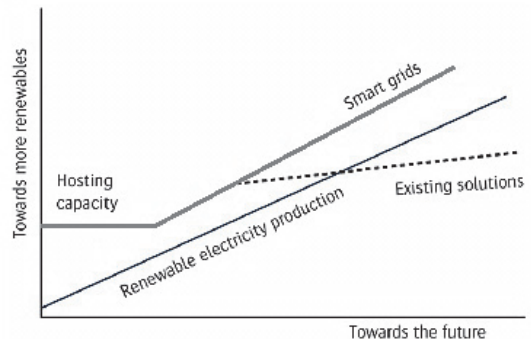

Fig. 2. The principle underlining hosting capacity [5].

IV. HARMONIC DISTORTION DUE TO DIFFERENT LOADS

Electrical devices, which are coming onto market, are becoming more and more complex. They may help to reduce energy consumption, but their performance regarding power quality is still rather improper.

The problem is that their current curve is not a perfect sinusoid. The widespread use of nonlinear loads may

implicate significant reactive power and problems with higher harmonics in a grid [6].

Harmonic currents produced by nonlinear loads are injected back into the supply systems. These currents can interact adversely with a wide range of power systems equipment causing additional losses, overheating and overloading. These harmonic currents can also cause interference with telecommunication lines and errors in power metering [7]–[9]. That problem may come more important when smart grid solutions where communication is very important are adapted.

Typical current curves of nonlinear loads are shown at Fig. 2. While the applied voltage is almost perfectly sinusoidal, the resulting current is heavily distorted.
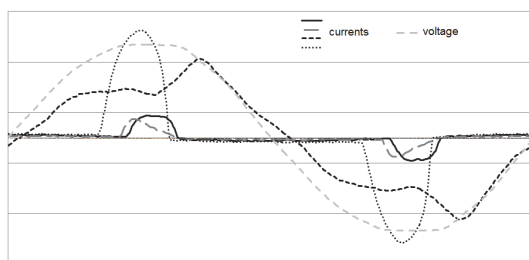

Fig. 3. Currents of typical nonlinear loads versus voltage.

Harmonics generated by consumer's appliances must not cause voltage rise in the connection point [6]. Fixing limits may become important before using numerous harmonics emitting devices together. In some papers [8] measurements with nonlinear loads are done when 5% current´s total harmonic distortion value at connection point is followed. For example most of the common compact fluorescence lamps have the total harmonic distortion over 100% [9].

Harmonic currents injected from individual end users on the system should be limited. These currents propagate toward the supply source through the system impedance, creating voltage distortion. Thus by limiting the amount of injected harmonic currents, the voltage distortion can be limited as well. This is the basic method of controlling the overall distortion levels proposed by IEEE standard 519-1992. Example for illustrating nonlinear loads influence on distribution grid a study with compact fluorescence lamps (CFLs) is made [8], [9].

V. POSSIBLE SOLUTIONS FOR POWER QUALITY FALL IN SMART GRID

Equipment responds very differently to harmonic distortions, depending on their method of operation. For example incandescent lights and different household heaters are not affected by them. On the other hand, induction motor windings are overheated by harmonics, causing accelerated degradation of insulation and so the lifetime of the machine can shorten in an abrupt way. The problem is that harmonic voltages can give correspondingly higher currents than do 50 Hz voltages and one can easily underestimate the degree of additional heating in the motor [10].

It is a widely known fact that faults such as the broken rotor bars induce sideband harmonic components to the stator current spectrum of the induction machine. Those harmonics can be used for detecting the faults. As most of electrical machines today are used in hand with frequency converters, then those converters add additional variables to the problem. Frequency converter causes supply frequency to vary slightly in time and, as a result, some additional harmonics in the current spectrum are induced and sidebands are reduced [11] or even hindered. This phenomenon also raises the amount of noise in the test signals, which makes the faults more difficult to detect.

In that sense it could prove to be useful to use a certain on-line diagnostic system in the grids with dispersed generation and the wind generators that are integrated to this system. This could be a helpful tool to detect the faults at an early stage where the repairing of the machines is still possible and reasonable. Also it would help to differentiate the deviations and harmonic distortions in the grid from the faulty cases of the machines.

VI. CONCLUSIONS

Irrespective of how the term smart grid is defined, one can safely state that electricity networks will face new challenges in the future, and that current and future challenges can be solved by a set of technologies that either exist today, or are being actively developed.

If more and more dispersed generation is going to be installed all over the power networks like it seems to go then it is most important to find measures for guarantying quality and security of supply.

From the example of Estonia we can see that the potential of dispersed generation is extensive. The impacts of using distributed generation may be massive even if bulk of that potential will not be installed.

In the situation where generation as well as consumption produces decrease of power quality in the grid, it is essential to analyze both generation and consumption in a very thorough way. If it proves to be necessary it might make sense to limit the usage of new plants and appliances or use some other methods to decrease their negative effect to power quality.

Usage of nonlinear loads like compact fluorescent lamps has risen rapidly in the last decade, but their harmonic emission, reactive power consumption and other drawbacks have been ignored.

Beside the problem that harmonics are extremely dangerous to electrical motors, distorted supply makes the diagnostics of them more difficult. A growing number of machines are driven through frequency converters. This means that also diagnostic for appropriate setups with frequency converters should be investigated. Frequency converters add additional noise and harmonics to the traditional current spectrum of the machines and thus such drives need a slightly different approach in diagnostics than traditional grid supplied machines. Nevertheless, appropriate on-line diagnostics of dispersed generation units must be applied to guarantee sufficient power quality, supply reliability and overall safety of customers and different

facilities connected to the grid.

REFERENCES

[1] Estonian Ministry of the Environment. Euroopa Liidu kliimapoliitika, 2012. [Online]. Available: http://www.envir.ee/1159209

[2] K.Purchala, R. Belmans, L. Exarchakos, A. D. Hawkes, "Distributed generation and the grid integration issue", KULeuven, Imperial College London.

[3] M. Bollen, *Understanding power quality problems: Voltage Sags and Interruptions,* 1st ed., Wiley-IEEE Press, 2000, p. 543.

[4] M.Bollen, M. Häger, "Power quality: interactions between distributed energy resources, the grid, and other customers", *Electric Power Quality and Utilisation Magazine,* vol. 1, no. 1, pp. 51–61, 2005.

[5] F. C. De La Rosa, *Harmonics and power systems*, CRC Press, 2006, pp. 1–184. [Online]. Available: http://dx.doi.org/10.1201/9781420004519.ch1

[6] T. Ackermann, G. Andersson, L. Söder, "Distributed generation: a definition", *Electric Power Systems Research,* vol. 57, pp. 195–204, 2001. [Online]. Available: http://dx.doi.org/10.1016/S0378-7796(01)00101-8

[7] T. Vaimann, J. Niitsoo, T. Kivipõld, "Dispersed generation accommodation into smart grid", in *Proc. of the 52nd International Scientific Conference of Riga Technical University. Section of Power and Electrical Engineering,* Riga Technical University Press, 2011, ID-42.

[8] European Standard, EN 50160:2011 Voltage characteristics of electricity, 2011.

[9] M. Bollen, *Adapting electricity networks to a sustainable– smart metering and smart grids*, Swedish Energy Markets Inspectorate, 2011, pp. 1–115.

[10] N. Watson, S. Hirsch, "The impact of compact flourescent lamps on power quality", in *Proc. of Conference of the Electric Power Supply Industry,* 1994, pp. 416–428.

[11] A. Miletic, M. Cettolo, "Frequency converter influence on induction motor rotor faults detection using motor current signature analysis – experimental research", *Symposium on Diagnostics for Electrical Machines, Power Electronics and Drives,* 2003, pp. 124–128.

Paper II

Kallaste, A.; Belahcen, A.; Kilk, A.; **Vaimann, T.** (2012). Analysis of the Eccentricity in a Low-Speed Slotless Permanent-Magnet Wind Generator. *Proceedings of the 8th International Conference PQ2012 Electric Power Quality and Supply Reliability*, Tartu, Estonia, June 11–13, 2012, pp. 47–52.

Analysis of the Eccentricity in a Low-Speed Slotless Permanent-Magnet Wind Generator

Ants Kallaste, Anouar Belahcen, Aleksander Kilk, and Toomas Vaimann

Abstract--This paper presents the analytical analysis of different eccentricities in the rotor of a novel slotless wind power generator. The analytical expressions for the air gap eccentricity have been derived and the effects of these eccentricities on the air gap flux density, the resultant unbalanced magnetic pull and the induced emf are investigated. The analysis shows a strong pull in the case of static eccentricity, which is not seen when the case of elliptic eccentricity for example. The analysis shows also that the induced emf per coil can vary very much but due to the series connection of the coil per phase emf is uniform but has higher rms value than in the case of healthy machine. The analytical equations are verified for the case of healthy machine on a constructed laboratory prototype.

Index Terms--Eccentricity, permanent magnet, slotless generator, wind generator.

I. INTRODUCTION

WIND generation industry is one of the most rapidly developing industries in the world, which also puts large pressure on the generators used in the windmills. There are many different generator solutions that have been described in the literature, such as induction generators [1], synchronous generators [2], and different permanent magnet generators [3]. There are a large number of different generator types, because the generators used in wind applications must fulfill a number of design requirements [4] and due to this fact it is difficult to find a universally acceptable and adaptable solution. The main requirements for the generators are as follows:

- simple construction,
- light weight,
- low speed,
- high output power,
- variable-speed generation,
- low starting torque,
- low cost.

Under these requirements one generator type that fulfills the needed criterions is selected for investigation. The idea of this solution is based on the iron free generator type that has been described in [5], [6]. During a more in-depth investigation it was found that it is more adequate to use a generator with added back iron [7]. Schematic of such gene-

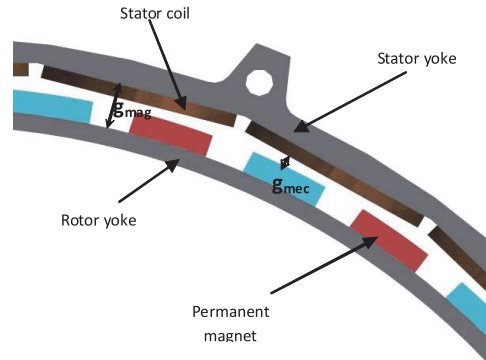rator is shown in Fig. 1, where both rotor and stator with coils are shown.

Fig. 1. Construction of a slotless permanent magnet generator under investigation in this study. The rotor consists of an iron ring on top of which permanent magnets are mounted whereas the stator consists of an outer iron ring holding the concentrated coils. The stator does not have any teeth.

The given generator fits well for usage in wind applications, because the solution enables the construction of light weight low-speed machines. The construction of the machine eliminates the problem of cogging torque thank to the toothless construction, which means that the starting torque of the machine is relatively low. As the construction is very simple, it is expected that also the construction cost of such machines is low.

One of the key issues in the generator design is the air-gap and its uniformity. Air-gap eccentricity is usually not taken into account during the design process of conventional generators, but as the generator under investigation has a large radius and is relatively thin, it is expected that there can be problems occurring due to air-gap eccentricity rising from the low mechanical stiffness of the generator construction. This paper is dealing with such possible problems from the point of view of analyzing the effect of the eccentricity on the operation parameters of the generator such as the induced voltage waveform and the mechanical stress acting on the stator and rotor of the machine.

Air-gap eccentricity can be related to different manufacturing inaccuracies, such as construction tolerances, bearings and shaft bending [8]. The eccentricity appears to some extends in all electrical machines and it has been studied from different points of views e.g. as related to its effect on the losses [9] or unbalanced magnetic pull [10], [11] or how to diagnose the fault [12], [13], [14]. However,

A. Kallaste, A. Kilk and T. Vaimann are with the Department of Fundamentals of Electrical Engineering and Electrical Machines, Tallinn University of Technology, Ehitajate tee 5, 19086 Tallinn, Estonia (e-mail:ants.kallaste@ttu.ee; kilk@cc.ttu.ee; toomas.vaimann@ttu.ee).

A. Belahcen is with the Department of Electrical Engineering, Aalto University, P.O. Box 13000, 0076 Aalto, Finland (e-mail: anouar.belahcen@aalto.fi).

it is not clear how much does a problem like this affects the performance of the electrical machines and is it important to take it into account during the design process. If one looks at a permanent magnet machine, then every magnet that is situated on the rotor causes some radial force that affects the stator. If the air-gap has a uniform width, then the resultant of these forces in all the construction of the machine equals to zero. On the other hand, if there is some eccentricity in the air-gap, the resulting force is different from zero and the additional force start to affect the bearings, which mean faster wearing. Another aspect related to the eccentricity is that the magnetic flux density in the air-gap will be asymmetrical, which causes a deviation of the electrical parameters of the machine from the designed ones. This can result in the deviations of the output voltage and current and also oscillations in the power of the machine. The oscillating power can cause unequal distribution of the load, which in turn causes local hot spots and wearing of coil insulation. Additionally, air-gap eccentricity always results in excessive mechanical vibrations.

This paper investigates the cases of static and dynamic air-gap eccentricities in a low-speed slotless permanent magnet generator. The investigation has been performed through analytical methods in order to better understand how the eccentricities affect to the machine. The methodology of how to consider the possible eccentricity faults in the analysis of the machine has been described and analytical calculations have been carried out and comparison with measurements made on a prototype machine has been presented. The measurements on the prototype have been made for a healthy machine only and for the purpose of validating the analytical methodology.

II. METHODS

Air-gap eccentricity can be caused by inaccurate construction as well as different problems during the exploitation. Fig. 2 shows possible types of eccentricity. A healthy machine (Fig. 2a), static eccentricity (SE) (Fig. 2b), elliptic eccentricity (EE) (Fig. 2c) and dynamic eccentricity (DE) (Fig. 2d and 2e) are shown on the figure.
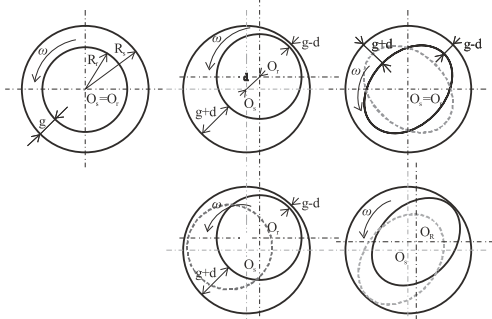

Fig. 2. Rotor eccentricity: a) healthy; b) static; c) elliptic; d) and e) dynamic. Other eccentricities mode emanating from the deformation of the stator can also occur but they are not investigated here

A. Static Eccentricity

In the SE fault, the rotational axis of the rotor coincides with the rotor symmetric axis, and it is displaced from the stator symmetric axis. Although the air-gap distribution around the rotor is not uniform, it is time independent. The

SE degree (δ_s) is defined as follows:

$$d_s = \frac{\left|O_sO_w\right|}{g} \ , \tag{1}$$

where O_s is the stator symmetry center, O_w is the rotational centre, and g is the air-gap length. Fig. 3a shows the position of the stator and rotor in the cross section plan of the machine in the case of SE. β_s is the initial angle of the SE and the vector O_sO_w is the static transfer vector. This vector is fixed for all angular position of the rotor.
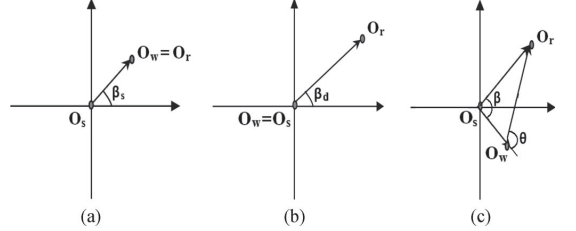

Fig. 3. Position of stator and rotor cross sections under (a) SE, (b) DE, and (c) EE in the stator reference frame.

In a SE fault, the width of the air-gap can be determined using the following equation:

$$g = R_s - R_r + \sqrt{R_r^2 - (d \cdot \sin \beta)^2} \ , \tag{2}$$

where R_s is the stator radius and R_r the rotor radius.

B. Elliptic Eccentricity

In case of elliptic eccentricity the centre points of the rotor and stator symmetry are matching, but due to the elliptic shape of the rotor, non uniform air-gap still exists. In such case, the deviations caused by the eccentricity change in time.

The width of the air-gap in the case of elliptic eccentricity can be found using the following equation:

$$g(t) = R_s - \sqrt{\left[(R_r + d)\cos(\frac{\omega t}{P} - \beta)\right]^2 + \left[(R_r - d)\cos(\frac{\omega t}{P} - \beta)\right]^2} \ , \tag{3}$$

where R_r is the radius of cylindrical rotor, d expresses the deviation of the ellipse from the circular shape and P is the number of rotor poles. Note that the angle β changes in time.

C. Dynamic and Mixed Eccentricity

Dynamic eccentricity is a situation where the center point of rotor symmetry is shifted depending on the stator center and the rotation of rotor is performed around the center point of stator symmetry. In such case the air-gap eccentricity is a time-varying phenomenon. The DE degree (δ_d) is defined as follows:

$$\delta_d = \frac{\left|O_wO_r\right|}{g} \ , \tag{4}$$

where O_r is the rotor symmetrical axis, and vector O_wO_r is the dynamic transfer vector. This vector is fixed for all angular positions of the rotor, but its angle varies in time as the rotor rotates. Fig. 3(b) shows the DE, where β_d is the initial angle of the DE.

Mixed eccentricity means that the center points of the rotor, the stator and the rotational symmetry are all shifted from each other. This means that both static and dynamic eccentricities are present in the generator. Mixed eccentricity is the result of static and dynamic transfer vectors and in that case MD degree (δ_m) can be defined:

$$d_d = \frac{\left|O_w O_r\right|}{g}$$
$$= \left|\frac{O_s O_w}{g} + \frac{O_w O_r}{g}\right| \qquad (5)$$
$$= \sqrt{d_s^2 + d_d^2 + 2 d_s d_d \cos q}$$

In case of mixed eccentricity the width of the air-gap depends on the mechanical position and it can be found as follows:

$$g(t) = R_s - \delta_m g \cos\left(\frac{\omega t}{P} - \beta\right) -$$
$$\sqrt{R_r^2 - \delta_m^2 g^2 \sin\left(\frac{\omega t}{P} - \beta\right)}. \qquad (6)$$

D. Stresses and Electrical Parameters

Knowing the width of the air-gap according to the mechanical angle, the magnetic flux density in the air-gap corresponding to each pole can be calculated. In the study the flux density was calculated by vector potential according to the equation:

$$\vec{B} = \nabla \times \vec{A} \qquad (7)$$

To know how large is the force that permanent magnets influence the stator with and also considering that $\mu_{iron} \gg \mu_0$, so that magnetic force is acting on the surface of the iron, Maxwell stress tensor can be used:

$$f_r = \sigma_{rr}^{air} - \sigma_{rr}^{iron} \approx \frac{1}{2\mu_0} B_g^2, \qquad (8)$$

where f_r denotes the radial traction

To find radial unbalanced force acting on the rotor center integrating radial force density along the rotor surface can be determined as in:

$$F_r = \int_0^{2\pi} f_r \cdot r d\theta. \qquad (9)$$

When calculating the generator emf it is assumed that the magnetic flux is uniform for the all the generator coil and thus the calculation of emf in one coil is enough. In such case every coil has to be considered as an independent case and the emf-s for each coil has to be calculated. The Emf can be calculated using:

$$emf = \oint_c (v \times B) \cdot dl \qquad (10)$$

III. RESULTS

As a result of the design process, a prototype generator of 5 kW rated power was constructed. The parameters of the generator are reported in Table I and a photo of the laboratory prototype is shown in Fig. 4.

TABLE I
SLOTLESS PERMANENT MAGNET GENERATOR PARAMETERS

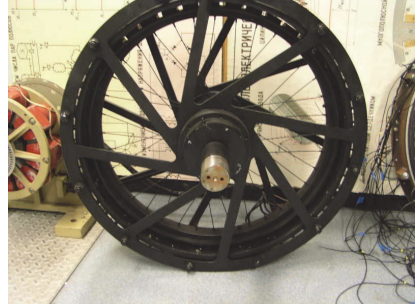|	
Rated power	5 kW
Rotational speed	230 rpm
Nominal voltage	340 Vac
Nominal current	8,5 Aac
Coils	24
Poles	40
Generator air-gap diameter	690 mm
Air-gap	2,5 mm

Fig. 4. Photo of the constructed prototype machine.

Based on the parameters of the generator under investigation and the above presented analytical expressions, the angular variation of the air gap was first calculated under different eccentricities. Fig. 5 shows the dimensions of the air-gap in case of different eccentricities. Calculations have been done assuming that in case of static eccentricity the offset of rotor symmetry center point compared to the stator symmetry center point is 2 mm what is 80% eccentricity of mechanical clearance. This high eccentricity is maximum what can be allowed from mechanical side. As in this type machine the coils are in the airgap and also magnet acts for magnetic path as airgap then from magnetic field side the eccentricity is 13%. It is the same in case of dynamic eccentricity and considering also that mechanical angle is changing with the angular position. In case of elliptic eccentricity, the offset of the ellipse from the circle is also set to 2 mm.
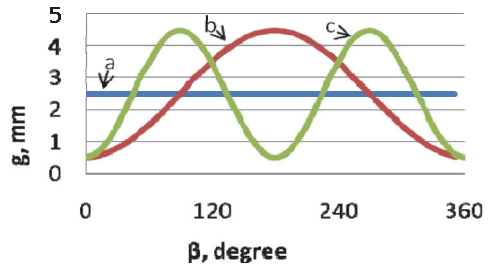

Fig. 5. Air-gap according to the mechanical position, a – healthy, b – static and dynamic, c – elliptic. Note that in the dynamic eccentricity case the position of the maximal and minimal air gap are changing in time as the rotor rotates.

In case of static and dynamic eccentricities it can be seen that one maximal and one minimal air-gap is emerging in the generator. Also the location of the air-gap is asymmetrical. With some simplifications, the location of the air-gap can be looked at as a sine function in such case.

In case of elliptic eccentricity two maximal and minimal values are forming, which are located symmetrically with respect to the mechanical angular position of the generator. With some simplification it can be looked at as a double sine function.

The magnetic flux density in the air-gap was calculated analytically in case of different eccentricities and it is shown on Figs. 6, 7, and 8 respectively for the cases of healthy machine, dynamic/static and elliptic eccentricity. In the case of dynamic eccentricity the waveform of the magnetic flux density is time dependent and it is moving along the angular position. The calculations are base on the assumption that in case of eccentricities the change of the air-gap is 2 mm. From the figures it can be seen that in case of a healthy machine, the waveform of the magnetic flux density along the angular position is uniform in the whole generator in the sense that the peak value is the same after each pole . In case of eccentricities, waveform of the magnetic flux density is asymmetrical in the sense that it is modulated by the varying air gap.
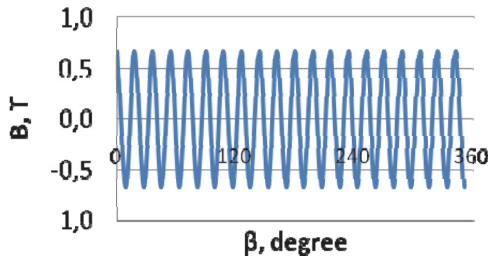

Fig. 6. Waveform of the magnetic flux density in the healthy machine. along the angular position.
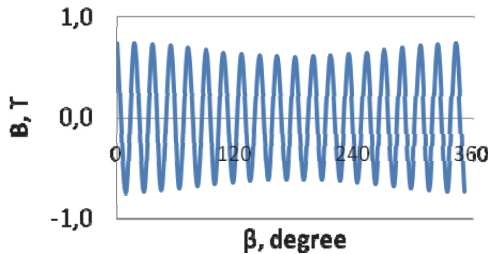

Fig. 7. Waveform of the magnetic flux density distribution along the angular position under static and dynamic eccentricity. Note that in the case of dynamic eccentricity the modulated waveform is moving along the angular position
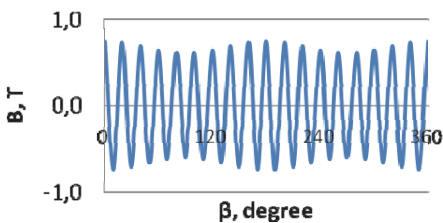

Fig. 8. Waveform of the magnetic lux density distribution along the angular position under elliptic eccentricity. The modulation is due to the modulated air gape as seen in Fig. 5.

In case of the healthy machine, the maximum magnetic flux density is 0,67 T. In the case of both dynamic and static eccentricities of 2 mm, at minimum air-gap dimensions the magnetic flux density rises 13,6% and at maximum air-gap dimensions the flux density falls 11%. Calculations of elliptic deviations show the similar results.

The Changes in the maximum values of the magnetic flux density with the eccenytricity deviations from rated air-gap dimensions were also investigated for different values of eccentricity. The results of such investigations are shown in Fig. 9.
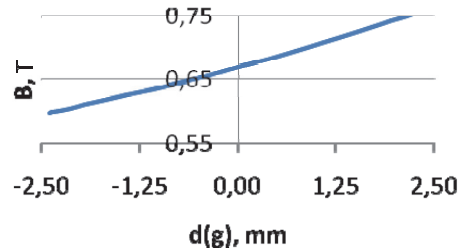

Fig. 9. Maximum values of the magnetic flux density as function of the eccentricity.

The total force acting on the stator caused by the primary magnetic field has also been investigated. In case of a healthy machine with uniform air-gap the magnetic forces are distributed in a homogeneous way across the air-gap. This means that the resultant force acting on the mechanical construction between the stator and the rotor is zero. In case of eccentricity, the air-gap becomes asymmetrical, and so are the forces, resulting in an unbalanced magnetic pull. Fig. 10 shows the calculated resultant force in the case of static eccentricity as function of the degree of deviation. It can be seen that the force acting on the construction in case of the shifted stator and rotor symmetry points is linear.
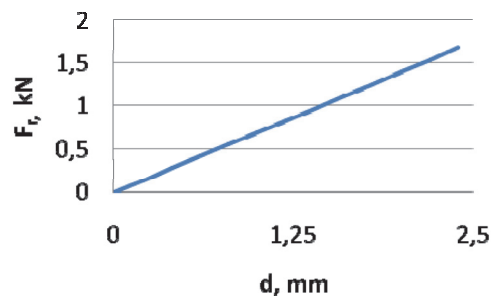

Fig 10. Resulting unbalanced magnetic pull as function of the degree of deviation in the case of static eccentricity. The linearity is due to the linearly assumed magnetic circuit

In the case of elliptic eccentricity, although the deviation of the air-gap dimensions is asymmetric in the generator, the resultant forces acting on the construction is zero due to the fact that the air gape deviation and also the magnetic flux density are in radial symmetry.

The next investigated parameter of the generator was the induced emf. The calculations show that in case of a healthy

machine, the induced emf in every coil has a constant effective value of 32 V. As the air-gap becomes asymmetrical due to assumed eccentricity the induced emf in different coils becomes asymmetric too. Fig. 11 shows the calculated value of induced emf in one coil as function of the eccentricity deviation of the air gap in case of static eccentricity.
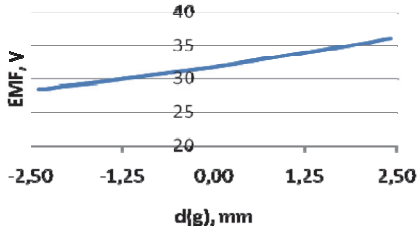

Fig. 11. EMF of a single coil as function of the air-gap change.

The investigated generator has its windings connect in a three-phase system, where the coils are distributed equally in the stator and all the coils corresponding to a given phase are connected in series. In case of eccentricity, the induced emf in the coils depends on the position of the eccentricity. Analytically it was found that the highest difference between the phases emerges when the shift vector of the rotor is oriented between two phases, i.e. 7,5 degrees. These calculations have been made for the case of a 2 mm rotor shift and the results are presented in Table II. In such case, similar voltages are induces in phases A and C, but the voltage of phase B differs from the two first ones. It can also be seen from Table II that when the coils are connected in series, the resultant emf in all the phases are equal, but the resulting voltages are higher than in the case of a healthy machine. This increase in the voltage is due to the additional motion of the rotor caused by the eccentricity which induces additional voltage in the coils.

TABLE II
CALCULATED EMF FOR STATIC AND DYNAMIC ECCENTRICITY

	Phase A	Phase B	Phase C
Static and dynamic eccentricity			
Min per coil	28,43	28,64	28,43
Max per coil	36,11	35,78	36,11
Serial connection	256,32	256,32	256,32
Elliptic eccentricity			
Min per coil	29,01	29,72	29,01
Max per coil	35,22	34,24	35,22
Serial connection	255,84	255,84	255,84
Healthy			
EMF per coil	31,82	31,82	31,82
Serial connection	254,56	254,56	254,56

Testing has been performed on the prototype generator and the load characteristic of the generator is shown on Fig. 12.

Testing showed that the used analytical methods are sufficient for the calculations of the charachteristics of the designed generator. The test results agree well with the calculated values. The verification of the eccentricity results through measurements has not been carried in view of keeping the generator helthy until all validations has been done as the introduction of faults in the prototype might destroy it.
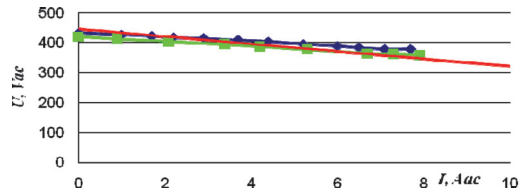

Fig 12. Generator load characteristic. Blue and green line are measured and red is calculated results

IV. ANALYSIS

Previous investigations showed that the slotless low-speed permanent magnet generator can be effectively used in wind applications due to its simple construction and light weight.

In the present investigation of how the eccentricity affects the generator it was found that any kind of eccentricity causes additional stresses to generator construction, which has to be taken into account in the design process of the generator mechanical support.

In case of static eccentricity it was found that even a small deviation of the rotor symmetry from the center point of the stator symmetry causes a significant increase in the unbalanced magnetic pull, which in turn causes the bearings to wear. It was also found that the force affecting the construction increases linearly with the eccentricity of the air-gap. As this force is not changing in time, it does not induce remarkable additional vibrations in the generator. At the same time the induced emf in the coils causes deviations in the phases voltage values. The Resulting voltage deviations and their presence in the generator system depends on the connection method of the coils. If the coils are connected in parallel, then the different voltage values between the coils induce circulating currents, which in turn in the case of static eccentricity cause additional resistive losses. In addition to these losses, static eccentricity causes the deviation of voltages between phases. On the other hand, when the coils are connected in series, there will be no difference of voltage between the phases, but the phase voltage rises when compared to a healthy machine. Dynamic eccentricity is quite similar to static eccentricity, except for the fact that the shift-vector changes in time. This causes additional vibrations in the generator.

In the case of elliptic eccentricity no additional forces are induced that affect the bearings, but as the forces are distributed un proportionally along the air gap angular position, the forces affecting the construction can cause additional bend and since they are time dependent they will case vibrations of the stator and rotor. The induced emf values are similar to the ones of dynamic eccentricity.

V. CONCLUSION

The Basics of a slotless low-speed permanent magnet wind generator design have been investigated with the different types of eccentricity taken into account. The causes for different types of air-gap eccentricities have been analyzed including static, dynamic, elliptic and mixed eccentricities. Analytical equations for calculating the dimensions of the air-gap eccentricities have been

developed and analysis of the consequences of the eccentricities on the operation of the machine have been presented. Both forces and induced emf values have been considered. Experiments have been performed on a prototype generator and the tested values were similar to the calculated ones under healthy operation.

Further investigation is needed to study different problems that are caused by air-gap eccentricity. The analytical methodology has to be improved to include losses and force distribution as well as vibrations. Part of the analytical methodology can be verified through numerical simulations and other parts have to be verified through the experiments.

VI. REFERENCES

[1] S. Muller, M. Deicke and R. W. DeDoncker, "Doubly fed induction generator systems for wind turbines" IEEE Industry Application Magazine, vol. 8 no. 3, May-June 2002, pp. 26-33.

[2] D. Bang, H. Polinder, G. Shrestha, J.A. Ferreira, "Promising Direct-Drive Generator System for Large Wind Turbine", Wind Power to the Grid - EPE Wind Energy Chapter 1st Seminar, 2008. EPE-WECS 2008, pp. 1-10.

[3] J. Pyrhönen, J. Nerg, P. Kurronen, J. Puranen and M. Haavisto, "Permanent Magnet Technology in Wind Power Generators", XIX International Conference on Electrical Machines - ICEM 2010, Rome. 2010, pp. 1-6.

[4] A. Kallaste, J. Järvik and A. Kilk (2006). "Permanent magnet axial flux generator with toroidal winding." In: 5th International Conference "Electric power quality and supply reliability" : conference proceedings : August 23-26, 2006, Viimsi, Estonia: Tallinn: Tallinn University of Technology, 2006, pp.167-171.

[5] E. Spooner, P. Gordon, J.R. Bumby and C.D. French, "Lightweight ironless-stator PM generators for direct-drive wind turbines", Electrical Power Applications, IEEE proceedings, Vol. 152, Issue 1, January 2005, pp. 17-26.

[6] P. J. Tavner and E. Spooner, "Light structures for large lowspeed machines for direct drive applications," in Proc. 2006 Int. Conf. Electr. Mach., Paper number 421, pp. 421.1-421.6.

[7] A. Kallaste, T. Vaimann and O. Pabut, "Slow-Speed Ring-Shaped Permanent Magnet Generator for Wind Application" 11th International Symposium "Topical Problems in the Field of Electrical and Power Engineering" and "Doctoral School of Energy and Geotechnology II, Tallinn: Elektriajam, 2012, pp. 66-69.

[8] T.J Kim, S.M Hwang, W.B Jung and C.U Kim, "Comparison of Dynamic Responses For IPM and SPM Motors by Considering Mechanical and Magnetic Coupling" Magnetics, IEEE, Vol. 37, No. 4. July, 2001, pp. 2818-2820.

[9] A. Belahcen, A. Arkkio , "Computation of additional losses due to rotor eccentricity in electrical machines" IET Electric Power Applications, Vol. 4, No. 4, pp. 259-266, 2010.

[10] D. G. Dorrell, M.-F. Hsieh, and Y. Guo, "Unbalanced magnet pull in large brushless rare-earth permanent magnet motors with rotor eccentricity," IEEE Trans. Magn., vol. 45, no. 10, pp. 4586-4589, Oct. 2009.

[11] Y. K. Chin, P. Kanninen, P. Maki-Ontto, R. Sakki and H. Lenden-mann, "Phenomenon of Magnetic Force in Permanent Magnet Wind Turbine Generarors" Electrical Machines and Systems, 2009. ICEMS 2009. pp. 1-6.

[12] B.M. Ebrahimi, J. Faiz and M.J. Roshtkhari, "Static-, Dynamic-, and Mixed-Eccentricity Fault Diagnoses in Permanent-Magnet Synchron-ous Motors" Industrial Electronics, IEEE proceedings, Vol. 56, No. 11. November, 2009, pp. 4727-4739.

[13] M. Hajiaghajani, Lei Hao, S. M. Madani, H. A. Toliyat, "A method for detection of eccentricity in permanent magnet machines" Industry Applications Conference, 2003. 38th IAS Annual Meeting, vol. 3, 2003, pp. 1833-1838.

[14] W. le Roux, R. G. Harley, T. G. Habetler, "Detecting Rotor Faults in Low Power Permanent Magnet Synchronous Machines," IEEE Trans. on Power Electronics, vol. 22, issue 1, 2007, pp. 322-328.

VII. BIOGRAPHIES

Ants Kallaste was born in Pärnu, Estonia in 1980 and received his BSc and MSc degrees in electrical engineering from Tallinn University of Technology, Estonia, in 2004 and 2006 respectively. He is currently a PhD student in Tallinn University of Technology department of Fundamental of Electrical Engineering and Electrical Machines.

He has been working in several companies as an electrical engineer. Presently he is working at the Tallinn University of Technology Department of Fundamentals of Electrical Engineering and Electrical Machines on research position and Goliath Wind on senior electric engineer position.

His main research interest includes PM machine design and wind generators.

Anouar Belahcen was born in Essaouira, Morocco, in 1963. He received the B.Sc. degree in physics (Licence es-science) from the University Sidi Mohamed Ben Abdellah, Fes, Morocco, in 1988 and the MSc. (Tech.), and Doctorate degrees from Helsinki University of Technology, Helsinki, Finland, in 1998 and 2004, respectively.

From 1996 to 1998, he was a Research Assistant at the Laboratory of Electromechanics, Helsinki University of Technology. From 1998 to 2004, he was a Research Scientist and from 2004 to 2008 he was a Senior Researcher at the same Laboratory. Since 2008, he has been working as an Adjunct Professor in the field of coupled problems and material modeling at the Department of Electrical Engineering, School of Science and Technology, Aalto University, Espoo, Finland. Since Sept. 2011, he has been appointed as part-time Professor of Electrical Machines at Tallinn University of Technology in Estonia.

His research interest deals with the numerical modeling of electrical machines, especially magnetic material modeling, coupled magnetic and mechanical problems, magnetic forces, and magnetostriction.

Aleksander Kilk was born in Karksi parish, Estonia, in 1946. He has graduated from Tallinn University of Technology and received a BSc degree in electric machines and electrical equipment in 1969. He received his MSc and PhD degree from Tallinn University of Technology in 1992 and 2008 respectively.

Since receiving his BSc degree in 1969 he has been working in the field of studies of electric machines, but also as a lecturer of the electrical engineering subjects. He is currently holding the position of associate professor as well as director of the department of Fundamentals of Electrical Engineering and Electrical Machines in Tallinn University of Technology.

His special field of research includes permanent magnet synchronous generators structures and properties.

Toomas Vaimann was born in Pärnu, Estonia, in 1984 and received his BSc and MSc degrees in electrical engineering from Tallinn University of Technology, Estonia, in 2007 and 2009 respectively. He is currently a PhD student in Tallinn University of Technology department of Fundamentals of Electrical Engineering and Electrical Machines.

He has been working in several companies as an electrical engineer. Presently he is working at the Tallinn University of Technology Depart-ment of Fundamentals of Electrical Engineering and Electrical Machines on engineer's position.

His main research interest includes diagnostics of electrical machines.

Paper III

Vaimann, T.; Belahcen, A.; Kallaste, A. (2014). Changing of Magnetic Flux Density Distribution in a Squirrel-Cage Induction Motor with Broken Rotor Bars. *Electronics and Electrical Engineering*, vol. XX, no. X, [to be published].

Changing of Magnetic Flux Density Distribution in a Squirrel-Cage Induction Motor with Broken Rotor Bars

Toomas Vaimann[1], Anouar Belahcen[1,2], Ants Kallaste[1]

[1]Department of Electrical Engineering, Tallinn University of Technology,
Ehitajate tee 5, 19086 Tallinn, Estonia
[2]Department of Electrical Engineering, Aalto University,
P.O. Box 13000, 0076 Espoo, Finland
toomas.vaimann@ttu.ee

Abstract—**This paper presents the finite element modelling of three-phase squirrel-cage induction motor with broken rotor bar faults. Finite element model based on a real machine is constructed, propagation of broken rotor bar fault and its influence on the magnetic flux density distribution of the machine cage is observed. As the propagation of the fault will result in total breakdown of the induction machine rotor, if the fault is not detected and solved, necessity of condition monitoring is pointed out. Analysis of the fault and its affect to the magnetic field in the rotor cage as well as changes in the phase voltage spectrum are presented.**

Index Terms— **Electric machines, induction motors, fault diagnosis, electromagnetic fields, rotors, finite element analysis.**

I. INTRODUCTION

Broken rotor bars of squirrel-cage induction machines have been the subject of interest in numerous scientific studies. A comprehensive yet ever growing list of the researches dealing with diagnostic problems of electrical machines is presented in [1]. As the given fault is one of the more usual types of failures, condition monitoring to predict the possible fault and detection of broken bars can be considered an important issue in the field of induction machine diagnostics.

Squirrel-cage induction machines are one of the most used machine types in the industry nowadays. They are preferred due to their rugged build, reliability and cost efficiency. This also means that induction machines are used in such applications, where sudden failures result with high economic loss and also possible threat to the surrounding environment as well as people manipulating them.

Induction machines are also often used as generators in small hydro and wind power plants. Failures of the machines used in such applications means a sudden drop of supply reliability and power quality to the customers using electricity produced in those units. With the world moving towards distributed generation, number of such small

generation units is expected to rise [2]. Due to that, rise in the use of induction machines can also be expected.

Induction machine rotor faults usually start from a fracture or a high resistivity spot in the rotor bar [3]. The fractured or cracked rotor bar starts to overheat around the crack until the bar breaks [4], [5]. This means that at the same time the resistance of such bars is rising and becomes significantly higher than the resistance of healthy bars in the rotor cage. As there is a lack of induced current in those bars, the magnetic field will become gradually more asymmetrical, which will lead to local saturation in stator and rotor teeth near the broken bar and disproportional distribution of magnetic field in the air-gap [6].

Breaking of the consecutive rotor bars is the most probable case in practice [7]. This happens, because currents that are unable to flow in the broken bars are flowing through the adjacent bars, which means that those bars situated next to the broken ones are under higher thermal stress due to higher current density. This means that if the fault is not treated, it will propagate in time resulting in the destruction of the whole rotor cage [8].

The aim of this paper is to show through a series of finite element modelling how the magnetic field in the machine is changing due to the presence of broken bars. Changes in the field are expected to be growing as the severity of the fault is rising and the fault propagates.

II. MODELLING OF THE INDUCTION MACHINE

Experiments of the induction machine's behavior were performed on a three-phase squirrel-cage induction motor with a healthy rotor and a rotor with up to three consecutive broken bars. These tests, where the same machine is fed through frequency converter supply are described in [9].

For the modelling of magnetic flux density distribution in case of broken rotor bar fault of an induction machine, the same motor as in previously mentioned experiments was used. Data of the machine is presented in Tab. 1.

Using the listed data and the machine layout, two dimensional finite element model of the induction machine was constructed. The model of the machine showing the magnetic flux density distribution in case of healthy rotor cage is presented in Fig. 1.

Parameter	Symbol	Value
Rated voltage	U_n	400V@60 Hz; 333V@50 Hz
Rated current	I_n	41 A
Rated speed	n_n	1680 rpm@60 Hz; 1400 rpm@50 Hz
Rated power	P_n	22 kW@60 Hz; 18 kW@50 Hz
Frequency	f	50-60 Hz
Power factor	$\cos\varphi$	0.86
Number of poles	p	4
Number of rotor bars	Q_r	40
Number of stator slots	Q_s	48

a lack of

Fig. 2. Magnetic flux density distribution of an induction motor with one broken rotor bar.

Fig. 1. Magnetic flux density distribution of a healthy induction motor.

Fig. 3. Magnetic flux density distribution difference between the healthy induction motor cage and the cage with one broken rotor bar.

III. EFFECT OF BROKEN BARS TO THE MAGNETIC FIELD

The necessity to detect the fault in an early stage, to prevent further damage of the equipment due to fault propagation, is one of the most important features of any condition monitoring or diagnostic techniques. At the same time, minor faults and early stages of the propagating fault are less obvious to detect and are significantly harder to grasp [10].

Based on this, the fault propagation in the given paper is modelled from healthy rotor cage up to three consecutive broken bars (which is 7.5% of all the rotor bars of the machine). The broken bars were modelled as areas with significantly higher resistance and low conductivity, so they would not contribute to the cage circuit [11], [12]. Fig. 2 presents the flux density distribution of the induction motor in case of one broken rotor bar.

As previously said, minor faults are very difficult to detect. Comparing Figs. 1 and 2, the difference between the flux density distributions is visible to some extent but not clearly detectable for the naked eye. The difference becomes easier to observe when one field distribution is subtracted from another and only the difference in the two presented flux density distributions remain. This difference of the flux density distributions of the healthy cage and the machine with one broken rotor bar is shown on Fig. 3.

It can be seen from Fig. 3 that already in case of one broken rotor bar in the cage, the magnetic field distribution is becoming distorted. Higher amount of magnetic saturation can be seen around the broken bar in the rotor as
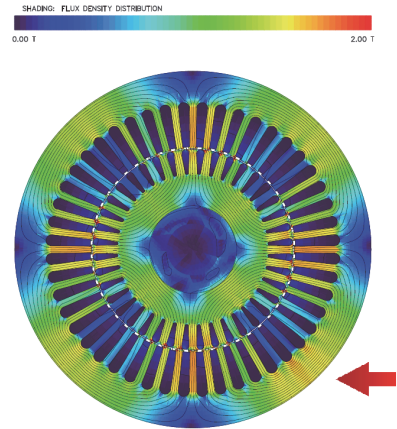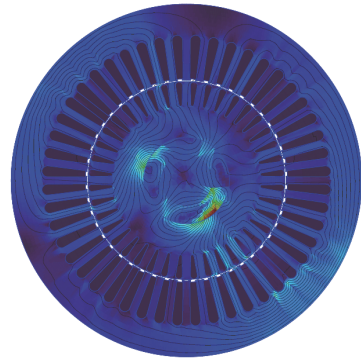
frequency-induced current in these rotor bars. Magnetic flux density in the studied machine is increasing by 0.15 T around the broken bar.

Additionally, as the rotor magnetic field distribution is distorted, this effect also influences the stator. In the stator higher saturation can be seen in the teeth facing the broken rotor bar and in stator yoke, where the magnetic flux density is also increasing by approximately 0.15 T.

Further study was made with two broken rotor bars. The simulation results of flux density distribution of this fault are given in the Fig 4. Fig. 5 presents a comparison of magnetic field distribution difference between healthy cage machine and an induction machine with two broken rotor bars.

It can be seen that in case of two broken rotor bars the magnetic field flux density is increasing around the broken rotor bars and also in the stator facing the broken rotor bar 0.2 T. The phenomenon can be described similarly to the one broken bar case, although the value of the magnetic flux density is rising even more. Also it can be seen that the magnetic flux density is increasing both in the stator and rotor yoke opposite to the broken rotor bars. It should be noted, that difference in the magnetic flux density

distribution between the healthy machine and the one with broken bars corresponds to an asymmetric field inducing
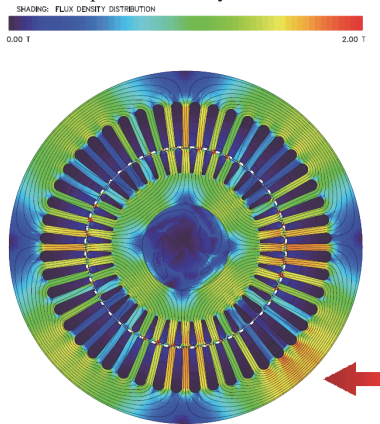

Fig. 4. Magnetic flux density distribution of an induction motor with two broken bars.
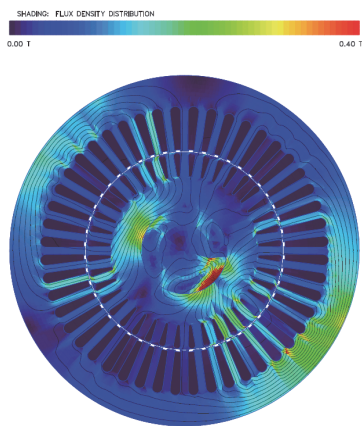

Fig. 5. Magnetic flux density distribution difference between the healthy induction motor cage and the cage with two broken bars.

eddy-currents in the shaft of the machine. Such current if free to circulate, will cause bearing currents that usually result in damaging the bearings.

Magnetic field distribution simulation results in case of three broken rotor bars are given in Fig. 6 and the comparison with healthy induction machine cage is presented in Fig. 7. It can be seen from Fig. 7 that three broken rotor bars lead to relatively high saturation of the iron around the broken rotor bars and opposite to the broken bars. Flux density is increasing up to 0.4 T compared to healthy machine and even more in the tooth between the broken bars as well as the shaft of the machine.

It can be said that due to the increased magnetic flux density, degradation in the mechanical performance of the induction machine can be expected. In the regions where the flux density is rising (around the broken bars and opposite to the broken bars), the core loss density is higher compared to other regions of the machine. These adjacent bars become more susceptible to thermal stress due to overheating and will lead to further breaking of rotor bar [13].

Although no currents pass through the broken bars and no heat losses are generated, it becomes obvious from the
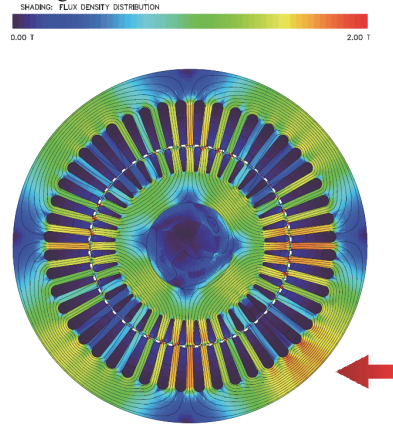

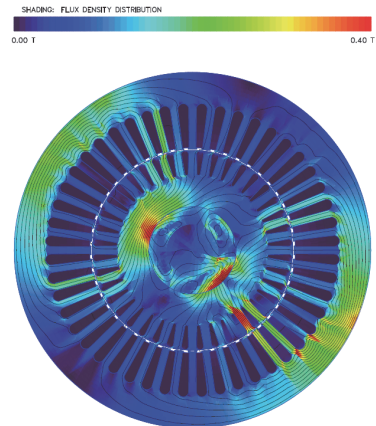Fig. 6. Magnetic flux density distribution of an induction motor with three broken bars.

Fig. 7. Magnetic flux density distribution difference between the healthy induction motor cage and the cage with three broken bars.

presented figures, that the currents passing through the bars adjacent to the broken ones are dramatically increased and the heat losses in the bars are increased in a large scale [14].

The air-gap field becomes asymmetrical due to the presence of broken bars in the rotor cage and the harmonic components of air-gap magnetic flux density vary significantly. As the flux density is fluctuating, it was assumed that it can also be traceable in the machine phase voltage due to the presence of counter-electromotive force. To visualize that effect, simulations were carried out and machine phase voltages were found. A comparison was made using the differences between healthy and faulty machine phase voltages. These results are presented in Fig. 8.

From Fig. 8 it can be seen that compared to healthy machine, the faulty machine phase voltage is fluctuating. The fluctuation is increasing with the amount of broken bars. In the studied machine, one broken bar in the cage leads to voltage difference up to ±10 V and three broken bars raise that difference up to ±15 V. It can also be seen that the third harmonic component is dominating the voltage

spectrum but also higher harmonic presence up to 21st and higher can be noted in the spectrum of the machine. The higher harmonic presence can also be detected on the bottom graph of Fig. 8, which shows phase voltage difference between one broken bar case and three broken rotor bars case.
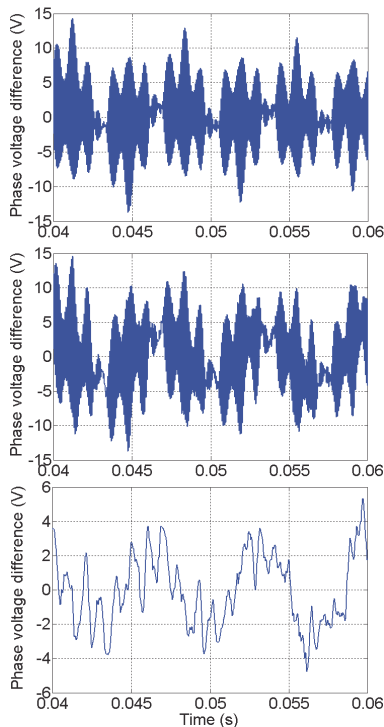

Fig. 8. Phase voltage difference: upper – phase voltage difference between healthy cage and one broken rotor bar case; middle – phase voltage difference between healthy cage and three broken rotor bars case; bottom – phase voltage difference between one broken bar case and three broken rotor bars case.

IV. CONCLUSIONS

Magnetic field modelling regarding the magnetic flux distribution of the induction machine in case of healthy machine and propagating severity of the broken rotor bars fault was made and analyzed. It was found that presence of broken rotor bars results in uneven distribution of magnetic field in the rotor cage and the whole machine.

Magnetic field strength is increasing around the broken bar in rotor and also in stator facing the broken bar. In addition to that, the magnetic field strength is also increasing on the opposite side of the broken rotor bar as well as the shaft of the machine. The latter can be explained by the asymmetric field that induces eddy-currents in the shaft and will most likely cause bearing currents, which in time will result in bearings damage.

When the fault propagates and the number of broken bars in the rotor cage increases, the magnetic field asymmetry is rising, resulting in higher local saturation in both rotor and stator teeth. Uneven magnetic field distribution starts affecting the machine phase voltage, resulting in the presence of higher harmonic components in the voltage spectrum. With increase of the number of consecutive broken bars, higher harmonic amplitude in phase voltage is also increasing, which means that various disturbances and undesired phenomena (i.e. increase of noise, increase of mechanical vibrations etc.) can be expected.

Based on the acquired magnetic field distribution figures, it can be estimated that broken rotor bars fault can lead to severe consequences if the fault is not dealt with in an early stage. The propagation of the fault will not only result in the destruction of the rotor cage but can also lead to various stator failures (i.e. stator winding turn to turn short circuits, lamination short circuits etc.) due to the broken rotor bar influenced local saturation in and around stator teeth. Additionally, such fault propagation can lead to bearings problems as mentioned previously.

To prevent the possible economic losses, danger to surrounding environment and people operating the machines, condition monitoring of the machines should be considered. This would grant the possibility of detecting the faults during the stage where repairing of the machine would still be reasonable and possible. Usage of sufficient diagnostic measures would also mean lower down-time for the industries where such machines are used.

REFERENCES

[1] M. Benbouzid, "Bibliography on induction motors faults detection and diagnosis", *IEEE Transactions on Energy Conversion*, vol. 14, no. 4, pp. 1065-1074, 1999.

[2] T. Vaimann, J. Niitsoo, T. Kivipõld, and T. Lehtla, "Power quality issues in dispersed generation and smart grids", *Electronics and Electrical Engineering*, vol. 10, no. 8, pp. 23-26, 2012.

[3] T. Lindh, *On the Condition Monitoring of Induction Machines*. Lappeenranta: Lappeenranta University of Technology, 2003. 148 p.

[4] A. Cardoso, S. Cruz, J. Carvalho, and E. Saraiva, "Rotor cage fault diagnosis in three-phase induction motors, by Park's vector approach", in *Proc. 1995 IEEE Industry Applications Conference*, vol. 1, pp. 642-646.

[5] B. Gaydon and D. Hopgood, "Faltering pulse can reveal an ailing motor", *Electrical Review*, vol. 205, no. 14, pp. 37-38, 1979.

[6] R. Fišer and S. Ferkolj, "Magnetic field analysis of induction motor with rotor faults", *COMPEL – The International Journal for Computation and Mathematics in Electrical and Electronic Engineering*, vol. 17, no. 1/2/3, pp. 206-211, 1998.

[7] R. Fišer and S. Ferkolj, "Application of a finite element method to predict damaged induction motor performance", *IEEE Transactions on Magnetics*, vol. 37, no. 5, pp. 3635-3639, 2001.

[8] T. Vaimann, A. Kallaste, and A. Kilk, "Using Clarke vector approach for stator current and voltage analysis on induction motors with broken rotor bars", *Electronics and Electrical Engineering*, vol. 123, no. 7, pp. 17-20, 2012.

[9] T. Vaimann, A. Belahcen, J. Martinez, and A. Kilk, "Detection of induction motor broken bars in grid and frequency converter supply", *Przeglad Elektrotechniczny (Electrical Review)*, vol. 90, no. 1, pp. 90-94, 2014.

[10] M. Nemec, K. Drobnic, D. Nedeljkovic, R. Fišer, and V. Ambrozic, "Detection of broken bars in induction motor through the analysis of supply voltage modulation", *IEEE Transactions on Industrial Electronics*, vol. 57, no. 8, pp. 2879-2888, 2010.

[11] D. Spyropoulos, K. Gyftakis, J. Kappatou, and E. Mitronikas, "The influence of the broken bar fault on the magnetic field and electromagnetic torque in 3-phase induction motors", in *Proc. 2012 International Conference on Electrical Machines*, pp. 1868-1874.

[12] J. Gierras, C. Wang, and J. Lai, "Noise of polyphase electric motors", CRC Press, Taylor & Francis Group, 2006, pp. 37-44.

[13] Li Weili, Xie Ying, Shen Jiafeng, and Luo Yingli, "Finite-element analysis of field distribution and characteristic performance of squirrel-cage induction motor with broken bars", *IEEE Transactions on Magnetics*, vol. 43, no. 3, pp. 1537-1540, 2007.

Paper IV

Vaimann, T.; Kallaste, A.; Kilk, A. (2011). Overview of Sensorless Diagnostic Possibilities of Induction Motors with Broken Rotor Bars. *Proceedings of the 12th International Scientific Conference Electric Power Engineering EPE 2011*, Kouty nad Desnou, Czech Republic, May 17–19, 2011, pp. 183–186.

Overview of Sensorless Diagnostic Possibilities of Induction Motors with Broken Rotor Bars

Toomas Vaimann[1], Ants Kallaste[2], Aleksander Kilk[3]

Tallinn University of Technology, Ehitajate tee 5, 19086 Tallinn, Estonia, http://www.ttu.ee
[1] tel: +372 620 3800, email: toomas.vaimann@ttu.ee,
[2] tel: +372 620 3800, email: ants.kallaste@ttu.ee
[3] tel: +372 620 3800, email: kilk@cc.ttu.ee

ABSTRACT

During the past few decades there has been a continually increasing interest and investigation into fault detection and diagnostics of induction motors. There are various different diagnostic approaches and methods to detect faults in induction motors. Attention should be paid to the fact that as induction motors are often used in critical duty drives, it is essential not to disturb the working cycle of the motor in any way while performing the needed diagnostic procedures. The needed measurements have to be carried out with the motor remaining in its normal operating mode, as changing of the working cycle can mean safety risks and economic losses in some applications where induction motors are used. This paper gives an overview of the sensorless diagnostic possibilities of three-phase squirrel-cage induction motors with broken rotor bars via the analysis of stator current.

Keywords: Induction motor, Rotor faults, Diagnostics, Stator current, Broken rotor bars, FFT, Clarke transformation, Current vector amplitude oscillation, Wavelet analysis, Finite element method

1 INTRODUCTION

Induction motors are critical for many industrial processes because they are cost effective and robust in the sense of performance. They are also critical components in many commercially available equipment and industrial processes [1]. In developed countries today there are more than 3 kW of electric motors per person and most of it is from induction motors [2]. Furthermore, induction motors are often used in critical duty drives where sudden failures can cause high safety risks and unnecessary economic expenses. Different failures can occur in electrical drives and one of the most common faults is the breaking of the rotor bars.

The majority of all stator and rotor faults are caused by a combination of various stresses, which can be thermal, electromagnetic, residual, dynamic, mechanical or environmental [3]. Broken rotor bars are not only one of the most common faults but also one of the most uncomfortable ones [4].

The worst case of such fault is when the broken rotor bars are situated closely one after another. This case is also most probable in practice as broken rotor bars are usually not detected at early stage. As the resistance of the broken bar is very high in comparison with the healthy ones, currents start to distribute unproportionally in the rotor cage. Parts of the rotor currents, which are unable to flow in broken bars, are flowing in adjacent bars. This increases the rms value of currents in the bars next to the broken ones [4]. As the healthy bars next to the broken one have too high current density, they will start to overheat, so these bars are under severe thermal stress. Those bars start cracking and breaking and when attention to the problem is not paid, the fault will continue to cascade, until the rotor cage is destroyed.

Broken rotors bars can lead to vibration problems, but more likely, in severe cases, the bar pounds out of the slot and makes contact with the stator core or winding [3]. The biggest problem of those faults is that it is often not worth or possible to repair the rotor. However all of this can be avoided, when the motor is supervised by an appropriate condition monitoring or diagnostic system.

2 SENSORLESS DIAGNOSTIC METHODS

The biggest advantage that sensorless diagnostic of induction motors provides is that testing and diagnostics can be done without any disturbances to the motor's normal working cycle. It means that in case of motors which are used in critical duty drives or perform on high risk conditions, no additional changes have to be made in order to perform the tests.

There are different possibilities to perform sensorless diagnostics on induction motors. One of the ways is to measure stator currents of the motor and analysing the measured signals. Some diagnostic methods for performing this analysis are described in this paper.

2.1 Fast Fourier Transform (FFT)

Fourier analysis is very useful for many applications where the signals are stationary, as in diagnostic faults of electrical machines [5].

Its purpose is to monitor a single-phase stator current. This is accomplished by removing the 50 Hz excitation component through low-pass filtering and sampling the resulting signal. Single-phase current is sensed by a current transformer and sent to a 50 Hz notch filter where the fundamental component is reduced. Analog signal is then amplified and low-pass filtered. Filtering removes the undesirable high-frequency components that produce aliasing of the sampled signal while the amplification maximizes the use of the analog-to-digital converter input range. Analog-to-digital converter samples the filtered current signal at a predetermined sampling rate that is an integer multiple of 50 Hz. This is

continued over a sampling period that is sufficient to achieve the required fast Fourier transform. [6]

Calculation of the fast Fourier algorithm can be performed with MATLAB-software where computing of this transform can be done in a simple way. The MATLAB functions $Y = fft(x)$ and $y = ifft(X)$ implement the transform and inverse transform pair given for vectors of length N by:

$$x(j) = \frac{1}{N} \sum_{k=1}^{N} X(k) \omega_N^{-(j-1)(k-1)} \qquad (1)$$

$$x(j) = \frac{1}{N} \sum_{k=1}^{N} X(k) \omega_N^{-(j-1)(k-1)} \qquad (2)$$

where

$$\omega_N = e^{\frac{2\pi i}{N}} \qquad (3)$$

is an Nth root of unity [7]. Equations 1 and 2 are known as fast Fourier transform algorithms, which have been developed from the discrete Fourier transform to reduce the amount of computations involved [8].

Induction motor faults detection, via fast Fourier transform based stator current signature analysis could be improved by decreasing the current waveform distortions. After all, it is well known that motor current is a non-stationary signal, the properties of which vary with the time-varying normal operating conditions of the motor. As a result, it is difficult to differentiate fault conditions from the normal operating conditions of the motor using Fourier analysis. [5]

The differentiation of faulty conditions of the motor will be easier, if the figures of healthy motor state are used as comparison material for the faulty rotor figures and peculiarities of local grid are noted. Differences between healthy and faulty rotor conditions are traceable as seen on Figs. 1 and 2.
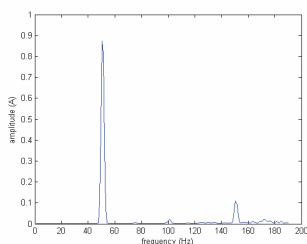

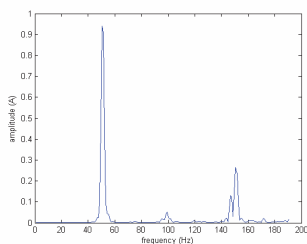Fig. 1 Stator current spectrum of healthy motor on nominal torque

Fig. 2 Stator current spectrum of faulty motor with seven broken rotor bars on nominal torque

2.2 Clarke Vector Approach

As fault detection based only on the fast Fourier transform can be quite difficult, other diagnostic methods should also be taken in consideration in order to make appropriate decisions on the state of the tested motor.

A two-dimensional representation can be used for describing three-phase induction motor phenomena. This transformation can be made using Clarke vector (or Park's vector)

$$\begin{cases} i_\alpha = i_a \\ i_\beta = \sqrt{2/3}\left(i_b + i_c\right) \end{cases} \qquad (4)$$

where i_a, i_b, and i_c are phase currents, i_α and i_β are alpha and beta components of the current.

Its representation is a circular pattern centered at the origin of the coordinates. This is a very simple reference figure, which allows the detection of an abnormal condition due to any fault of the machine by observing the deviations of the acquired picture from the reference pattern [9].

The healthy pattern differs slightly from the expected circular one, because supply voltage is generally not exactly sinusoidal [10]. Pattern of the rotor with broken bars is however more like an ellipse shaped one. Patterns of healthy and faulty motors are shown on Figs. 3 and 4.
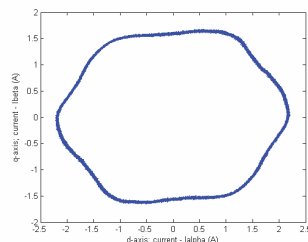

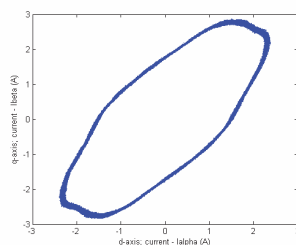Fig. 3 Stator current Clarke vector pattern of healthy motor on nominal torque

Fig. 4 Stator current Clarke vector pattern of faulty motor with seven broken rotor bars on nominal torque

2.3 Current Vector Amplitude Oscillation

Clarke transformation can be followed by monitoring the current vector amplitude oscillation. This method is not commonly described in the literature concerning induction motor rotor fault diagnostics, but it can prove to be a good indicator for the state of the rotor. The aim is primarily to find out whether there are changes in the figures according to the state of the motor and torque applied to it or not. This is also a simple procedure if the Clarke transformation is already

performed or in other words, the three-dimensional system is transformed into a two-dimensional system. After the Clarke transformation only one simple formula is required to acquire the graph of the current vector amplitude oscillation:

$$Cvao = \sqrt{i_\alpha{}^2 + i_\beta{}^2} \qquad (5)$$

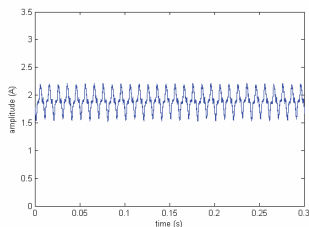After completing this calculation, Figs. 5 and 6 can be plotted.

Fig. 5 Current vector amplitude oscillation of healthy motor on nominal torque
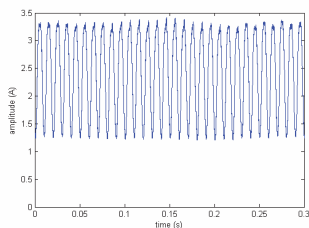

Fig. 6 Current vector amplitude oscillation of faulty motor with seven broken rotor bars on nominal torque

Difference is clear. The amplitude of a faulty rotor current vector is much higher, especially when the nominal torque is applied. It should be mentioned that the rise of the amplitude results also from the torque applied. This leads to a rise in current. Nevertheless, this method allows deciding on the state of the motor based on the analysis of the stator current measurements.

2.4 Other Possible Methods

In addition to the described methods that have been used by the authors for induction motor diagnostics there are various other methods for analyzing the measured stator current. Hereby a brief overview of some other existing analyzing methods is given.

Wavelet Analysis

As it was said before it can be difficult to differentiate fault conditions from the normal operating conditions of the motor using FFT. To overcome this problem wavelet analysis can be used.

Wavelet is a time frequency analysis tool originated from seismic signal analysis, which uses narrow windows for high frequency component [11]. Continuous wavelet transforms (CWTs) have constant frequency to bandwidth ratio analysis and therefore, CWTs provide powerful multi-resolution in time-frequency analysis for characterizing the transitory features of non-stationary signals [12]. Wavelet analysis can be used for localized analysis in the time-frequency or time scale domain, which makes it a powerful tool for condition monitoring and fault diagnosis [5].

Examples of the stator current spectra of healthy and faulty motors which are gained using wavelet theory are shown on Figs. 7 and 8.
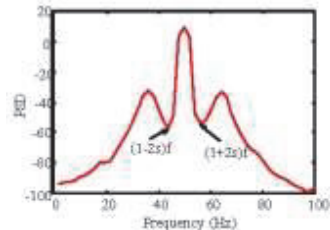

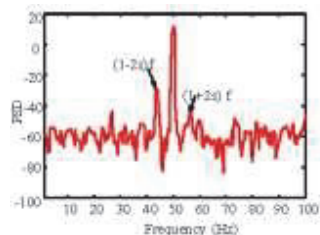Fig. 7 Stator current spectrum of healthy motor [13]

Fig. 8 Stator current spectrum of healthy motor with three broken rotor bars [13]

Finite Element Method

The finite element method, which is well established for induction motors modeling, could be used to provide an accurate evaluation of the magnetic field distribution inside the motor [6]. To assess the magnetic saturation effect on faults detection, the time-stepping finite-element method is recommended [14]. Faults in the rotor can be simulated using the finite element method and this would give an opportunity to estimate the magnetic field anomalies, based on the motor simulation. One example of the results of such simulation is shown on Fig 9.

Fig. 9 Magnetic field distribution in the cross section of a 3 kW induction motor at nominal load operating condition: left – healthy rotor cage, right – faulty rotor cage with seven broken bars (shaded) [15]

3 CONCLUSION

In general, it is certainly possible to decide upon the state of the rotor, and the whole induction motor respectively, using only the signals of stator currents and analyzing them. All of the methods described can be used as indicators of the motor state. However, there are some aspects that should be considered when such methods of sensorless diagnostics are used.

Firstly, it is essential to know the characteristics of the tested motor under normal operating conditions, as well as the peculiarities of the local grid where the motor is being tested. Deviations such as not perfectly sinusoidal supply voltage can have an effect on the outcomes of the current figures and can produce some unexpected peaks and curves in the graphs.

Secondly, to prove that the performed measurements and analyses are correct, the tests should not be performed using only one of the methods. For example the resolution of the obtained figure of FFT is directly related to the length of the sampling time. In order to get fine and correctly readable figures, the motor has to be in steady state during the sampling of the signal. It is however often not possible to keep the motor in a steady state during a prolonged sampling time. As a result it can be difficult to differentiate fault conditions from the normal operating conditions of the motor using only FFT, due to variability of properties of the non-stationary motor current signal. This problem can be solved when figures are proved by some other diagnostic method that is used simultaneously or in cooperation with the chosen one.

Another drawback of this kind of diagnosis is that the computational power required for the analysis is rather large. Without appropriate knowledge and software it is not possible to make all the transformations and graphs so easily. Interpretation of the figures require the operator or the user to have some degree of expertise and experience as well, because the deviations on the graphs can result from a number of sources, including the normal operating conditions for number of reasons, some of which have been described.

On the other hand, online monitoring makes the detection of a fault easy. If all the procedures are done correctly, the faults will appear on the graphs. Also, when the drive is monitored, the faults of the rotor will be detected on an early stage. When using this kind of monitoring it will not be necessary to stop the motor of running in its stage of work. All the needed procedures can be done without changing the working cycle of the tested motor.

REFERENCES

[1] Kim K., Parlos A., Bharadwaj R. Sensorless Fault Diagnosis of Induction Motors. IEEE Transactions on Industrial Electronics, vol. 50, no. 5, October 2003, pp. 1038–1051.

[2] Boldea I., Nasar S. The Induction Machine Handbook. Boca Raton, FL: CRC Press, 2002.

[3] Bonnett A., Soukup G. Cause and Analysis of Stator and Rotor Failures in Three-Phase Squirrel-Cage Induction Motor. IEEE Transactions on Industry Applications, vol. 28, no. 4, July/August 1992, pp. 921–937.

[4] Fišer R., Ferkolj S. Calculation of Magnetic Field Asymmetry of Induction Motor with Rotor Faults. Pro-ceedings of the 1998 IEEE Mediterranean Electrotechnical Conference, Tel Aviv (Israel), vol. 2, pp. 1175–1179.

[5] Benbouzid M., Kliman G. What Stator Current Processing-Based Technique to Use for Induction Motor Rotor Faults Diagnosis. IEEE Transactions on Energy Conversion, vol. 18, no. 2, June 2003, pp. 238–244.

[6] Benbouzid M. A Review of Induction Motors Signature Analysis as a Medium for Faults Detection. Proceedings of the 1998 International Conference of the IEEE Industrial Electronics Society, Aachen (Germany), vol. 4, pp. 1908–1913.

[7] MathWorks: http://www.mathworks.com/help/techdoc/ref/fft.html

[8] Ingle V., Proakis J., Digital Signal Processing Using MATLAB, 2nd edition. Toronto: Thompson, 2007. 605 p.

[9] Szabo L., Kovacs E., Toth F., Fekete G., Dobai J. Rotor Faults Detection Method for Squirrel Cage Induction Machines Based on the Park's Vector Approach. Annals of the University of Oradea, Fascicle of Electrotechnics, Section of Computer Science and Control Systems, 2007.

[10] Cardoso A., Saraiva E. Computer-aided Detection of Airgap Eccentricity in Operating Three-Phase Induction Motors by Park's Vector Approach. IEEE Transactions on Industrial Applications, vol. 29, no. 5, September/October 1993, pp. 897–901.

[11] Cao Z., Chen H., He G., Ritchie E. Rotor Fault Diagnosis of Induction Motor Based on Wavelet Reconstruction. Electrical Machines and Systems, ICEMS 2001, Proceedings of the Fifth International Conference, vol. 1, 2001, pp. 374-377.

[12] Tse P., Yang W., Tam H. Machine Fault Diagnosis Through an Effective Exact Wavelet Analysis. Journal of Sound and Vibration, vol. 277, 2004, pp. 1005-1024.

[13] Askari, M. Broken Bars Detection in Squirrel Cage Induction Motors Using Wavelet Theory. Journal of Applied Science, vol. 10, 2010, pp. 471-478.

[14] Kim C., Jung Y., Yoon S., Im D. The Fault Diagnosis of Rotor Bars in Squirrel Cage Induction Motors by Time Stepping Finite Element Method. IEEE Transactions on Magnetics, vol. 33, March 1997, pp. 2131-2134

[15] Fišer R., Ferkolj S. Application of a Finite Element Method to Predict Damaged Induction Motor Performance, IEEE Transactions on Magnetics, vol. 37, no. 5, September 2001, pp. 3635–3639.

Paper V

Vaimann, T.; Belahcen, A.; Martinez, J.; Kilk, A. (2014). Detection of induction motor broken bars in grid and frequency converter supply. *Przeglad Elektrotechniczny*, vol. 90, no.1, pp. 90–94.

Toomas VAIMANN[1], Anouar BELAHCEN[1,2], Javier MARTINEZ[2], Aleksander KILK[1]

Tallinn University of Technology (1), Aalto University (2)

Detection of induction motor broken bars in grid and frequency converter supply

Abstract. This paper presents the experimental study of three-phase squirrel cage induction motor broken rotor bars diagnostics. Tests have been performed with two different machines, one through a frequency converter and the other supplied directly from grid. This comparison has been presented, as the use of frequency converters changes the traditional current spectrum of the machine and hence the diagnostic of such machines becomes more difficult. Necessity for further study on the behavior of the frequency converter in the weak grid is pointed out.

*Streszczenie. W artykule zaprezentowano metodę diagnostyki trójfazowego silnika indukcyjnego z uszkodzonymi prętami. Zaprezentowano widmo sygnału prądowego różnych silników. (**Wykrywanie uszkodzonych prętów silnika indukcyjnego na podstawie widma częstotliwościowego prądu**)*

Introduction

Induction machines are by far the most widely industrial electrical machine type in nowadays world and considering their rugged build and cost-efficiency, their popularity can be expected to stay the same if not increase in the near future. In fact, in developed countries today there are more than 3 kW of electric motors per person and most of it is from induction motors [1]. Failures and faults in such machines can often have dramatic results and pose danger for the people and surroundings and cause economic problems for the industries, whose production depends on them.

The majority of all stator and rotor faults are caused by a combination of various stresses, which can be thermal, electromagnetic, residual, dynamic, mechanical or environmental [2]. These stresses can cause a number of different failures in electrical machines. In the case of squirrel cage induction machines, one of the most common faults is the cracking and eventually breaking of rotor bars. The main concern regarding such faults is that it is often not worth or possible to repair the rotor, if the fault has been detected too late. However all of this can be avoided, when the motor is supervised by an appropriate condition monitoring or diagnostic system allowing the anticipation of the fault and its propagation.

With the development of power electronics, many machines are today supplied by frequency converters, which enables good control of the torque and speed and thus energy saving in ,e.g., pumping and ventilation applications. However, the frequency converter supply changes the natural and traditional current spectrum of electrical machines. This also means that diagnostic measures have to be changed to match the peculiarities in the behavior of electrical machines connected to converters. However, the main requirements for diagnostic methods still stay the same, such as no additional changes or disturbances to the working cycle of the machines, when performing condition monitoring.

This paper describes an experimental study where broken rotor bars diagnostics of induction motor is performed on a machine that is supplied directly from grid and also a machine that is driven though a frequency converter. The studied parameters are the motor terminal currents and voltages. The first part of the paper describes the measurement set up and the following parts reviews the Clarke's vector equations and analyzes the measurements based on these equations.

Measurements

Measurements described in this paper were performed in two separate series. For the experiments, where the induction motor is supplied straight from the grid, a motor with a healthy rotor and a rotor with seven broken bars was used. In the experiments with supply through a frequency converter, a motor with a healthy rotor and a rotor with three broken bars was used. Broken rotor bars were situated next to each other in both cases. Schematics of the setups for the tests are presented in Fig. 1.
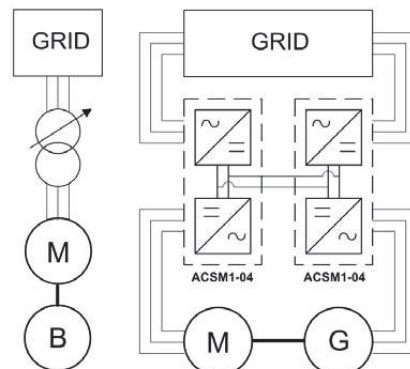

Fig.1. Schematics of experimental setups used for testing. Left – motor is fed directly from the grid through an autotransformer and loaded with an electromagnetic brake; right – motor is fed through frequency converters and loaded by an identical motor and frequency converter in regeneration mode.

In case of Motor 1, the machine is supplied directly from the grid through an autotransformer. The motor is loaded using an electromagnetic brake. Tested induction machine was connected in star during the tests.

Motor 2 is supplied from the grid through ABB ACSM1-04 frequency converters. Scalar control was used for driving the machine. Motor was loaded using an identical machine in generator mode and the machine was also connected to star during the testing period. The DC-links of the frequency converters were connected in parallel and only the power losses from both machines and frequency converters were drawn from the grid. Table 1 presents more precise data of the tested induction motors.

Table 1. Technical data of the tested induction motors

Parameter	Symbol	Motor 1 Value	Motor 2 Value
Rated voltage	U_n	177 V	380-415 V
Rated current	I_n	14.8 A	41 A
Rated speed	n_n	1456 rpm	1700 rpm
Rated power	P_n	3 kW	22 kW
Frequency	f	50 Hz	60 Hz
Power factor	$\cos\varphi$	0.785	0.860
Number of poles	p	4	4
Number of rotor bars	Q_r	44	40
Number of stator slots	Q_s	36	48

Analysis and discussion

Clarke's vector approach is an easy way to decide if the motor is healthy or not [5]. It means that the phase currents (i_a, i_b, i_c) are transformed to current alpha and beta components (i_α, i_β) and placed on α-axis and β-axis respectively. In other words, a three-dimensional system is transformed to a two-dimensional one assuming the zero component of the space vector is not allowed to flow, which holds true in case of star connection of the machine. The two components of the Clarke's current vector are then given as:

$$(1) \quad \begin{cases} i_\alpha = i_a \\ i_\beta = \dfrac{1}{\sqrt{3}}\left(2i_b + i_a\right) \end{cases}$$

Its representation at steady state operation of the machine is a circular pattern centered at the origin of the αβ-coordinate system. This is a very simple reference figure, which allows the detection of an abnormal condition due to any fault of the machine by observing the deviations of the acquired picture from the reference pattern [6].

The healthy pattern differs slightly from the expected circular one, because of the distortion and unbalance of the supply voltage and thus of the current space vector [7]. Clarke's vector current pattern of the rotor with broken bars is however more ellipse-shaped and its discrepancy from the circular pattern could be used for fault detection [8].

The Clarke's vector can be also used to transform the three-phase voltages at the terminal of the machine into α- and β-axis components:

$$(2) \quad \begin{cases} u_\alpha = u_a \\ u_\beta = \dfrac{1}{\sqrt{3}}\left(2u_b + u_a\right) \end{cases}$$

where u_a, u_b, and u_c are the phase voltages and u_α, u_β are the voltage alpha and beta components. This gives the opportunity to monitor the stator voltage as well as current and make the decisions upon the analyses of the obtained graphs [6].

Using Park's vector (and also Clarke's vector) approach for diagnostic purposes of electrical machines is not a novel idea itself. It has been proposed in the end of 80's by Cardoso et al [9]-[11], however, the method did not become widely used as there were significant doubts on the automation possibilities of the process. Nowadays, when computation technologies have advanced, the method can be implemented far more easily, e.g., with pattern recognition algorithms [12]. In addition, usage of Clarke's vector approach on stator voltage instead of current will grant a wider segment of possible diagnostic usage as the supply voltage of electrical machines is generally held at a constant value and is not much affected by the scalar control, which is by far the most used control methodology in applications with less requirements on the dynamic behavior of the drive system.

Grid operation (Motor 1)

In the tests with direct grid supply, the induction motor with a healthy rotor and a rotor with seven broken bars was used. All the broken rotor bars were situated next to each other, as it is the most probable case in practice and the asymmetry in such case is more severe. It should be noted that Motor 1 has die-cast aluminum cage, which is prone to bad casting and thus could present several broken bars not only at operation but right away after the manufacturing process. MATLAB software was used to analyze the data.

If one looks at the presented figures (Figs. 2-9), it can be observed that there are some unexpected curves and declinations from the expected vector pattern. This is caused mainly by the supply voltage used during the tests. As the supply was not exactly sinusoidal, the deviations from ideal sinusoid can also be traced in the resulting figures. However, this phenomenon can be left aside, as the healthy and faulty conditions of the motor are clearly visible from the figures regardless of the imperfection in the supply.

First two figures (Figs. 2 and 3) show Clarke's vector pattern of the stator current while the machine is working at no load conditions.
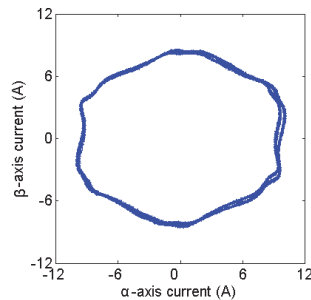

Fig.2. Stator current Clarke's vector pattern of healthy motor at no load conditions (Motor 1)
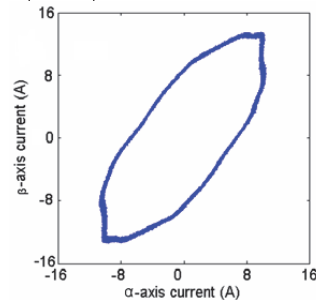

Fig.3. Stator current Clarke's vector pattern of faulty motor at no load conditions (Motor 1)

As the figures show, the healthy motor Clarke's vector current pattern has indeed a more or less circular shape and the faulty one looks more close to an ellipse as referred to in the literature [9]. In addition, it was found that the absolute value of current is higher in the case of faulty motor, which was also expected prior to the testing.

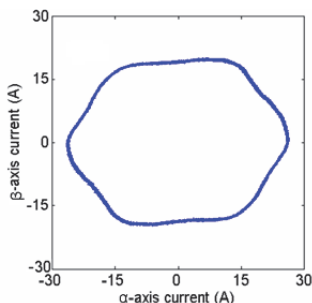Next figures (Figs. 4 and 5) are showing the machine at rated torque conditions.

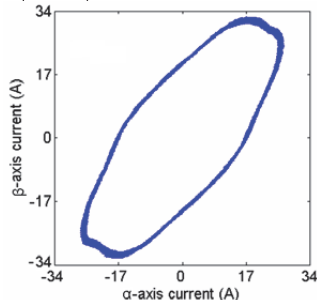Fig.4. Stator current Clarke's vector pattern of healthy motor at full load conditions (Motor 1)

Fig.5. Stator current Clarke's vector pattern of faulty motor at full load conditions (Motor 1)

Faulty case can be traced easily in the full load figures as well, due to the major differences in the pattern shape of healthy and faulty conditions. If one compares the figures of no load and full load operations, it can also be clearly seen that the current amplitude rises as more torque is applied to the machine.

Next figures (Figs. 6 and 7) are plotted using the Clarke's vector approach on stator voltage at the same time moment as the current data was gathered. Usage of stator voltage should yield better results and no load condition is observed first.

The figures show that the voltage pattern of the healthy motor looks again more as a circle and that of the faulty motor more like an ellipse. Such a dramatic change would not be expected if the supply network was enough rigid to withstand to effect of fault in the motor. Furthermore, changes in scale are more drastic and better traceable in case of the voltage graphs. Additionally, from the healthy case graph it can be seen that deviations due to the non-ideal sine voltage supply are not so vivid in the voltage case.

Figs. 8 and 9 are from the full load test, again taken in the same time moment as for the current figures.
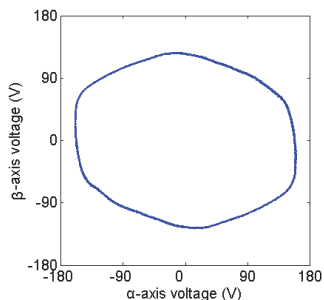

Fig.6. Stator voltage Clarke's vector pattern of healthy motor at no load conditions (Motor 1)
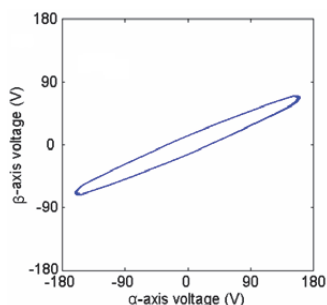

Fig.7. Stator voltage Clarke's vector pattern of faulty motor at no load conditions (Motor 1)
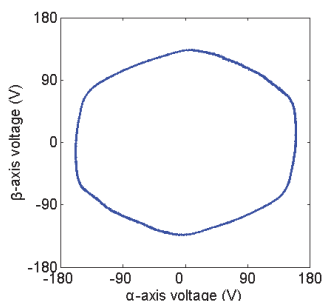

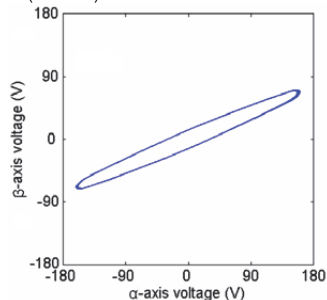Fig.8. Stator voltage Clarke's vector pattern of healthy motor at full load conditions (Motor 1)

Fig.9. Stator voltage Clarke's vector pattern of faulty motor at full load conditions (Motor 1)

When no load situation and full load situation are compared, it can be seen that they match in to a very large extend, which means that most of the changes in the patterns are due to the voltage unbalance caused by the seven broken rotor bars in the induction motor and not any other deviations in the grid or other variables.

Frequency converter operation (Motor 2)
A three-phase squirrel cage induction motor with a healthy rotor and a rotor with three broken bars situated next to each other was used for performing these tests. The machine was not supplied directly from grid but through a frequency converter using scalar control instead.

It is a commonly known fact that faults such as the broken rotor bars induce sideband harmonic components to the stator current spectrum of the induction motor. Those harmonics are used as fault indicators in the diagnostic process. Frequency converter causes supply frequency to slightly vary in time and, as a result, some additional harmonics in the current spectrum are induced and sidebands are reduced [13]. Depending on the type of the frequency converter the damping of sideband frequencies can be varying in a very large scale due to the raised

amount of noise in the test signals, which makes the faults more difficult to detect.

In the tests with frequency converters both current and voltage changes are observed as they were in the tests with direct grid supply. Figs. 10 and 11 present stator current Clarke's vector patterns of healthy and faulty cases under no load conditions.

If the figures of different cases are compared, no large scale changes can be detected as it was in the case with the grid supplied machine. Main difference compared to previous figures is the thicker line of the vector pattern, which is caused by the slightly changing supply frequency of the used frequency converter. As the supply frequency changes, it causes a slight change in the trajectory of the Clarke's vector and thus the vector pattern line becomes thicker.
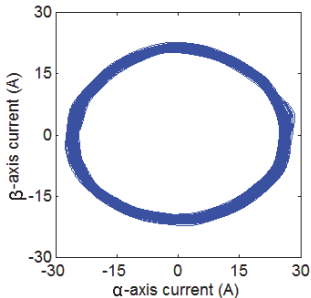

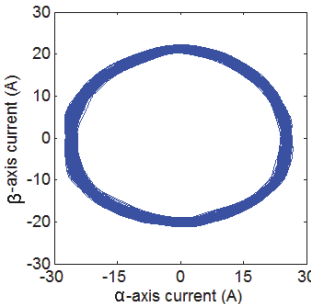Fig.10. Stator current Clarke's vector pattern of healthy motor at no load conditions (Motor 2)

Fig.11. Stator current Clarke's vector pattern of faulty motor at no load conditions (Motor 2)

Next figures (Figs. 12 and 13) describe stator current Clarke's vector pattern of both healthy and faulty cases on nominal load operation.
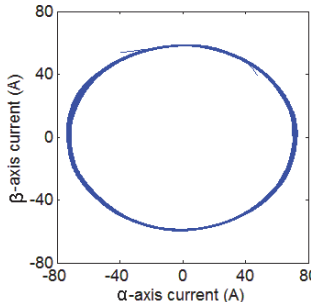

Fig.12. Stator current Clarke's vector pattern of healthy motor at full load conditions (Motor 2)
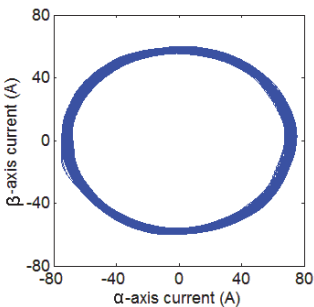

Fig.13. Stator current Clarke's vector pattern of faulty motor at full load conditions (Motor 2)

Those figures again do not show as large changes as it could be expected from the grid operation tests. Some change in the thickness of the stator current pattern can be observed, but change of shape is minuscule. The detection of the fault however is very complicated if not impossible when analyzing the stator current pattern of the machine equipped with a frequency converter. It can be said that it is very complicated to differentiate the faulty rotor from the healthy rotor in the case where induction motor is used with a frequency converter. As usage of voltage gave some benefits in the grid operation tests, it can be expected also when frequency converters are used. No load tests in such case are presented in Figs. 14 and 15.

As expected, the differences are more traceable when stator voltage pattern analysis is used. However, the signals are very noisy due to the additional harmonic components induced by the converter. Again the trajectory of the vector pattern is wider, which results in a thicker pattern line, but results are better and allow differentiation of the faulty case.

Last figures (Figs. 16 and 17) present the stator voltage Clarke's vector pattern under full load conditions.
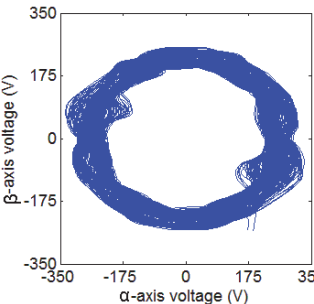

Fig.14. Stator voltage Clarke's vector pattern of healthy motor at no load conditions (Motor 2)
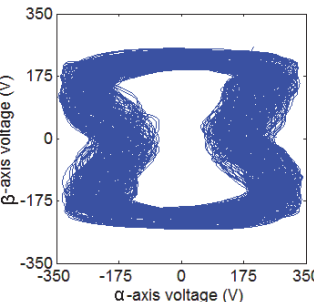

Fig.15. Stator voltage Clarke's vector pattern of faulty motor at no load conditions (Motor 2)
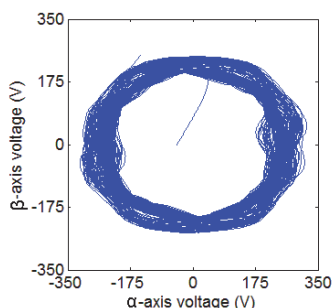
Fig.16. Stator voltage Clarke's vector pattern of healthy motor at full load conditions (Motor 2)
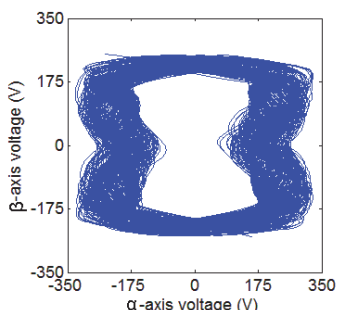

Fig.17. Stator voltage Clarke's vector pattern of faulty motor at full load conditions (Motor 2)

Both full load and no load figures are very similar to each other. The faulty case does not look like an ellipse, as it could be expected and this can be related to the switching frequencies, additional harmonics and varying supply frequency caused by the converter. It should be noted that the filtration level during the analysis of the result has been kept the same both in grid and frequency converter operation figures. Nevertheless, as the changes in the pattern shapes are clearly visible, it means that analysis of stator voltage in case of broken bars of the frequency converter driven induction motor can be used more effectively for determination of the rotor fault than the analysis of stator current [14].

Conclusion

Conducted experiments and analyses show that although traditionally used for transformation of current data, Clarke's vector approach can be very effectively used for transformation of three-phase voltage. For diagnostic purposes this might be a better use of the method, as supply voltage of electrical machines is generally held at a constant value. Also using voltage as a diagnostic parameter will gain a wider range of possible setups that can be monitored as scalar control and load conditions do not affect the voltage pattern. This peculiarity of voltage patterns gives the opportunity for better and more precise decisions as healthy and faulty case data can be compared without any changes or recalculations of amplitudes.

Frequency converters, due to slightly time-varying supply frequency, induce additional harmonics to the current spectrum of the machines, which reduces or even hinders the sideband frequencies that are used as fault indicators. Also they create more noise in the signals, which makes detection of the fault more complicated. As seen from the figures, presented in this paper, current pattern cannot be used for diagnostic purposes as the fault

indicators are not visible, which is not the case when voltage is used.

When diagnostics via the comparison of induction motor performance models is desired, the described method could be used in a sufficiently effective way to decide upon the state of the motor [13]. This can be automated using various algorithms and thus would be an effective way of diagnostics, which does not need vast computational resources due to the simplicity of the mathematical model. The model or figure of the healthy case of the motor can be used as a master model, to which other graphs would be compared to. It could prove to be a very good way for performing diagnostics also in the sense that no disturbance in the working cycle of the motor is needed in order to perform the needed measurements and analysis. The method could also be for testing the success of die cast aluminum cages of low power motors.

REFERENCES

[1] Boldea I., Nasar S., The Induction Machine Handbook. Boca Raton: CRC Press, (2002), 950
[2] Bonnett, A., Soukup, G., Cause and Analysis of Stator and Rotor Failures in Three-Phase Squirrel-Cage Induction Motor, *IEEE Trans. Ind. Appl.,* 28 (1992), No.5, 921-937
[3] Vaimann, T., Kallaste, A., Kilk, A., Using analysis of stator current for squirrel-cage induction motor rotor faults diagnostics, *in Proc. ECT 2011,* (2011), 245-251
[4] Vaimann, T., Kallaste, A., Kilk, A., Sensorless detection of induction motor rotor faults using the Clarke vector approach, *Scientific Journal of Riga Technical University,* 29 (2011), 43-48
[5] Cardoso, A., Saraiva, E., Computer-aided detection of airgap eccentricity in operating three-phase induction motors by Park's vector approach, *IEEE Trans. Ind. Appl.,* 29 (1993), No. 3, 897-901
[6] Vaimann, T., Kallaste, A., Kilk, A., Overview of sensorless diagnostic possibilities of induction motors with broken rotor bars, *in Proc. EPE 2011,* (2011), 183-186
[7] Benbouzid, M., A review of induction motor signature analysis as a medium for faults detection, *in Proc. IEEE IECON 1998,* 4 (1998), 1908-1913
[8] Miletic, A., Cettolo, M., Frequency converter influence on induction motor rotor faults detection using motor current signature analysis – experimental research, *in Proc. SDEMPED 2003,* (2003), 124-128
[9] Cardoso, A., Saraiva, E., On-line diagnostics of three-phase induction motors, by Parks Vector, *in Proc. ICEM,* 1 (1988), 231-234
[10] Cardoso, A., Saraiva, E., On-line diagnostics of current source inverter-fed induction machines, by Park's Vector Approach, *in Proc. ICEM,* (1990), 1000-1005
[11] Cardoso, A., Cruz, S., Carvalho, J., Saraiva, E., Rotor Cage Fault Diagnosis in Three-phase Induction Motors, by Park's Vector Approach, *in Proc. IAC,* 1 (1995), 642-646
[12] Amaral, T., Pires, V., Martins, J., Pires, A., Crisostomo, M., Image processing to a neuro-fuzzy classifier for detection and diagnosis of induction motor stator fault, *in Proc. IEEE IECON 2007,* (2007), 2408-2413
[13] Vaimann, T., Belahcen, A., Martinez, J., Kilk, A., Detection of Broken Bars in Frequency Converter Fed Induction Motor Using Park's Vector Approach, *in Proc. PQ 2012,* (2012), 53-56
[14] Vaimann, T., Kallaste, A., Kilk, A., Using Clarke Vector Approach for Stator Current and Voltage Analysis on Induction Motors with Broken Rotor Bars, *Electronics and Electrical Engineering,* 123 (2012), No. 7, 17-20

Authors: M.Sc. Toomas Vaimann, E-mail: *toomas.vaimann@ttu.ee;* prof. Anouar Belahcen, E-mail: *anouar.belahcen@aalto.fi;* M.Sc Javier Martinez, E-mail: *javier.martinez@aalto.fi;* ass.prof. Aleksander Kilk, E-mail: *aleksander.kilk@ttu.ee;* Tallinn University of Technology, Department of Electrical Engineering, Ehitajate tee 5, 19086 Tallinn, Estonia; Aalto University, Department of Electrical Engineering, P.O. Box 13000, FI-00076 Aalto, Finland.

Paper VI

Vaimann, T.; Belahcen, A.; Martinez, J.; Kilk, A. (2012). Park's Vector Approach for Detection Broken Rotor Bars in Frequency Converter Fed Induction Generator. *Proceedings of the 13th International Scientific Conference Electric Power Engineering EPE 2012*, May 23–25, 2012, Brno, Czech Republic, vol. 2, pp. 985–988.

Park's Vector Approach for Detection of Broken Rotor Bars in Frequency Converter Fed Induction Generator

Toomas Vaimann[1], Anouar Belahcen[1,2], Javier Martinez[2], Aleksander Kilk[1]

[1] Tallinn University of Technology, Department of Fundamentals of Electrical Engineering and Electrical Machines, Ehitajate tee 5, 19086 Tallinn, Estonia, www.ttu.ee
tel: +372 620 3800, email: toomas.vaimann@ttu.ee

[2] Aalto University, Department of Electrical Engineering, P.O. Box 13000, 0076 Aalto, Finland, elen.aalto.fi/en/

ABSTRACT

This paper presents the experimental study of induction generator broken rotor bars diagnostics. As induction generators are often used in renewable energy applications, such as wind and hydro power plants where they are also equipped with frequency converters, diagnostics of such machines is becoming more important. Tests are performed with an induction machine with a healthy rotor and a rotor with three broken bars, supplied through a frequency converter. Park's vector approach is used as an analyzing tool to detect the broken rotor bars. Park's vector pattern using stator current and voltage is investigated. Results of the tests and discussion of the results are presented. The necessity for further study is pointed out.

Keywords: Broken Rotor Bars, Diagnostics, Generator, Frequency Converter, Induction Machine, Park's Vector

1 INTRODUCTION

Renewable energy use and generation is getting more and more important in nowadays world. CO_2 emissions policies and the search for alternative energy sources to decrease the use of fossil fuels have lead to increasing need for wind and hydro power plants. Due to this, wind generation industry has become one of the fastest developing industries in the world today. In those appliances, induction generators are often used and preferred due to their robustness and low manufacturing costs [1].

Like all machine types, also induction generators, performing responsible tasks, are under high stress that can lead to different failures. Those faults are not particularly welcomed, because reliability of the machines decreases and there are vast economical and safety risks to the users of those machines. Main parts of the machine that can more likely be broken are the bearings, the stator and the rotor.

The majority of all stator and rotor faults are caused by a combination of various stresses, which can be thermal, electromagnetic, residual, dynamic, mechanical or environmental [2]. Broken rotor bars are not only one of the most common faults but also one of the most uncomfortable ones [3].

The worst case of such fault is when the broken rotor bars are situated closely one after another. This case is also most probable in practice as broken rotor bars are usually not detected at early stage. As the resistance of the broken bar is very high in comparison with the healthy ones, currents start to distribute unproportionally in the rotor cage. Parts of the rotor currents, which are unable to flow in broken bars, are flowing in adjacent bars. This increases the rms value of currents in the bars next to the broken ones [3]. As the healthy bars next to the broken one have too high current density, they will start to overheat, so these bars are under severe thermal stress. Those bars start cracking and breaking and when attention to the problem is not paid, the fault will continue to cascade, until the rotor cage is destroyed.

Broken rotors bars can lead to vibration problems [4], but more likely, in severe cases, the bar pounds out of the slot and makes contact with the stator core or winding [2]. The biggest problem of those faults is that it is often not worth or possible to repair the rotor. However all of this can be avoided, when the machine is supervised by an appropriate condition monitoring or diagnostic system.

When choosing an appropriate method for condition monitoring or diagnostics of the machines, it should be noted, that changes of the working cycle are not desired while diagnostic process is performed. In other words, in case of machines which are used in critical duty drives or perform on high risk conditions, no additional changes should be made in order to perform the tests.

A growing number of machines are driven through frequency converters. This means that also diagnostic for appropriate setups with frequency converters should be investigated. Frequency converters add additional noise and harmonics to the traditional current spectrum of the machines and thus such drives need a slightly different approach in diagnostics than traditional grid supplied machines. This paper describes an experimental study where broken rotor bars diagnostics of induction generator is performed on a machine that is driven though a frequency converter.

2 MEASUREMENTS

Measurements described in this paper were performed in two separate series. For the experiments a generator with a healthy rotor and a rotor with three broken bars was used. Broken rotor bars were situated next to each other. Schematic of the experimental setup is presented in Fig. 1.

The tested generator was supplied from the grid through ABB ACSM1-04 frequency converters. Scalar control was used for driving the machine. Generator was loaded using an identical machine in motor mode and the machine was connected to star during the testing period. Table 1 presents more precise data of the tested induction machine.
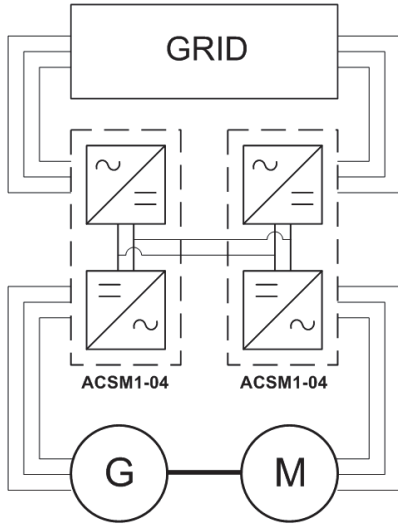
Fig. 1 Schematic of experimental setup

Tab. 1 Technical data of the tested induction machine

Parameter	Symbol	Value
Rated voltage	U_n	380-415 V
Rated current	I_n	41 A
Rated speed	n_n	1700 rpm
Rated power	P_n	22 kW
Frequency	f	60 Hz
Power factor	$\cos\varphi$	0.860
Number of poles	p	4
Number of rotor bars	Q_r	40
Number of stator slots	Q_s	48

3 ANALYSIS

Park's vector approach is an easy way to decide if the machine is healthy or not [5]. It means that the phase currents (i_a, i_b, i_c) are to be transformed into current alpha and beta components (i_α, i_β) and placed on d-axis and q-axis respectively. In other words, transforming a three-dimensional system into a two-dimensional one:

$$\begin{cases} i_\alpha = i_a \\ i_\beta = \sqrt{2/3}\left(i_b + i_c\right) \end{cases} \quad (1)$$

Its representation is a circular pattern centered at the origin of the coordinates. This is a very simple reference figure, which allows the detection of an abnormal condition due to any fault of the machine by observing the deviations of the acquired picture from the reference pattern [5].

The healthy pattern differs slightly from the expected circular one, because supply voltage is generally not exactly sinusoidal [6]. Pattern of the rotor with broken bars is however more like an ellipse shaped one [7].

Exactly the same transformation can be used to transform the three-phase voltage into a two-dimensional system:

$$\begin{cases} u_\alpha = u_a \\ u_\beta = \sqrt{2/3}\left(u_b + u_c\right) \end{cases} \quad (2)$$

where u_a, u_b, u_c are the phase voltages and u_α, u_β are the voltage alpha and beta components. This gives the opportunity to monitor the stator voltage as well as current and make the decisions upon the analyses of the obtained graphs [5].

3.1 Stator Current Analysis

To perform analysis on the data received from the measurements, MATLAB software was used. This makes it very simple to perform Park's transformation on the gained data. Generator with a healthy rotor and a rotor with three broken bars situated next to each other was used for performing these experiments. The machine was supplied through a frequency converter.

It is a widely known fact that faults such as the broken rotor bars induce sideband harmonic components to the stator current spectrum of the induction machine. Those harmonics can be used for detecting the faults. Frequency converter causes supply frequency to vary slightly in time and, as a result, some additional harmonics in the current spectrum are induced and sidebands are reduced [8]. This phenomenon also raises the amount of noise in the test signals, which makes the faults more difficult to detect.

In the tests both current and voltage changes are observed. The first figures (Figs. 2 and 3) present stator current Park's vector patterns of healthy and faulty cases on no load conditions.

Both healthy and faulty cases are very similar to each other. The thick line of the stator current Park's vector pattern is caused by the use of frequency converter and the phenomenon described before – slightly changing supply frequency. As the supply frequency changes, it causes a slight change in the trajectory of the Park's vector and thus the vector pattern becomes thicker. If the stator current Park's vector pattern of a machine supplied directly from grid would be observed, it could be seen that the line is thinner and plainer than in the case seen in the presented figures, even though the same amount of filtering has been applied [5].
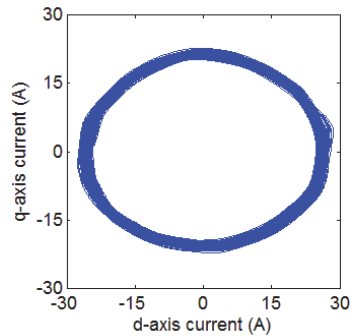

Fig. 2 Stator current Park's vector pattern of healthy generator at no load conditions
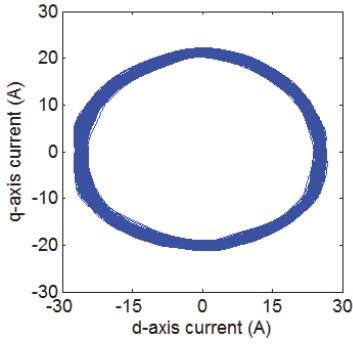
Fig. 3 Stator current Park's vector pattern of faulty generator at no load conditions

Next figures (Figs. 4 and 5) are describing the stator current Park's vector pattern of healthy and faulty generators on full load conditions.
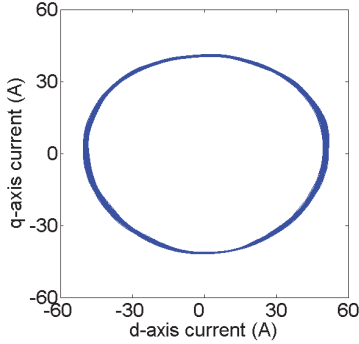

Fig. 4 Stator current Park's vector pattern of healthy generator at full load conditions
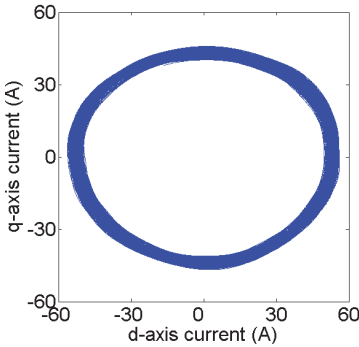

Fig. 5 Stator current Park's vector pattern of faulty generator at full load conditions

As seen from the figures, the changes are there, but they are not as large as expected. Some change in the thickness of the stator current pattern can be observed, but change of shape is minuscule if any. It can be said that it is very complicated to differentiate the faulty rotor from the healthy one through the analysis of stator current when induction generator is used with a frequency converter.

3.2 Stator Voltage Analysis

Previous studies from the authors have shown that differentiation of the fault can be easier when stator voltage is used instead of current to perform the Park's transformation. As voltage is not largely affected by loading of the machine, deviations in the figures are expected to derive solely from the fault signals of the generator. Figs 6 and 7 show the stator voltage Park's vector pattern of the healthy and faulty cases on no load conditions.
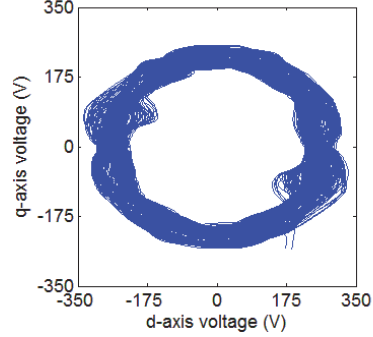

Fig. 6 Stator voltage Park's vector pattern of healthy generator at no load conditions
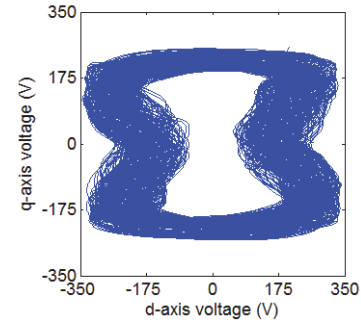
Fig. 7 Stator voltage Park's vector pattern of faulty generator at no load conditions

Figures show that indeed the changes are more traceable in the case when stator voltage is analyzed instead of current. As the use of frequency converter induces additional harmonics, the signals are very noisy. This can clearly be seen on the voltage figures. Additionally, the deviations of supply frequency make the trajectory line thicker than it has been in other described cases. Nevertheless, the drastic changes in the shapes of Park's vector pattern allow the differentiation of the faulty case.

Last two figures (Figs. 8 and 9) show stator voltage Park's vector pattern on full load conditions.

Full load figures are very similar to the no load ones. This means that load does not affect the figures when voltage is observed. The changes are clearly visible, which means that analysis of stator voltage in case of broken bars of the frequency converter driven induction generator can be used more effectively for determination of the rotor fault than the analysis of stator current.

Fig. 8 Stator voltage Park's vector pattern of healthy generator at full load conditions

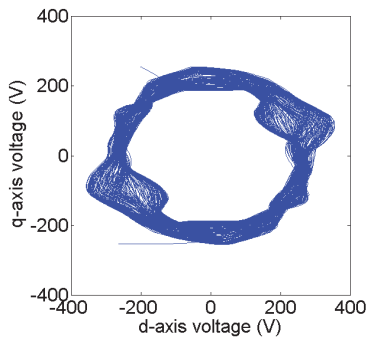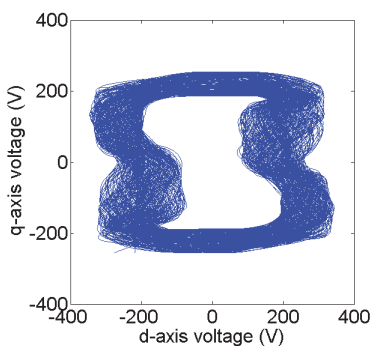Fig. 9 Stator voltage Park's vector pattern of faulty generator at full load conditions

4 CONCLUSION

Conducted experiments and analyses show that although traditionally used for transformation of current data, Park's vector approach can be very effectively used for transformation of three-phase voltage. For diagnostic purposes this might be a better use of the method, as in the case of voltage, load conditions, as well as deviations of supply voltage do not have as high effect on the outcomes as in the case of current.

When diagnostics via the comparison of induction machine performance models is desired, the described method could be used in a sufficiently effective way to decide upon the state of the machine. The needed information is the model or figure of the healthy case of the generator, which would also be the master model, to which other graphs would be compared to. It could prove to be a very good way for performing diagnostics also in the sense that no disturbance in the working cycle of the generator is needed in order to perform the needed measurements and analysis.

This could prove to be especially beneficial, when the diagnostics is performed in wind applications or small hydro power plants, where induction generators are often used. Usage of diagnostic systems in such applications would help improve the reliability and stability of energy generation from renewable energy sources. It would decrease the downtime and maintenance costs of the plant as well as increase overall safety of such applications.

Frequency converters, due to slightly time-varying supply frequency, induce additional harmonics to the current spectrum of the machines, which reduces or even hinders the sideband frequencies that are used as fault indicators. Also they create more noise in the signals, which makes detection of the fault more complicated.

Further study in the field is needed to find more accurate and effective solutions to detect faults in machines driven through frequency converters. Furthermore, investigation is needed for better understanding the impact of frequency converters to the Park's vector pattern of stator voltage. Park's vector approach seems to be a sufficient method of detecting a fault in induction machines regardless of the supply, but segregation of the nature of the fault requires more investigations. Simulation of the broken rotor bars in a machine that is supplied through frequency converter is planned in near future.

REFERENCES

[1] Albizu, A., Tapia, A., Saenz, J., Mazon, A., Zamora, I. On-line Stator Winding Fault Diagnostics in Induction Generators for Renewable Generation. Proceedings of the 12th Mediterranean Electrotechnical Conference, 2004, vol. 3, pp. 1017-1020.

[2] Bonnett, A., Soukup, G. Cause and Analysis of Stator and Rotor Failures in Three-Phase Squirrel-Cage Induction Motor. IEEE Transactions on Industry Applications, 1992, vol. 28, no. 4, pp. 921–937.

[3] Fišer, R., Ferkolj, S. Calculation of Magnetic Field Asymmetry of Induction Motor with Rotor Faults. Proceedings of the 1998 IEEE Mediterranean Electrotechnical Conference, vol. 2, pp. 1175–1179.

[4] Rodriguez, P., Belahcen, A., Arkkio, A. Signatures of Electrical Faults in the Force Distribution and Vibration Pattern of Induction Motors. IEE Proceedings - Electric Power Applications, 2006, vol. 153, no. 4, pp. 523-529.

[5] Vaimann, T., Kallaste, A., Kilk, A. Sensorless Detection of Induction Motor Rotor Faults Using the Clarke Vector Approach. Scientific Journal of Riga Technical University, 2011, vol. 29, pp. 43-48.

[6] Cardoso, A., Saraiva, E. Computer-Aided Detection of Airgap Eccentricity in Operating Three-Phase Induction Motors by Park's Vector Approach. IEEE Transactions on Industrial Applications, 1993, vol. 29, no. 5, pp. 897–901.

[7] Vaimann, T., Kallaste, A., Kilk, A. Overview of Sensorless Diagnostic Possibilities of Induction Motors with Broken Rotor Bars, Proceedings of the 12th International Scientific Conference on Electrical Power Engineering EPE 2011, pp. 183-186.

[8] Miletic, A., Cettolo, M. Frequency Converter Influence on Induction Motor Rotor Faults Detection Using Motor Current Signature Analysis – Experimental Research. Proceedings of Symposium on Diagnostics for Electric Machines, Power Electronics and Drives SDEMPED 2003, pp. 124-128

CURRICULUM VITAE

1. Personal data

Name:	Toomas Vaimann
Date and place of birth:	11.05.1984, Pärnu, Estonia
Citizenship:	Estonian
Marital status:	Married

2. Contact information

Address:	Keskuse 14a-43, 12911 Tallinn, Estonia
Phone:	(+372) 5061921
E-mail:	toomas.vaimann@ttu.ee

3. Education

Educational Institution	Graduating year	Education (field of study / degree)
Tallinn University of Technology	2009	Electrical drives and power electronics / Master's degree
Tallinn University of Technology	2007	Electrical drives and power electronics / Bachelor's degree
Pärnu Co-educational gymnasium	2002	Secondary education

4. Language competence/skills

Language	Level
Estonian	fluent
English	fluent
Russian	fluent
German	average
Finnish	basic

5. Special Courses

Period	Course name	Educational or other organisation
2013 (3 days)	Tooth Contour Method for Electric Machine Analysis	Lappeenranta University of Technology, Finland
2012 (3 days)	Uncertainty Quantification in Engineering – Application to Electrical Machines and Devices	Aalto University, Finland
2012 (3 days)	Elements of Synchronous Machine Design	Lappeenranta University of Technology, Finland
2011 (3 days)	PM machine: Design, Analysis, and Control	Lappeenranta University of Technology, Finland
2010–2013	Different intensive courses	Doctoral school of energy and geotechnology II, Tallinn University of Technology
2010 (5 days)	Basic course on legislature and standards of safety in electrical engineering	Auditron LLC
2009 (1 day)	BIM design course for electrical field specialists	Kymdata Oy
2009 (2 days)	CADS Planner Electric Pro for Building Systems – course on switch board schematics and installation drawings	Kymdata Oy

6. Professional Employment

Period	Organisation	Position
2013–…	Tallinn University of Technology, Department of Electrical Engineering	engineer/assistant
2010–2013	Tallinn University of Technology, Department of Fundamentals of Electrical Engineering and Electrical Machines	engineer/assistant
2009–2010	Amhold Ltd	designer of electrical installations
2008–2009	Elwo Ltd	designer of electrical installations
2006–2007	EE AIA Ltd	supervisor
2006–2006	EE AIA Ltd	electrician
2004–2004	Elwo Ltd	foreman (internship)

7. Scientific work

- Project "Analysis and Improvement of Analytical Model of Permanent Magnet Generator", Domestic project, 08.02.2010 – ... Research staff.
- Project "Design and Optimization Methodology for Electrical Motor-Drives", Estonian Ministry of Education and Science base financing fund, 01.05.2013 – 30.04.2016. Research staff.
- Project "Permanent magnets for sustainable energy application (MagMat)", National R&D program „Materials technology", 17.03.2012 – 31.12.2014. Research staff.
- Project "Power Quality and Safety Requirements for People and Electrical Equipment in Smart Grid Customer Domain", ERA-Net SmartGrids, 01.11.2010 – 31.10.2013. Research staff.

8. Defended theses

- Aasma, R. (2013). Composition of electricity supply documentation for scientific laboratory of electrical machines (Master's thesis).
- Kresla, T. (2013). Restoration of slow-speed permanent magnet synchronous generator (Bachelor's thesis).
- Kulp, J. (2012). Building of study model of DC machine (Bachelor's thesis).
- Vendelin, K. (2012). Investigation of diagnostic possibilities of synchronous machines (Bachelor's thesis).

9. Main areas of scientific work / Current research topics

Electrical machines, diagnostics of electrical machines.

ELULOOKIRJELDUS

1. Isikuandmed
    Ees- ja perekonnanimi: Toomas Vaimann
    Sünniaeg ja -koht: 11.05.1984, Pärnu
    Kodakondsus: Eesti
    Perekonnaseis: abielus

2. Kontaktandmed
    Aadress: Keskuse 14a-43, 12911 Tallinn
    Telefon: 5061921
    E-posti aadress: toomas.vaimann@ttu.ee

3. Hariduskäik

Õppeasutus (nimetus lõpetamise ajal)	Lõpetamise aeg	Haridus (eriala/kraad)
Tallinna Tehnikaülikool	2009	elektriajamid ja jõuelektroonika / tehnikateaduste magister
Tallinna Tehnikaülikool	2007	elektriajamid ja jõuelektroonika / tehnikateaduste bakalaureus
Pärnu Ühisgümnaasium	2002	keskharidus

4. Keelteoskus

Keel	Tase
Eesti keel	emakeel
Inglise keel	kõrgtase
Vene keel	kõrgtase
Saksa keel	kesktase
Soome keel	algtase

5. Täiendõpe

Õppimise aeg	Täiendõppe nimetus	Täiendõppe läbiviija
2013 (3 päeva)	Tooth Contour Method for Electric Machine Analysis	Lappeenranta Tehnikaülikool, Soome
2012 (3 päeva)	Uncertainty Quantification in Engineering – Application to Electrical Machines and Devices	Aalto Ülikool, Soome
2012 (3 päeva)	Elements of Synchronous Machine Design	Lappeenranta Tehnikaülikool, Soome
2011 (3 päeva)	PM machine: Design, Analysis, and Control	Lappeenranta Tehnikaülikool, Soome
2010–2013	Erinevad intensiivkursused	Energia- ja geotehnika doktorikool II, Tallinna Tehnikaülikool
2010 (5 päeva)	Elektriohutuse seadusandluse ja ohutusstandardite põhikursus	Auditron OÜ
2009 (1 päev)	BIM-projekteerimise koolitus elektriala spetsialistidele	Kymdata Oy
2009 (2 päeva)	CADS Planner Electric Pro for Building Systems – paigaldus-jooniste ja kilbiskeemide projekteerimise koolitus	Kymdata Oy

6. Teenistuskäik

Töötamise aeg	Tööandja nimetus	Ametikoht
2013–…	Tallinna Tehnikaülikool, elektrotehnika instituut	insener/assistent
2010–2013	Tallinna Tehnikaülikool, elektrotehnika aluste ja elektrimasinate instituut	insener/assistent
2009–2010	Amhold AS	elektripaigaldiste projektiinsener
2008–2009	Elwo AS	elektripaigaldiste projektiinsener
2006–2007	EE AIA AS	töödejuhataja
2006–2006	EE AIA AS	elektrik
2004–2004	Elwo AS	meister (praktika)

7. Teadustegevus
- Püsimagnetgeneraatori arvutusliku mudeli analüüs ja täiustamine, siseriiklik leping, 08.02.2010 – … Põhitäitja.
- Elektrimootorajamite projekteerimis- ja optimeerimismetodoloogia, HTM baasfinantseerimine, 01.05.2013 – 30.04.2016. Põhitäitja.
- Püsimagnetid jätkusuutliku energeetika rakendustes (MagMat), SA Archimedes, 17.03.2012 – 31.12.2014. Põhitäitja.
- Elektri tarkvõrgu kliendivalduse elektrikvaliteedi ja inimeste ning elektriseadmete ohutusnõuded, ERA-Net SmartGrids, 01.11.2010 – 31.10.2013. Põhitäitja.

8. Juhendatud lõputööd
- Aasma, R. (2013). Elektrimasinate teaduslaboratooriumi elektripaigaldise projektdokumentatsiooni koostamine. (Magistritöö)
- Kresla, T. (2013). Madalakiiruselise püsimagnetitega sünkroongeneraatori restaureerimine. (Bakalaureusetöö)
- Kulp, J. (2012). Alalisvoolumasina õppemudeli valmistamine. (Bakalaureusetöö)
- Vendelin, K. (2012). Sünkroonmasinate diagnostikavõimaluste uurimine. (Bakalaureusetöö)

9. Teadustöö põhisuunad
Elektrimasinad, elektrimasinate diagnostika.

DISSERTATIONS DEFENDED AT
TALLINN UNIVERSITY OF TECHNOLOGY ON
POWER ENGINEERING, ELECTRICAL ENGINEERING, MINING ENGINEERING

1. **Jaan Tehver**. Boiling on Porous Surface. 1992.

2. Salastatud.

3. **Endel Risthein.** Electricity Supply of Industrial Plants. 1993.

4. **Tõnu Trump**. Some New Aspects of Digital Filtering. 1993.

5. **Vello Sarv.** Synthesis and Design of Power Converters with Reduced Distortions Using Optimal Energy Exchange Control. 1994.

6. **Ivan Klevtsov**. Strained Condition Diagnosis and Fatigue Life Prediction for Metals under Cyclic Temperature Oscillations. 1994.

7. **Ants Meister**. Some Phase-Sensitive and Spectral Methods in Biomedical Engineering. 1994.

8. **Mati Meldorf**. Steady-State Monitoring of Power System. 1995.

9. **Jüri-Rivaldo Pastarus**. Large Cavern Stability in the Maardu Granite Deposit. 1996.

10. **Enn Velmre**. Modeling and Simulation of Bipolar Semiconductor Devices. 1996.

11. **Kalju Meigas**. Coherent Photodetection with a Laser. 1997.

12. **Andres Udal**. Development of Numerical Semiconductor Device Models and Their Application in Device Theory and Design. 1998.

13. **Kuno Janson**. Paralleel- ja järjestikresonantsi parameetrilise vaheldumisega võrgusageduslik resonantsmuundur ja tema rakendamine. 2001.

14. **Jüri Joller**. Research and Development of Energy Saving Traction Drives for Trams. 2001.

15. **Ingo Valgma**. Geographical Information System for Oil Shale Mining – MGIS. 2002.

16. **Raik Jansikene**. Research, Design and Application of Magnetohydrodynamical (MHD) Devices for Automation of Casting Industry. 2003.

17. **Oleg Nikitin**. Optimization of the Room-and-Pillar Mining Technology for Oil-Shale Mines. 2003.

18. **Viktor Bolgov**. Load Current Stabilization and Suppression of Flicker in AC Arc Furnace Power Supply by Series-Connected Saturable Reactor. 2004.

19. **Raine Pajo**. Power System Stability Monitoring – an Approach of Electrical Load Modelling. 2004.

20. **Jelena Shuvalova**. Optimal Approximation of Input-Output Characteristics of Power Units and Plants. 2004.

21. **Nikolai Dorovatovski**. Thermographic Diagnostics of Electrical Equipment of Eesti Energia Ltd. 2004.

22. **Katrin Erg**. Groundwater Sulphate Content Changes in Estonian Underground Oil Shale Mines. 2005.

23. **Argo Rosin**. Control, Supervision and Operation Diagnostics of Light Rail Electric Transport. 2005.

24. **Dmitri Vinnikov**. Research, Design and Implementation of Auxiliary Power Supplies for the Light Rail Vehicles. 2005.

25. **Madis Lehtla**. Microprocessor Control Systems of Light Rail Vehicle Traction Drives. 2006.

26. **Jevgeni Šklovski**. LC Circuit with Parallel and Series Resonance Alternation in Switch-Mode Converters. 2007.

27. **Sten Suuroja**. Comparative Morphological Analysis of the Early Paleozoic Marine Impact Structures Kärdla and Neugrund, Estonia. 2007.

28. **Sergei Sabanov**. Risk Assessment Methods in Estonian Oil Shale Mining Industry. 2008.

29. **Vitali Boiko**. Development and Research of the Traction Asynchronous Multimotor Drive. 2008.

30. **Tauno Tammeoja**. Economic Model of Oil Shale Flows and Cost. 2008.

31. **Jelena Armas**. Quality Criterion of road Lighting Measurement and Exploring. 2008.

32. **Olavi Tammemäe**. Basics for Geotechnical Engineering Explorations Considering Needed Legal Changes. 2008.

33. **Mart Landsberg**. Long-Term Capacity Planning and Feasibility of Nuclear Power in Estonia under Certain Conditions. 2008.

34. **Hardi Torn**. Engineering-Geological Modelling of the Sillamäe Radioactive Tailings Pond Area. 2008.

35. **Aleksander Kilk**. Paljupooluseline püsimagnetitega sünkroongeneraator tuuleagregaatidele. 2008.

36. **Olga Ruban**. Analysis and Development of the PLC Control System with the Distributed I/Os. 2008.

37. **Jako Kilter**. Monitoring of Electrical Distribution Network Operation. 2009.

38. **Ivo Palu**. Impact of Wind Parks on Power System Containing Thermal Power Plants. 2009.

39. **Hannes Agabus**. Large-Scale Integration of Wind Energy into the Power System Considering the Uncertainty Information. 2009.

40. **Kalle Kilk**. Variations of Power Demand and Wind Power Generation and Their Influence to the Operation of Power Systems. 2009.

41. **Indrek Roasto**. Research and Development of Digital Control Systems and Algorithms for High Power, High Voltage Isolated DC/DC Converters. 2009.

42. **Hardi Hõimoja**. Energiatõhususe hindamise ja energiasalvestite arvutuse metoodika linna elektertranspordile. 2009.

43. **Tanel Jalakas**. Research and Development of High-Power High-Voltage DC/DC Converters. 2010.

44. **Helena Lind**. Groundwater Flow Model of the Western Part of the Estonian Oil Shale Deposit. 2010.

45. **Arvi Hamburg**. Analysis of Energy Development Perspectives. 2010.

46. **Mall Orru**. Dependence of Estonian Peat Deposit Properties on Landscape Types and Feeding Conditions. 2010.

47. **Erik Väli**. Best Available Technology for the Environmentally Friendly Mining with Surface Miner. 2011.

48. **Tarmo Tohver**. Utilization of Waste Rock from Oil Shale Mining. 2011.

49. **Mikhail Egorov**. Research and Development of Control Methods for Low-Loss IGBT Inverter-Fed Induction Motor Drives. 2011.

50. **Toomas Vinnal**. Eesti ettevõtete elektritarbimise uurimine ja soovituste väljatöötamine tarbimise optimeerimiseks. 2011.

51. **Veiko Karu**. Potential Usage of Underground Mined Areas in Estonian Oil Shale Deposit. 2012.

52. **Zoja Raud**. Research and Development of an Active Learning Technology for University-Level Education in the Field of Electronics and Power Electronics. 2012.

53. **Andrei Blinov**. Research of Switching Properties and Performance Improvement Methods of High-Voltage IGBT based DC/DC Converters. 2012.

54. **Paul Taklaja**. 110 kV õhuliinide isolatsiooni töökindluse analüüs ja töökindluse tõstmise meetodid. 2012.

55. **Lauri Kütt**. Analysis and Development of Inductive Current Sensor for Power Line On-Line Measurements of Fast Transients. 2012.

56. **Heigo Mõlder**. Vedelmetalli juhitava segamisvõimaluse uurimine alalisvoolu kaarleekahjus. 2012.

57. **Reeli Kuhi-Thalfeldt**. Distributed Electricity Generation and its Possibilities for Meeting the Targets of Energy and Climate Policies. 2012.

58. **Irena Milaševski**. Research and Development of Electronic Ballasts for Smart Lighting Systems with Light Emitting Diodes. 2012.

59. **Anna Andrijanovitš**. New Converter Topologies for Integration of Hydrogen Based Long-Term Energy Storages to Renewable Energy Systems. 2013.

60 **Viktor Beldjajev**. Research and Development of the New Topologies for the Isolation Stage of the Power Electronic Transformer. 2013.

61. **Eduard Brindfeldt**. Visually Structured Methods and Tools for Industry Automation. 2013.

62. **Marek Mägi**. Development and Control of Energy Exchange Processes Between Electric Vehicle and Utility Network. 2013.

63. **Ants Kallaste**. Low Speed Permanent Magnet Slotless Generator Development and Implementation for Windmills. 2013.

64. **Igor Mets**. Measurement and Data Communication Technology for the Implementation in Estonian Transmission Network. 2013.

65. **Julija Šommet**. Analysis of Sustainability Assessment in Carbonate Rock Quarries. 2014.

66. **Tanel Kivipõld**. Real-Time Electricity Tariff System for Retail Market. 2014.

67. **Priit Uuemaa**. Industrial CHP Optimal Management Model in the Energy Market under Incomplete Information. 2014.